MycoKeys 40: 1–12 (2018)
doi: 10.3897/mycokeys.40.23828
http://mycokeys.pensoft.net

RESEARCH ARTICLE

A peer-reviewed open-access journal
MycoKeys
Launched to accelerate biodiversity research

Classicula sinensis, a new species of basidiomycetous aquatic hyphomycetes from southwest China

Min Qiao[1], Wenjun Li[1], Ying Huang[1], Jianping Xu[1], Li Zhang[1], Zefen Yu[2]

1 *Laboratory for Conservation and Utilization of Bio-resources, Key Laboratory for Microbial Resources of the Ministry of Education, Yunnan University, Kunming, Yunnan, 650091, P. R. China* **2** *School of Life Sciences, Yunnan University, No. 2 North, Kunming, Yunnan, 650091, P. R. China*

Corresponding author: *Zefen Yu* (zfyuqm@hotmail.com)

Academic editor: *D. Begerow* | Received 24 January 2018 | Accepted 5 September 2018 | Published 18 September 2018

Citation: Qiao M, Li W, Huang Y, Xu J, Zhang L, Yu Z (2018) *Classicula sinensis*, a new species of basidiomycetous aquatic hyphomycetes from southwest China. MycoKeys 40: 1–12. https://doi.org/10.3897/mycokeys.40.23828

Abstract

Classicula sinensis, isolated from decaying leaves from Mozigou, Chongqing Municipality, China, is described as a new species. The new species is a member of basidiomycetous aquatic hyphomycetes which represent a small proportion of all aquatic hyphomycetes. This species falls within the genus *Classicula* (Classiculaceae, Pucciniomycotina) and is closely related to *C. fluitans*, based on multiple gene sequence analyses. Morphologically, it is characterised by the apical, hyaline, obclavate or navicular conidia with several hair-like lateral appendages and by its holoblastic and monoblastic conidiogenesis, with a flat un-thickened conidiogenous locus. Clamp connections and haustorial branches were often observed in culture.

Keywords

fresh water fungi, mycoparasites, Pucciniomycotina, taxonomy

Introduction

Aquatic hyphomycetes constitute a dominant mycoflora on submerged decaying plant debris, both in lotic and lentic systems (Khan 1987). Phylogenetically, most aquatic hyphomycetes belong to Ascomycota, with only a small percentage belonging to Basidiomycota (Shearer 2007). Most known basidiomycetous aquatic hyphomycetes have been reported from North America (Marvanová 1977, Marvanová and Barlocher 1988, 1998, 2000, Marvanová and Suberkropp 1990, Raj and Kendrick 1981), Aus-

tralia (Shaw 1972), Asia (Hudson and Ingold 1960, Nawawi 1985, Marvanová and Bandoni 1987, Kirschner 2013) and Europe (Scheuer et al. 2008).

There are more than 8000 known species in the Pucciniomycotina (previously Urediniomycetes) and these comprise about one-third of all described basidiomycetes (Aime et al. 2006). Classification of the Pucciniomycotina has been reviewed and revised multiple times. Based on sequences at large and small subunits of the nuclear rDNA, Aime et al. (2006) grouped them into 8 classes. More recently, two new classes, Tritirachiomycetes (Schell et al. 2011) and Spiculogloeomycetes (Wang et al. 2015), were added to Pucciniomycotina. Amongst these 10 classes in Pucciniomycotina, one class, the Classiculomycetes, contains a single order, the Classiculales, with only two monotypic fungi, *Jaculispora* H. J. Huds. & Ingold and *Classicula* R. Bauer, Begerow, Oberw. & Marvanová. As early as 1960, *Jaculispora* was erected to accommodate a single anamorphic fungal species, *J. submerse* H. J. Huds. & Ingold. The genus is characterised by having narrow and delicate conidiophores and obclavate conidia with 0–3 hair-like lateral appendages (Hudson and Ingold 1960). Later, Naiadella Marvanova & Bandoni was established with *N. fluitans* Marvanova & Bandoni (synomy of *C. fluitans*) as the type species (Marvanová and Bandoni 1987). Bauer et al. (2003) observed the basidial stage of *N. fluitans* and connected it to the teleomorphic state *Classicula*. *Classicula* was recommended over *Naiadella* because *Classicula* is the base of the higher level taxonomy (Aime et al. 2018). The conidia of *Classicula* are similar to those of *Jaculispora* in shape. *Classicula* is characterised by the production of clamped hyphae with tremelloid haustorial cells and binucleate fusoid conidia with 3–4 bristle-like lateral branches (Marvanová and Bandoni 1987). Bauer et al. (2003) defined the phylogenetic positions of genera *Jaculispora* and *Classicula* based on the small subunit of ribosomal DNA (18S rDNA). Subsequent analyses of both the 18S and the large subunit ribosomal DNA (28S rDNA) data also supported the conclusion that the two genera are closely related and both belong to class of Classiculomycetes (Schell et al. 2011).

During a study of aquatic hyphomycetes on submerged decaying leaves collected from a stream in south-western China, we encountered two fungi which resembled species in the genus *Classicula*. Combining the morphological and phylogenetic analyses, we identified that the fungi belonged to *Classicula*. In this paper, we describe these specimens as a new species and discuss its phylogenetic placement based on the combined sequences of the 18S and 28S rDNA, the internal transcribed spacer regions of rDNA (ITS 1 and 2, including the 5.8S rDNA gene) and the translation elongation factor 1-a (TEF1).

Materials and methods

Collection of samples, isolation and characterisation

Samples of submerged dicotyledonous plant leaves collected from a stream in Chongqing Municipality were transported to the laboratory in zip-locked plastic bags. The

rotten leaves were cut to several 0.5–1.5 × 1–1.5 cm sized fragments in the laboratory and spread on to the CMA medium (20 g cornmeal, 18 g agar, 40 mg streptomycin, 30 mg ampicillin, 1000 ml distilled water). After incubation at 27 °C for about 10 days, a single conidium was isolated and cultivated on CMA in Petri plates using a sterilised toothpick under a BX51 microscope. Morphological observations were made from cultures on CMA after incubation at 27 °C for one week. Pure cultures and a permanent slide were deposited in the Herbarium of the Laboratory for Conservation and Utilization of Bio-resources, Yunnan University, Kunming, Yunnan, P.R. China (YMF; formerly Key Laboratory of Industrial Microbiology and Fermentation Technology of Yunnan). Ex-holotype living cultures were deposited in the China General Microbiological Culture Collection Center (CGMCC).

DNA extraction, PCR and sequencing

The cultures were grown on potato dextrose agar (PDA) and incubated at 27 °C for about 10 days. Fungal mycelia were harvested and transferred to a 2.0 ml Eppendorf tube. Total DNA was extracted using a CTAB method as described by Pratibha et al. (2014).

Three regions of the nuclear ribosomal DNA gene cluster and one nuclear protein-coding genes, translation elongation factor 1a (TEF1) were amplified: Primer pairs ITS4 and ITS5 (White et al. 1990) were used to amplify the complete ITS regions (including 5.8 S); NS1 and NS8 for the 18S rDNA; and LR5 and LROR for the 28S rDNA (Vilgalys and Hester 1990). Primer pairs EF1-983F and EF1-2218R were used for amplifying the TEF1 gene (Rehner and Buckley 2005). PCR amplifications were performed using the methods described previously (Wang et al. 2014). The PCR products were then sent to the Beijing Tsingke Biotechnology Co. of China, Ltd and sequenced on both strands with the same primers that were used for amplification.

Sequence alignment and phylogenetic analysis

Preliminary BLAST searches with 18S and 28S rDNA gene sequences of the new isolates indicated that they had a close phylogenetic relationship with sequences from the genera *Jaculiapora* and *Naiadella* (*Classicula*). Based on the phylogenetic positions of the two genera, we downloaded 18S, 28S, ITS and TEF1 sequences of representative species of 8 class within Pucciniomycotina, but Cryptomycocolacomycetes and Spiculogloeomycetes were not included as Cryptomycocolacomycetes only includes two known species, *Cryptomycocolax abnormis* and *Colacosiphon filiformis* and only 18S rDNA of two species are available. Spiculogloeomycetes only comprises yeast and yeast-like species, which has an affinity to Mixiomycetes within Pucciniomycotina. Based on our main aim of identifying new hyphomycetes species within Classiculomycetes, another 8 classes were chosen to carry out phylogenetic analysis. Four sequences

Table 1. The species used in the phylogenetic analyses. Also included in the Table are the representative isolate name of each species and the GenBank accession numbers for each of the four analysed gene fragments of each isolate.

Class	Species	Isolate No.	GenBank accession No.				Reference
			ITS	28S	18S	TEF	
Agaricostilbomycetes	*Bensingtonia changbaiensis*	AS 2.2310	AY233339	AY233339	AY233339	KJ707751	Wang et al. 2003; 2015
	Agaricostilbum hyphaenes	CBS 7811	AF444553	AF177406	AY665775	KJ707749	Scorzetti et al. 2002; Wang et al. 2015
	Chionosphaera apobasidialis	CBS 7430	AF444599	AF177407	U77662	KJ707883	Scorzetti et al. 2002; Wang et al. 2015
	Bensingtonia ciliata	AS 2.1945	AF444563	AF189887	D38234	KF706486	Scorzetti et al. 2002; Wang et al. 2015
	Kurtzmanomyces insolitus	JCM 10409	AF444594	AF177408	KJ708424	KJ707893	Scorzetti et al. 2002; Wang et al. 2015
	Sporobolomyces sasicola	AS 2.1933	AF444548	AF177412	AB021688	KJ707900	Scorzetti et al. 2002; Wang et al. 2015
	Mycogloea nipponica	CBS 11308	KJ778629	KJ708456	KJ708370	KJ707882	Wang et al. 2015
	Sterigmatomyces elviae	JCM 1602	AB038053	KP216512	KP216516	KJ707852	Wang et al. 2015
	Kondoa aeria	CBS 8352	AF444562	AF189901	KJ708417	KJ707905	Scorzetti et al. 2002
Cystobasidiomycetes	*Bannoa* sp.	MP 3490	DQ631900	DQ631898	DQ631899	DQ631902	Matheny et al. 2006
	Naohidea sebacea	CBS 8477	DQ911616	DQ831020	KP216515	KF706487	Wang et al. 2015
	Sporobolomyces coprosmae	JCM 8772	AF444578	AF189980	D66880	KJ707798	Scorzetti et al. 2002
	Sakaguchia dacryoidea	JCM 3795	AF444597	AF189972	D13459	KP216514	Scorzetti et al. 2002
	Sporobolomyces bischofiae	JCM 10338	AB035721	AB082572	AB035721	KJ707777	Hamamoto et al. 2002
	Rhodotorula armeniaca	JCM 8977	AF444523	AF189920	AB126644	KJ707762	Scorzetti et al. 2002; Wang et al. 2015
	Occultifur externus	JCM 10725	AF444567	AF189910	AB055193	KJ707829	Scorzetti et al. 2002; Wang et al. 2015
	Cyrenella elegans	CBS 274.82	KJ778626	KJ708454	KJ708360	KJ707830	Wang et al. 2015
	Erythrobasidium hasegawianum	AS 2.1923	AF444522	AF189899	D12803	KJ707776	Scorzetti et al. 2002; Wang et al. 2015
Pucciniomycetes	*Chrysomyxa arctostaphyli*	CFB22246	DQ200930	AY700192	AY657009	DQ435789	Matheny et al. 2007
	Endocronartium harknessii	CFB22250	DQ206982	AY700193	AY665785	DQ234567	Matthias et al. 2004
	Helicobasidium mompa	CBS 278.51	AY292429	AY254179	U77064	EF100614	Matthias et al. 2004
	Platygloea disciformis	IFO32431	DQ234556	AY629314	DQ234563	DQ056288	Matheny et al. 2007
	Puccinia graminis tritici	CRL75-36-700-3/ ECS	AF468044	AF522177	AY125409	XM_003333024	Weber et al. 2003
	Insolibasidium deformans	TDB183-1	–	AF522169	AY123292	–	Wang et al. 2015
	Septobasidium canescens	DUKE:DAH(323)	DQ241446	DQ241479	DQ241410	–	Henket al. 2007
Tritirachiomycetes	*Tritirachium oryzae*	CBS 164.67	GQ329853	KF258732	JF779647	JF779645	Schell et al. 2011
	Tritirachium sp.	CBS 473.93	JF779664	JF779649	JF779650	JF779651	Schell et al. 2011
	Tritirachium sp.	CBS 265.96	JF779668	JF779652	JF779653	-	Schell et al. 2011

Class	Species	Isolate No.	GenBank accession No.				Reference
			ITS	28S	18S	TEF	
Mixiomycetes	*Mixia osmundae*	CBS 9802	DQ831010	DQ831009	D14163	KJ707837	Matheny et al. 2006
Microbotryomycetes	*Leucosporidium scottii*	JCM 9052	AF444495	AF070419	X53499	KJ707788	Scorzetti et al. 2002; Wang et al. 2015
	Sphacelotheca hydropiperis	CBS 179.24	KJ708463	KJ708463	KJ708394	KJ707807	Wang et al. 2015
	Microbotryum biolaceum	CBS 143.21	KJ708462	KJ708462	KJ708388	KJ707811	Wang et al. 2015
	Sporobolomyces bannaensis	AS 2.2285	AY274824	AY274823	KJ708405	KJ707934	Zhao et al. 2003
	Rhodosporidium babjevae	JCM 9279	AF444542	AF070420	AB073270	KJ707874	Scorzetti et al. 2002; Wang et al. 2015
	Rhodotorula rosulata	CBS 10977	EU872492	EU872490	KJ708384	KJ707854	Wang et al. 2015
Atractiellomycetes	*Helicogloea lagerheimii*	FO 36341	–	AY512849	AY124476	–	Bauer et al. 2003
	Helicogloea variabilis	KW 1540	–	L20282	U78043	–	Berres et al. 1995
	Platygloea vestita	DB 1280	–	AY512872	AY124480	–	Bauer et al. 2003
Classiculomycetes	*Classicula fluitans*	ATCC 64713	–	AY512838	AY124478	–	Schell et al. 2011
	Classicula sinense	**YMF 1.04613**	**KY548838**	**KY548836**	**KY468515**	**MG787169**	This study
	Classicula sinense	**YMF 1.04389**	**KY548837**	**KY548835**	**KY468514**	**MG787170**	This study
	Jaculispora submersa	CCM 8127	–	AY512853	AY124477	–	Schell et al. 2014
Agaricomycotina	*Auricularia* sp.	AFTOL-ID 676	DQ200918	AY634277	DQ234542	DQ408144	Schell et al. 2014
	Coprinus comatus	AFTOL-ID 626	AY854066	AY635772	AY665772	AY881026	Schell et al. 2014

of each representative strain of 8 classes were combined with those from our own cultures. (see Table 1 for all GenBank accession numbers).

Raw sequences were aligned using CLUSTAL W 1.6 (Thompson et al. 1994); then manually adjusted to minimise the number of uninformative gaps and to improve alignments using MEGA 6.06 (Kumar et al. 2012). Ambiguously aligned regions were excluded from downstream analyses. Missing data at the 5'- and 3'-end of partial sequences were coded by a '?'. To select the most appropriate model of sequence evolution, JMODEL TEST 2.1.1 was run for each gene (ITS, TEF1, 18S, 28S) and the GTR þ I þ G model was chosen according to the Akaike information criterion (AIC). Before phylogenetic analysis, the ITS, TEF1, 18S and 28S matrices were concatenated with BIOEDIT 7.5.0.3. The tree construction procedure was performed in MrBAYES 3.2 (Ronquist et al. 2012). Maximum likelihood was performed with MEGA 6.06. *Auricularia* sp. and *Coprinus comatus* of Agaricomycotina were used as outgroups. Phylogenetic trees were imported into FIGURETREE 1.4.2 and exported as SVG vector graphics

for Figure assembly in ADOBE ILLUSTRATOR CS6. The phylogenetic analyses of different datasets were performed using Bayesian and maximum likelihood algorithms.

Results

Phylogenetic analysis

In our Bayesian and maximum likelihood analyses (Figure 1), our isolates representing the new species named *C. sinensis* was a sister group to *C. fluitans* and consistently had *J. submerse* as the next closest relative with a strong statistical support. The close relationship between *C. sinensis* and *C. fluitans* was supported with a posterior probability of 1.00 in the Bayesian analysis and with a bootstrap value of 0.93 in the maximum likelihood analysis. Phylogenetic relationships amongst the taxa inferred from the combined four gene sequences are in general agreement with those based on SSU rDNA and LSU rDNA D1/D2 domains by Wang et al. (2015). Although there are some minor variations in the relationships amongst the classes between the two studies, taxa within each class still formed a single clade.

BLAST searches using the complete ITS regions of our *C. sinensis* strains (YMF 1.04613 and YMF 1.04389) aligned them only to the 5.8S rDNA of a variety of uncultured fungus. There are a few ITS1 matches at about 87% sequence identity to specimens in Pucciniomycotina. Since the study of Classiculomycetes by Bauer et al. (2003) did not employ ITS sequences, we were unable to use ITS sequences for species confirmation with those in *Classicula*. Sequences of accession numbers AY512838 and AY512853 were those of 18S rDNA of *C. fluitans* R. Bauer, Begerow, Oberw. & Marvanová and *J. submerse*, respectively, but were mistaken for ITS by Wang et al. (2015).

Taxonomy

Classicula sinensis **Y. Huang & Z.F. Yu, sp. nov.**
MycoBank MB819813
Figure 2

Etymology. Sinensis refers to the country in which this species was found.

Diagnosis. ***Classicula sinensis*** differs from *C. fluitans* by having fusiform conidiogenous cells growing from the hyphae directly.

Type. CHINA. From leaves of an unidentified dicotyledonous plant submerged in a stream, Chongqing Municipality, Mozigou, 29°25'38"N, 107°24'19"E, ca. 750 m elev. Oct 2014, ZeFen Yu, YMF 1.04613–holotype[live culture], YMFT1.04613 [dried specimen], CGMCC–3.18938–ex-type culture. Other strain: YMF 1.04389, CGMCC–3.18937, Chongqing Municipality, Mozigou, 29°28'N, 107°25'E, ca. 750 m elev.

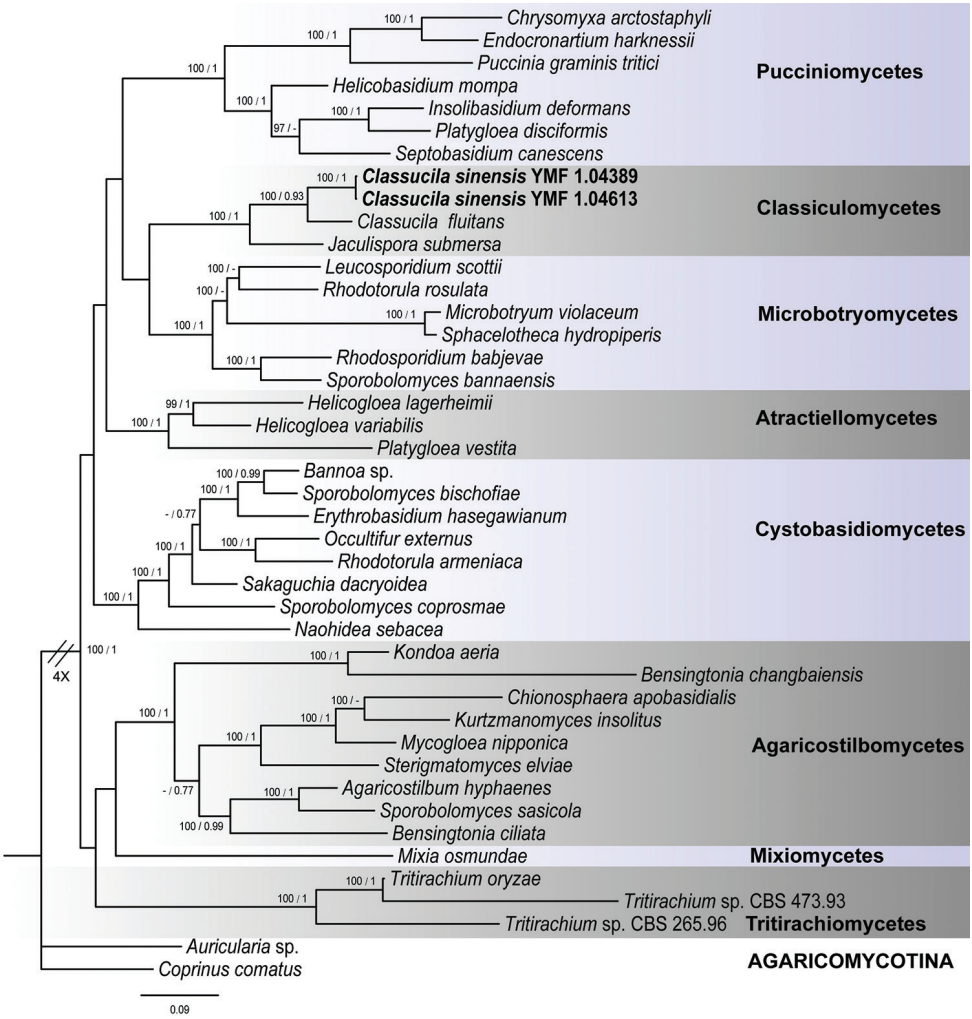

Figure 1. Phylogenetic tree based on Bayesian analysis of the combined ITS, TEF1, 18S and 28S rDNA sequences. *Auricularia* sp. and *Coprinus comatus* of Agaricomycotina are used as outgroups. Clades and taxa are labelled according to Schell et al. (2011). Bayesian posterior probabilities, greater than 0.95, are given above the nodes (out of 100). Maximum likelihood bootstrap values, greater than 75%, are given below the nodes (out of 100). The scale bar shows the expected changes per site.

Description. Colonies on CMA reach about 10 mm diameter after incubating for 7 days at 27 °C. Colony effuse, mycelium partly superficial, partly immersed in substratum, composed of hyaline, branched, thin-walled, septate, smooth, binucleated hyphae, 1.5–4.8 µm wide, often 1.8–2.7 µm wide. Clamp connection and haustorial branches on hyphae present. Haustorial branches with basal clamps, tapering distally or obclavate, 9–14.2 (–16.5) µm long, 1.2–2.6 µm wide, one or two terminal filaments of 3–8.5 × 1.3 µm located on the top of it. Conidiophores absent. Conidiogenous cells fusiform, monoblastic, 7.5–11×2–2.8 µm, attaching directly on

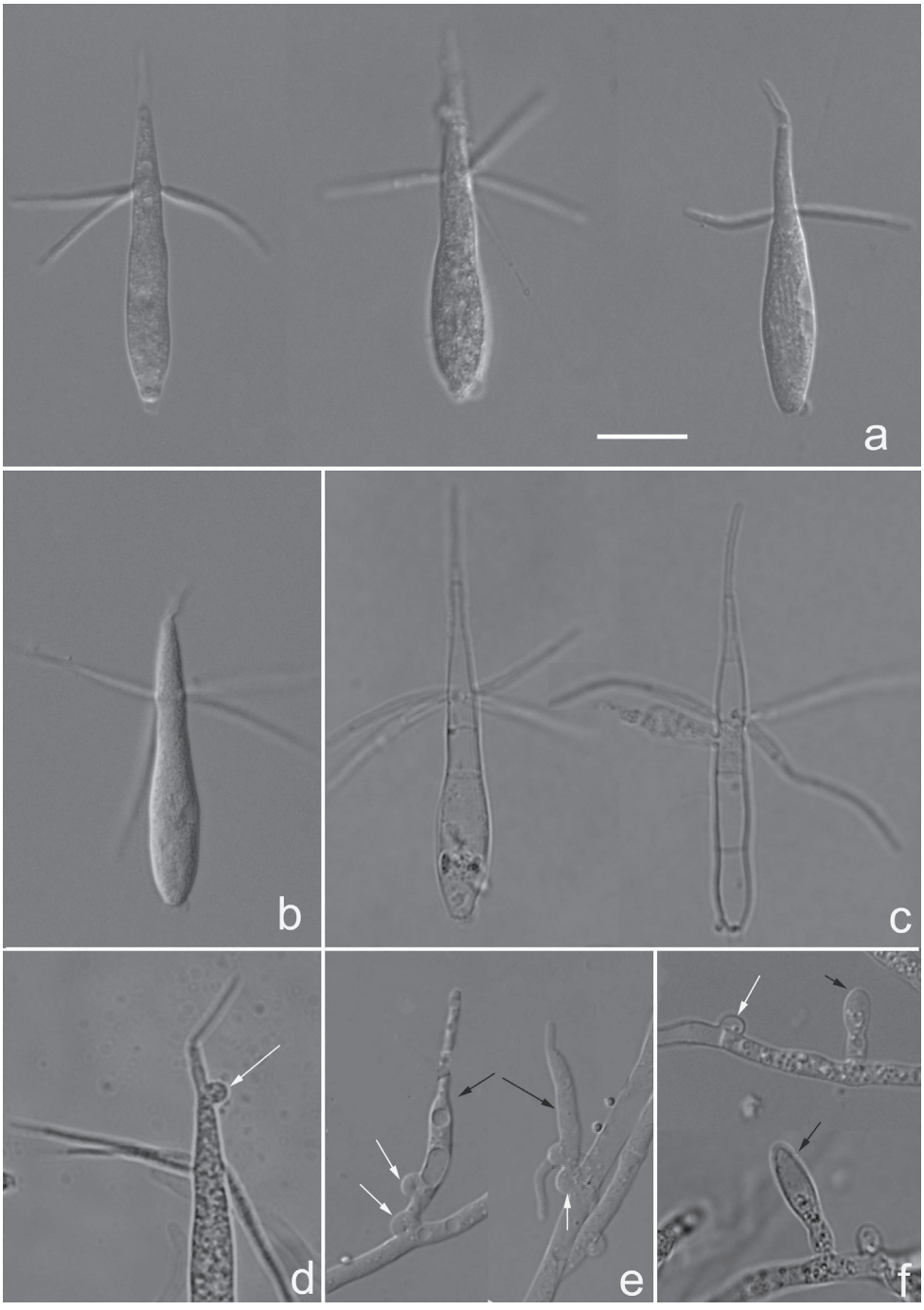

Figure 2. Microscopic features of *Classicula sinensis* (holotype YMF 1.04613). **a, b** Conidia **c** empty conidia **d** clamp connection on conidia **e** Haustorial branches with basal clamps on hyphae **f** Conidiogenous cells (black arrow) and clamp connection on hyphae (white arrow). Scale bar: 10 μm **(a–f).**

the hyphae, solitary or in aggregates of two. Conidia solitary, acrogenous, navicular or obclavate, attenuating upwards, 25–38 (–42) μm long, 3.8–6.2 μm wide, 1.3–3.4 μm wide at the truncate base, (0–) 2–5 (–7) septa appear in those conidia without cytoplasm, with 1–5 (mainly 3–4) lateral appendages, attaching to the upper part of conidia, opposite or verticillate, filiform, smooth, divergent, pendulous or straight (–7) 13–21 (–25) μm long, 0.8–1.2 μm wide, 0–2(–3) septate. Occasionally, 1(–2) appendages also arise from apex of the main axis. Sometimes clamp connections appear at the top of conidia.

Discussion

Classicula is phylogenetically related to *Jaculispora* and morphologically similar to the latter. When *Jaculispora* was established, Hudson and Ingold (1960) did not mention clamp connections or haustorial cells. Later, Matsushima (1987) observed clamps on hyphae from *J. submersa* (isolate MFC 12864), but did not see haustorial cells. Bauer et al. (2003) reported that *J. submersa* also presented tremelloid haustorial cells similar to *C. flutitans* and both species have septal-spore architecture surrounded by microbodies. Further phylogenetic analysis inferred from the 18S rDNA gene revealed that the two species belonged to the family Classiculaceae of Urediniomycetes. In fact, both *Classicula* and *Jaculispora* are very similar in having navicular conidia with 3–4 distal setose branches. However, conidiogenous cells of *Classicula* are discrete fusiform, differentiated obviously and those of *Jaculispora* are integrated. Conidiogenous cells of *C. sinensis* are also integrated, but in the analysis of concatenated dataset of four sequences, *C. sinensis* and *C. flutitans* formed a well-supported clade separated from *Jaculispora*, so we treated our strains as a member of the genus *Classicula*.

C. fluitans is similar to *C. sinensis* in having haustorial branches and obclavate or navicular conidia with hair-like lateral and apex appendages. However, their conidiophores and conidiogenous cells were totally different. First, *C. sinensis* has no conidiophore and its conidiogenous cells grow from hyphae directly, while conidiophores of *C. fluitans* are determinate, micronematous to semi-macronematous. Second, typical conidiogenous cells of *C. fluitans* are discrete fusiform formed successively, clamped basally, but *C. sinensis* has no clamps at the base of conidiogenous cells and conidiogenous cells of *C. sinensis* are integrated, which resemble that of *Jaculispora*. Besides the main differences described above, conidia of *C. fluitans* are shorter and wider [(18–)25– 32(–45) × (4–)5–6.5(–9)] than those of *C. sinensis*, lateral branches of *C. fluitans* are 2–3, while 4 lateral branches often appear in *C. sinensis*. Furthermore, coralloid structures were interpreted as appressoria in *C. fluitans* but were not observed in *C. sinensis* (Bauer et al. 2003).

C. sinensis is similar to *J. submersa* in conidia form, but conidia of the latter grow on the tip of long micronematous conidiophores, while that of *C. sinensis* grow from conidiogenous cells directly produced on hyphae. Besides, conidia of *J. submersa* are longer

than those of *C. sinensis* (type strain: 35–55 × 5–7, MFC-12864:35–56 × 4–6 μm). Septa of conidia without cytoplasm were not mentioned in the type strain of *J. submerse*. In strain MFC-12864, there is a septum obscurely presented at the attenuated part, while conidia of *C. sinensis* have 3–4 septa after cytoplasm drained out of the conidia.

A combination of morphological and molecular characters was used to establish *C. sinensis*. Conidiogenous cells of *C. sinensis* and *C. flutitans* were sufficiently different to support the molecular data and to suggest the new species. This situation has not been observed often in other fungi of the same genus, thus more isolates belonging to Classiculomycetes are needed to circumscribe genus characteristics of *Classicula* better and in more detail.

Acknowledgements

This work was financed by the National Natural Science Foundation Program of PR China (31770026, 31570023). We are grateful to two reviewers for critically reviewing the manuscript and providing helpful suggestions to improve this paper.

References

Aime MC, Matheny PB, Henk DA, Frieders EM, Nilsson RH, Piepenbring M, McLaughlin DJ, Szabo LJ, Begerow D, Sampaio JP, Bauer R (2006) An overview of the higher level classification of Pucciniomycotina based on combined analyses of nuclear large and small subunit rDNA sequences. Mycologia 98: 896–905. https://doi.org/10.1080/15572536.2006.11832619

Aime MC, Castlebury LA, Abbasi M, Begerow D, Berndt R, Kirschner R, Marvanová L, Ono Y, Padamsee M, Scholler M, Thines M, Rossman AY (2018) Competing sexual and asexual generic names in Pucciniomycotina and Ustilaginomycotina (Basidiomycota) and recommendations for use. IMA FUNGUS 9: 75–90. https://doi.org/10.5598/imafungus.2018.09.01.06

Bauer R, Begerow D, Oberwinkler F, Marvanova L (2003) *Classicula*: the teleomorph of *Naiadell afluitans*. Mycologia 95: 756–764. https://doi.org/10.1080/15572536.2004.11833077

Hudson HJ, Ingold CT (1960) Aquatic hyphomycetes from Jamaica. Transactions of the British Mycological Society 43: 469–478. https://doi.org/10.1016/S0007-1536(60)80029-0

Khan MA (1987) Interspecies interactions in aquatic hyphomycetes. The botanical magazine Tokyo 100: 295–303. https://doi.org/10.1007/BF02492836

Kumar S, Stecher G, Peterson D, Tamura K (2012) MEGA-CC: computing core of molecular evolutionary genetics analysis program for automated and iterative data analysis. Bioinformatics 28: 2685–2686. https://doi.org/10.1093/bioinformatics/bts507

Kirschner R, Okuda T (2013) A new species of *Pseudocercospora* and new record of Bartheletia paradoxa on leaves of Ginkgo biloba. Mycological Progress 12: 421–426. https://doi.org/10.1007/s11557-012-0849-3

Marvanová L (1977) *Taeniospora gracilis* gen. et sp. nov. Transactions of the British Mycological Society 69: 146–148. https://doi.org/10.1016/S0007-1536(77)80128–9

Marvanová L, Bandoni RJ (1987) *Naiadella fluitans* gen. et sp. nov.: a conidial basidiomycete. Mycologia 79: 578–586. https://doi.org/10.2307/3807598

Marvanová L, Barlocher F (1988) Hyphomycetes from Canadian streams. I. Basidiomycetous anamorphs. Mycotaxon 32: 339–351.

Marvanová L, Suberkropp K (1990) *Camptobasidium hydrophilum* and its anamorph, *Crucella subtilis*: a new heterobasidiomycete from streams. Mycologia 82: 208–217. https://doi.org/10.2307/3759849

Marvanová L, Bärlocher F (1998) Hyphomycetes from Canadian streams. III. *Arcispora bisagittaria* anam. gen. and sp. nov. Mycologia 90: 531–536. https://doi.org/10.2307/3761413

Marvanová L, Bärlocher F (2000) Hyphomycetes from Canadian streams. V. Two new conidial basidiomycetes. Mycotaxon 75: 409–423.

Matsushima T (1987) Matsushima mycological memoirs No. 5. Matsushima Fungus Collection, Kobe, Japan, 100 pp.

Nawawi A (1985) Basidiomycetes with branched, waterborne conidia. Botanical Journal of the Linnean Society 91: 51–60. https://doi.org/10.1111/j.1095-8339.1985.tb01134.x

Pratibha J, Nguyen HDT, Mel'nik VA, Bhat DJ, White GP, Seifert KA (2014) Lectotypification, epitypification, and molecular phylogeny of the synnematous hyphomycete *Pseudogliophragma indicum*, the second genus in the Wiesneriomycetaceae. Mycoscience 56: 387–395. https://doi.org/10.1016/j.myc.2014.12.002

Raj TRN, Kendrick B (1981) *Infundibura*, a new hyphomycete with unique appendages. Canadian Journal of Botany 59: 542–546. https://doi.org/10.1139/b81-076

Rehner SA, Buckley EA (2005) Beauveria phylogeny inferred from nuclear ITS and EF1-α sequences: evidence for cryptic diversification and links to *Cordyceps* teleomorp-hs. Mycologia 97(1): 84–98.

Ronquist F, Teslenko M, van der Mark P, Ayres DL, Darling A, Hohna S, Larget B, Liu L, Suchard MA, Huelsenbeck JP (2012) MrBayes 3.2: efficient Bayesian phylogenetic inference andmodel choice across a large model space. Systematic Biology 61: 539–542. https://doi.org/10.1093/sysbio/sys029

Schell WA, Lee AG, Aime MC (2011) A new lineage in Pucciniomycotina: class Tritirachiomycetes, order Tritirachiales, family Tritirachiaceae. Mycologia 103:1331–1340. https://doi.org/10.3852/10-333

Shaw DE (1972) *Ingoldiella hamata* gen. et sp. nov., a fungus with clamp connexions from a stream in north Queensland. Transactions of the British Mycological Society 59: 255–259. https://doi.org/10.1016/S0007-1536(72)80010-X

Shearer CA, Descals E, Kohlmeyer B, Kohlmeyer J, Marvanová L, Padgett D, Porter D, Raja HA, Schmit JP, Thorton HA, Voglymayr H (2007) Fungal biodiversity in aquatic habitats. Biodiversity and Conservation 16: 49–67. https://doi.org/10.1007/s10531-006-9120-z

Scheuer C, Bauer R, Lutz M, Stabentheiner E, Mel'nik VA, Grube M (2008) *Bartheletia paradoxa* is a living fossil on Ginkgo leaf litter with a unique septal structure in the Basidiomycota. Mycological Research 112: 1265–1279. https://doi.org/10.1016/j.mycres.2008.06.008

Thompson JD, Higgins DG, Gibson TJ (1994) CLUSTAL W: improving the sensitivity of progressive multiple sequence alignment through sequence weighting, position-specific gap penalties and weight matrix choice. Nucleic Acids Research 22: 4673–4680. https://doi.org/10.1093/nar/22.22.4673

Vilgalys R, Hester M (1990) Rapid genetic identification and mapping of enzymatically amplified ribosomal DNA from several Cryptococcus species. Journal of Bacteriology 172: 4238–4246. https://doi.org/10.1128/jb.172.8.4238-4246.1990

Wang QM, Groenewald M, Takashima M, Theelen B, Liu XZ (2015) Phylogeny of yeasts and related filamentous fungi within Pucciniomycotina determined from multigene sequence analyses. Studies in Mycology 81: 27–53. https://doi.org/10.1016/j.simyco.2015.08.002

Wang QM, Theelen B, Groenewald M, Bai FY, Boekhout T (2014) Moniliellomycetes and Malasseziomycetes, two new classes in Ustilaginomycotina. Persoonia: Molecular Phylogeny and Evolution of Fungi 33: 41–47. https://doi.org/10.3767/003158514X682313

White TJ, Bruns T, Lee S, Taylor J (1990) Amplification and direct sequencing of fungal ribosomal RNA genes for phylogenetics. In: Innins MA, Gelfand DH, Sninsky JJ, White TJ (Eds) PCR Protocols: a guide to methods and applications. Academic Press, San Diego, California, 315–322. https://doi.org/10.1016/B978-0-12-372180-8.50042-1

MycoKeys 40: 13–28 (2018)
doi: 10.3897/mycokeys.40.26724
http://mycokeys.pensoft.net

RESEARCH ARTICLE

A peer-reviewed open-access journal
MycoKeys
Launched to accelerate biodiversity research

Phylogenetic study and taxonomic revision of the *Xanthoparmelia mexicana* group, including the description of a new species (Parmeliaceae, Ascomycota)

Alejandrina Barcenas-Peña[1], Steven D. Leavitt[2], Jen-Pan Huang[1], Felix Grewe[1], H. Thorsten Lumbsch[1]

1 *Science & Education, The Field Museum, 1400 South Lake Shore Drive, Chicago, IL 60605-2496, USA*
2 *Department of Biology and M.L. Bean Life Science Museum, Brigham Young University, 4102 Life Science Building, Provo, UT 84602, USA*

Corresponding author: *H. Thorsten Lumbsch* (tlumbsch@fieldmuseum.org)

Academic editor: *Pradeep Divakar* | Received 16 May 2018 | Accepted 2 September 2018 | Published 18 September 2018

Citation: Barcenas-Peña A, Leavitt SD, Huang J-P, Grewe F, Lumbsch HT (2018) Phylogenetic study and taxonomic revision of the *Xanthoparmelia mexicana* group, including the description of a new species (Parmeliaceae, Ascomycota). MycoKeys 40: 13–28. https://doi.org/10.3897/mycokeys.40.26724

Abstract

Xanthoparmelia (Parmeliaceae, Ascomycota) is the most species-rich genus of lichen-forming fungi. Species boundaries are based on morphological and chemical features, varying reproductive strategies and, more recently, molecular sequence data. The isidiate *Xanthoparmelia mexicana* group is common in arid regions of North and Central America and includes a range of morphological variation and variable secondary metabolites – salazinic or stictic acids mainly. In order to better understand the evolutionary history of this group and potential taxonomic implications, a molecular phylogeny representing 58 ingroup samples was reconstructed using four loci, including ITS, mtSSU, nuLSU rDNA and MCM7. Results indicate the existence of multiple, distinct lineages phenotypically agreeing with *X. mexicana.* One of these isidiate, salazinic acid-containing lineages is described here as a new species, *X. pedregalensis* sp. nov., including populations from xerophytic scrub vegetation in Pedregal de San Angel, Mexico City. *X. mexicana* s. str. is less isidiate than *X. pedregalensis* and has salazinic and consalazinic acid, occasionally with norstictic acid; whereas *X. pedregalensis* contains salazinic and norstictic acids and an unknown substance. Samples from the Old World, morphologically agreeing with *X. mexicana,* are only distantly related to *X. mexicana* s. str. Our results indicate that *X. mexicana* is likely less common than previously assumed and ongoing taxonomic revisions are required for isidiate *Xanthoparmelia* species.

Keywords
Cryptic species, lichenised fungi, Mexico, phylogeny, taxonomy

Introduction

The family *Parmeliaceae* is the largest family of lichenised fungi (Jaklitsch et al. 2016) currently classified in approximately 70 genera with almost 2,800 species (Lumbsch and Huhndorf 2010, Divakar et al. 2017). *Xanthoparmelia*, with about 800 described species, is the largest genus of lichen-forming fungi (Lücking et al. 2016), with two centres of distribution in Australia and southern Africa; a smaller number of species occur in the Holarctic (Blanco et al. 2004, Eriksson et al. 2004, Crespo et al. 2010, Thell et al. 2012, Leavitt et al. 2018). To date, 74 species have been reported from Mexico, amongst these species, 27 are isidiate (Nash et al. 2016).

Isidiate *Xanthoparmelia* species are distributed in boreal, temperate and tropical regions. However, they commonly occur in semi-arid to arid regions worldwide especially on siliceous rocks, such as granite and sandstone. In North and Central America, *Xanthoparmelia mexicana* (Gyelnik) Hale ranks amongst the most common isidiate species. This taxon is widely distributed and has been reported from western USA, Mexico, Dominican Republic, Argentina, Kenya, Australia, New Zealand, Japan, China and Nepal (Hale 1990, Elix 1994, Nash and Elix 2004). *X. mexicana* is part of a complex of morphologically similar species, with adnate to slightly attached thalli, cylindrical isidia and a brown lower side of the thalli, which are primarily separated by their secondary metabolites. The species complex also includes *X. ajoensis* (T. H. Nash) Egan (diffractaic acid), *X. dierythra* (Hale) Hale (norstictic acid), *X. joranadia* (T. H. Nash) Hale (lecanoric acid), *X. maricopensis* T. H. Nash & Elix (norstictic and hyposalazinic acids), *X. moctezumensis* T. H. Nash (3-α-hydroxybarbatic acid), *X. plittii* (Gyelnik) Hale (stictic acid), *X. schmidtii* Hale (barbatic, norstictic and salazinic acids), *X. subramigera* (Gyelnik) Hale (fumarprotocetraric acid) and *X. weberi* (Hale) Hale (hypoprotocetraric acid) (Hale 1990, Nash et al. 2016). However, previous studies indicate that current interpretations of morphological features and secondary metabolites likely fail to accurately characterise species-level diversity in isidiate *Xanthoparmelia* species (Leavitt et al. 2011, 2013).

To better understand the evolutionary history of the *Xanthoparmelia mexicana* complex and potential taxonomic implications, isidiate *Xanthoparmelia* specimens were collected from different locations throughout arid regions of Mexico and supplemented with previously available sequence data. The new samples came from xerophytic scrublands in the states Puebla, Oaxaca, San Luis Potosí, Querétaro, Estado de México, Mexico City, Guanajuato, Zacatecas and Hidalgo, all in the central part of Mexico. We focused on sampling *Xanthoparmelia* populations that were phenotypically similar to *X. mexicana*, e.g. isidiate specimens containing salazinic acid. *X. mexicana* was originally described by Gyelnik (1931) as *Parmelia mexicana* and was later combined into *Xanthoparmelia* by Hale (1974). The type specimen was collected from San Jerónimo,

in Pedregal de San Angel, Mexico City. The syntype in the Bouly de Lesdain herbarium was destroyed during World War II, whereas the lectotype in the Budapest herbarium (BP) was not available for molecular study. Therefore, we attempted to recollect material at the type locality of *X. mexicana* and other regions throughout Mexico. Based on the results of this study, we formally describe a previously unrecognised species-level lineage comprised of isidiate specimens as new to science.

Material and methods

Taxon sampling

Specimens were studied from the herbaria ASU, BRY, F, MAF and new collections from different localities throughout arid regions from the central part of Mexico (Table 1, Fig. 1). A total of 83 specimens, representing 43 species were included, with an emphasis on isidiate species/populations from Central and North America (all epithets are validly published, with the exception of *X. isidiomontana nom prov* assigned to the clade 'D2' from Leavitt et al. 2013). New sequences were generated from 25 specimens and supplemented with 34 sequences from a previous analysis (Leavitt et al. 2018) and 24 additional sequences from GenBank (Table 1). Four species in the genus *Xanthoparmelia* that have previously been shown to be distantly related to *X. mexicana* were used as outgroup – *X. beatricea*, *X. austroafricana*, *X. subramigera* and *X.* aff. *subramigera* (Leavitt et al. 2018).

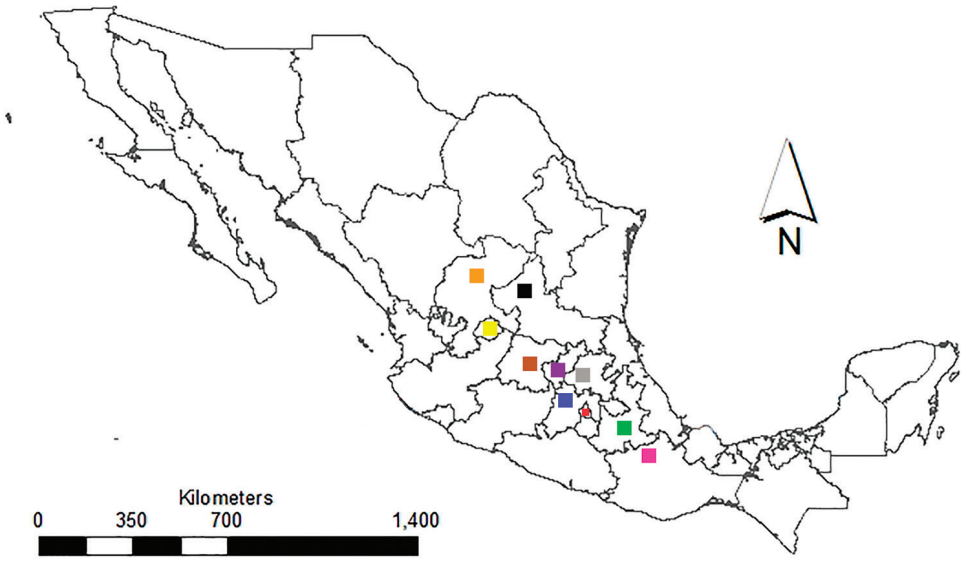

Figure 1. Location of new *Xanthoparmelia* recollection sites from arid regions from central part of Mexico. Oaxaca (pink), Puebla (green), Mexico City (red), Estado de México (blue), Querétaro (purple), Guanajuato (brown), Hidalgo (grey), Aguas Calientes (yellow), San Luis Potosí (black), Zacatecas (orange).

Table 1. Collection information for specimens included in the present study: Species, morphological/chemical species identification; DNA code, individual code associated with specimen label in multiple sequence alignments; Species distribution; Voucher information; and GenBank accession numbers for sampled loci in bold text indicates new sequences generated for this study. Specimens sequenced using Illumina technology are indicated by a • with the associated DNA code.

Species	DNA code	Voucher	ITS	MCM7	mtSSU	nuLSU
X. aff. chlorochroa	082f	USA: Utah; Leavitt et al. 55225 (BRY-C)	MG695498	MG695699	MG695746	MG695599
X. aff. chlorochroa	9866	USA: Nevada; Leavitt & St. Clair 9866 (BRY-C)	MG695499	MG695700	MG695747	MG695600
X. aff. coloradoensis	135f	USA: Utah; Leavitt et al. 55255 (BRY-C)	MG695500	MG695701	MG695748	MG695601
X. aff. protomatrae	GenBank	Spain: Zamora; Blanco & Crespo 6216 (MAF-Lich)	AY581104	–	AY582339	AY578972
X. aff. subramigera	9664	Kenya: Coast, Kirika & Lumbsch 4117 (F)	MG695515	–	MG695764	MG695616
X. ajoensis•	14908	Mexico: Puebla; Barcenas-Peña 5898 (F)	MH580218	MH686124	MH699893	MH699913
X. ajoensis•	14920	Mexico: Puebla; Barcenas-Peña 5900 (F)	MH580219	MH686125	MH699894	MH699914
X. ajoensis•	14934	Mexico: Puebla; Barcenas-Peña 5914 (F)	MH580220	MH580220	MH699895	MH699915
X. angustiphylla	GenBank	USA: Blanco et al. 6768 (MAF)	AY581092	–	AY582328	–
X. atticoides	GenBank	USA: Blanco et al. 6744 (MAF)	AY581066	–	AY582302	AY578929
X. austroafricana	9549	Kenya: Coast Prov., Kirika 4485 (F)	MG695542	–	–	MG695644
X. beatricea	E467	Kenya: E467 (MAF-Lich 17174)	JQ912367	–	MG695793	JQ912462
X. camtschadalis 1	GenBank	USA: Leavitt et al. 55174 (BRY-C)	HM578630	–	–	HM579042
X. camtschadalis 2	GenBank	USA: Leavitt et al. 55291 (BRY-C)	HM578744	–	–	HM579156
X. cf. mexicana	016m	Pakistan: Tattu; Kahlid, Usman & Khan MKF16 (LAH)	MH580221	–	–	–
X. cf. mexicana	016m2	Pakistan: Swat Valley; Khan & Khalid SW-16 (LAH)	MH580222	–	–	–
X. chlorochroa	536f	USA: North Dakota; G. Lind 1213 (BRY-C)	HM578887	HM579688	KR995372	HM579298
X. conspersa	GenBank	Spain: Zamora, Blanco & Crespo s.n. (MAF-Lich 6793)	AY581096	–	AF351186	AY578962
X. cordillerana	E422	Chile: E422 (MAF-Lich 17198)	JQ912358	–	MG695797	JQ912453
X. coreana 1	GenBank	South Korea: Hur, J.-S. 005561	KJ170890	–	–	KJ170890
X. coreana 2	GenBank	South Korea: Hur, J.-S. 005589	KJ170883	–	–	KJ170883
X. coreana 3	GenBank	South Korea: Hur, J.-S. 013905	KJ170873	–	–	KJ170873
X. cumberlandia	nybg02	USA: Maine; R. Harris 55563 (NY)	MG695545	–	MG695798	MG695646
X. dierythra	226f	USA: Leavitt et al. 55300 (BRY-C)	HM578753	HM579569	–	HM579165
X. dierythra	439f	USA: Leavitt et al. 55383 (BRY-C)	HM578833	–	–	HM579245
X. dierythra	098f	Mexico: Puebla; Leavitt et al. 55234 (BRY-C)	HM578689	HM579504	–	HM579099
X. hirolsakiensis	GenBank	South Korea: Hur, J.-S. 010532	KJ170876	–	–	KJ170876

Species	DNA code	Voucher	ITS	MCM7	mtSSU	nuLSU
X. hypofusca	8837	USA: West Virginia; Streets (02086946 NY)	MG695550	MG695717	MG695803	MG695651
X. idahoensis 1	GenBank	USA: Leavitt et al. 55463 (BRY-C)	HM578915	HM579708	–	HM579323
X. idahoensis 2	GenBank	USA: Leavitt et al. 55354 (BRY-C)	HM578805	HM579620	–	HM579216
X. infrapallida	9904	USA: Arizona; Leavitt 9904 (BRY-C)	MG695555	MG695720	MG695809	MG695656
X. isidiovagans	GenBank	Spain: 9956 (MAF-Lich)	AY581094	JX974718	AY582330	AY578960
X. lavicola	GenBank	USA: Leavitt et al. 55230 (BRY-C)	HM578685	HM579500	–	–
X. lavicola	15489	Mexico: Morelos; Nash III 46261 (WIS)	MH580227	MH686131	–	MH699920
X. lavicola•	14894	Mexico: Puebla; Barcenas-Peña 5857 (F)	MH580223	MH686127	MH699896	MH699916
X. lavicola•	14905	Mexico: Puebla; Barcenas-Peña 5884 (F)	MH580224	MH686128	MH699897	MH699917
X. lavicola•	14906	Mexico: Oaxaca; Barcenas-Peña 5905 (F)	MH580225	MH686129	MH699898	MH699918
X. lavicola•	14910	Mexico: Puebla; Barcenas-Peña 5888 (F)	MH580226	MH686130	MH699899	MH699919
X. lineola	245f	USA: Arizona; EA collection 31–259 (55306 BRY-C)	MG695556	MG695721	MG695810	MG695657
X. maricopensis	6698	USA: Arizona; J. Leavitt 001 (BRY-C)	MG695558	MG695723	MG695812	MG695659
X. mexicana	291f	USA: Leavitt et al. 55328 (BRY-C)	HM578780	HM579596	–	HM579192
X. mexicana	786f	USA: Leavitt et al. 55462 (BRY-C)	HM578914	HM579707	–	HM579322
X. mexicana	097f	Mexico: Leavitt et al. 55233 (BRY-C)	HM578688	HM579503	-	HM579098
X. mexicana	GenBank	South Korea: Jang et al. 005486 (KoLRI)	KM250123	–	–	–
X. mexicana	15479	Mexico: San Luis Potosí; Barcenas-Peña 7316 (F)	MH580231	MH686135	MH699904	MH699923
X. mexicana	15472	Mexico: San Luis Potosí; Barcenas-Peña 7408 (F)	MH580229	MH699932	–	MH699922
X. mexicana	15466	Mexico: San Luis Potosí; Barcenas-Peña 7441 (F)	MH686404	MH686133	MH699902	–
X. mexicana	15461	Mexico: Querétaro; Barcenas-Peña 7178 (F)	MH686401	MH699930	MH699901	–
X. mexicana	15485	Mexico: Querétaro; Barcenas-Peña 7209 (MEXU)	MH686402	MH686136	MH699905	–
X. mexicana	15471	Mexico: San Luis Potosí; Barcenas-Peña 7273 (F)	MH686403	MH699931	MH699903	–
X. mexicana	15473	Mexico: Hidalgo; Nash III 45126 (WIS)	MH580230	MH686134	–	–
X. mexicana	156f	USA: Leavitt et al. 55267 (BRY-C)	HM578721	HM579536	–	HM579132
X. mexicana	15487	Mexico: Hidalgo; Barcenas-Peña 7470 (F)	MH580232	MH686137	MH699906	–
X. mexicana•	14899	Mexico: Oaxaca; Barcenas-Peña 5918 (F)	MH580228	MH686132	MH699900	MH699921
X. moctezumensis•	14897	Mexico: Puebla; Barcenas-Peña 5891(F)	MH580233	MH686138	MH699907	MH699924

Species	DNA code	Voucher	ITS	MCM7	mtSSU	nuLSU
X. norchlorochoroa 1	GenBank	USA: Leavitt et al. 55157 (BRY-C)	HM578613	HM579432	–	HM579025
X. norchlorochoroa 2	GenBank	USA: Leavitt et al. 55447 (BRY-C)	HM578899	HM579693	–	HM579307
X. orientalis	GenBank	South Korea: Hur, J.-S. 005613	KJ170884	–	–	KJ170884
X. pedregalensis	527	Mexico: Mexico City; Ruiz-Cazares 1552 (F)	MH580238	MH707353	MH699912	MH699929
X. pedregalensis	526	Mexico: Mexico City; Ruiz-Cazares 1553 (MEXU)	MH580234	MH707352	MH699908	MH699925
X. pedregalensis	533	Mexico: Mexico City; Ruiz-Cazares 1557 (F)	MH580236	–	MH699910	MH699927
X. pedregalensis	529	Mexico: Mexico City; Ruiz-Cazares 1555 (F)	MH580235	MH686139	MH699909	MH699926
X. pedregalensis	531	Mexico: Mexico City; Ruiz-Cazares 1559 (MEXU)	MH580237	MH707354	MH699911	MH699928
X. plittii	498f	USA: North Carolina; Leavitt et al. (55422 BRY-C)	MG695562	MG695727	–	MG695664
X. psoromifera 1	GenBank	USA: Leavitt et al. 55314 (BRY-C)	HM578766	HM579582	–	HM579178
X. psoromifera 2	GenBank	USA: Leavitt et al. 55313 (BRY-C)	HM578765	HM579581	–	HM579177
X. pulvinaris	GenBank	Hungary: Molnar et al. 93943 (BP)	JQ362484	–	JQ362485	JQ362486
X. isidiomontana nom. prov.	292f	USA: Nevada; Leavitt (55329 BRY-C)	MG695579	MG695733	MG695834	MG695679
X. isidiomontana nom. prov.	E1010	Spain: E1010 (MAF-Lich 17181)	JQ912354	–	MG695835	JQ912451
X. isidiomontana nom. prov.	E984	USA: E984 (MAF-Lich 17199)	JQ912386	–	MG695836	JQ912479
X. stenophylla	5040	Kazakhstan: Karkaralinsk; Tshernyshev (BRY-C)	MG695583	MG695737	MG695843	MG695683
X. stenophylla	E708	Turkey: E708 (MAF-Lich 17196)	JQ912372	–	MG695844	JQ912467
X. subcumberlandia	121f	USA: Utah; Leavitt et al. (55242 BRY-C)	MG695584	MG695738	MG695845	MG695684
X. subdifluens 1	GenBank	Spain: de Paz et al. 17178 (MAF-Lich)	JQ912381	–	–	JQ912474
X. subdifluens 2	GenBank	Spain: Blanco et al. 9910 (MAF)	AY581105	–	AY582340	AY578973
X. sublaevis	GenBank	Spain: Tenerife, Canary Islands; Blanco et al. 7460 (MAF)	AY581106	–	AY582341	AY578974
X. subramigera	9668	Kenya: Coast, Kirika 4583 (F)	MG695525	MG695709	MG695774	MG695626
X. tuberculiformis	GenBank	South Korea: Jang et al. 012058 (KoLRI)	KM250131	–	–	KM250131
X. vicentei	GenBank	Spain: Salamanca; Crespo & Molina (7248 MAF-Lich)	AY581112	–	AY582347	AY578980
*X. viriduloumbrina*1	GenBank	USA: Pennsylvania; Lendemer 13314: 1049917 (NY)	HM066945	–	–	–
X. viriduloumbrina 2	GenBank	USA: Pennsylvania; Lendemer 13325: 1049906 (NY)	HM066944	–	–	–
X. wyomingica	001f	USA: Utah; Leavitt et al. (55151 BRY-C)	MG695598	MG695745	MG695864	MG695698
X. wyomingica	826f	USA: Wyoming; Leavitt 826 (55501 BRY-C)	HM578953	HM579746	–	HM579360

Morphology and chemistry

Morphological characters were observed using a Zeiss Stemi 2000-C stereoscope. Ascomatal anatomy, ascospore in addition to conidia shape and size were observed using a Zeiss Axioscope. Secondary metabolites were identified using spot test KOH 10%, KC, C, PD and high-performance thin layer chromatography (HPTLC), using solvent systems C following established methods (Culberson and Johnson 1982, Arup et al. 1993, Lumbsch 2002, Orange et al. 2010).

Molecular methods

Total genomic DNA was extracted from thallus fragments following the manufacturers' instructions using the ZR Fungal/Bacterial DNA Miniprep Kit (Zymo Research Corp., Irvine, CA). DNA sequences were generated for four markers using polymerase chain reaction (PCR): the nuclear ribosomal internal transcribed spacer region (ITS), a fragment of nuclear large subunit rDNA (nuLSU), the nuclear protein-coding marker minichromosome maintenance complex component 7 (*MCM7*) and a fragment of the mitochondrial small subunit rDNA (mtSSU). PCR reactions contained 6.25 ml of MyTaq Mix, 25 ml H_2O, 0.25 ml forward and reverse primer and 0.5 ml template DNA, for a total reaction volume of 12.5 ml. The ITS region was amplified using primers ITS1F (Gardes and Bruns 1993) and ITS4 (White et al. 1990); *MCM7* using primers MCM7-709f and Mcm7-1348r (Schmitt et al. 2009), mtSSU using primers mrSSU1 and mrSSU3R (Zoller et al. 1999) and nuLSU rDNA using primers AL2R (Mangold et al. 2008) and LR6 (Vilgalys and Hester 1990). PCR products were sequenced using an ABI PRISM 3730 DNA Analyser (Applied Biosystems) at the Pritzker Laboratory for Molecular Systematics and Evolution at The Field Museum, Chicago, Illinois, USA. Nine specimens were obtained previously for a global phylogenetic study of the genus and sequenced using next generation sequencing technology as described in Leavitt et al. (2018) (Table 1). In short, metagenomic Nextera libraries (prepared from total DNA extraction) were sequenced on the Nextseq platform at the Core Genomics Facility at the University of Illinois at Chicago, USA. Illumina reads of each specimen were mapped to reference marker sequences downloaded from Genbank (ITS AY581063, nuLSU HM125760, MCM7 HM579689, mtSSU KR995373) using the mapping feature implemented in Geneious v11.0.3 (http://www.geneious.com, Kearse et al. 2012). The consensus sequence of each locus was extracted and added to the data set of Sanger sequences to build a combined alignment.

Sequence alignment and phylogenetic analysis

Sanger sequences, consensus Illumina reads and sequences available on GenBank were added to an alignment published in Leavitt et al. (2018) using Mafft v7 with the option

'add sequence' (Table 1). ITS, MCM7, mtSSU and nuLSU sequences were aligned independently using the 'automatic' option in Mafft v7, with the remaining parameters set to default values. Ambiguous positions of each one-locus alignment were removed using options for a "less stringent" selection on Gblocks 0.91b (Castresana 2000). SequenceMatrix software (Vaidya et al. 2011) was used for the alignment concatenation. Phylogenetic analyses were performed using Maximum Likelihood (ML) and Bayesian Analysis (BA). ML trees were calculated with RAxML-HPC2 on XSEDE 8.2.10 (Stamatakis 2014) on the Cipres Science Gateway (Miller et al. 2010) using GTR+G+I substitution model with 1000 bootstrap pseudoreplicates. For the BA, substitution models for each locus were estimated using jModelTest-2.1.9 (Guindon and Gascuel 2003, Darriba et al. 2012): in ITS the TIM2ef+I+G, in MCM7 the K80+G, in mtSSU the TPM2uf+I and in nuLSU the TrN+I were used. Two parallel Markov chain Monte Carlo (MCMC) runs were performed in MrBayes 3.2.6 (Huelsenbeck and Ronquist 2001, Ronquist and Huelsenbeck 2003), each using 10,000,000 generations which were sampled every 100 steps. A 50% majority rule consensus tree was generated from the combined sampled trees of both runs after discarding the first 25% as burn-in. Tree files were visualised with FigTree 1.4.2 (Rambaut 2014). The ITS, MCM7, mtSSU and nuLSU sequences are deposited in GenBank (Table 1).

Results and Discussion

Phylogeny

Results from phylogenetic analyses presented here clearly indicate that the taxonomy in the *Xanthoparmelia mexicana* group requires revision because different samples assigned to the same species based on phenotypical characters may not form a monophyletic group. Specimens identified as *X. mexicana* from Asia (Pakistan and South Korea) were distantly related to samples of the species collected in North America and Europe (included in *X. isidiomontana nom prov*) (Fig. 2). The latter specimens fell into three distinct and well supported clades (clade I-III in Fig. 2). Note that the three distinct and well supported clades did not form a monophyletic group.

Clade 'I' (=*X.* '*isidiomontana*' *nom prov*, 'D2' in Leavitt et al. 2013) included isidiate specimens from North America and Europe and samples identified as *X. dierythra*, *X. mexicana* (Figs. 2A and B) and *X. plittii*, in addition to a number of non-isidiate, fertile specimens. Additional studies will be necessary to better understand the delimitation of *X. dierythra*, which is also polyphyletic and is currently accommodating specimens with norstictic acid and lacking salazinic acid (Hale 1990). This clade likely represents another species-level lineage lacking formal taxonomic recognition and a formal description of this lineage will be proposed once the phylogenetic placement of *X. dierythra* s. str. is ascertained.

Clade 'II' included specimens collected in the Pedregal, south of Mexico City, which is also the type locality of *X. mexicana*. However, the new material does not correspond phenotypically with the type specimen of *X. mexicana* in BP (Fig. 2G). These specimens

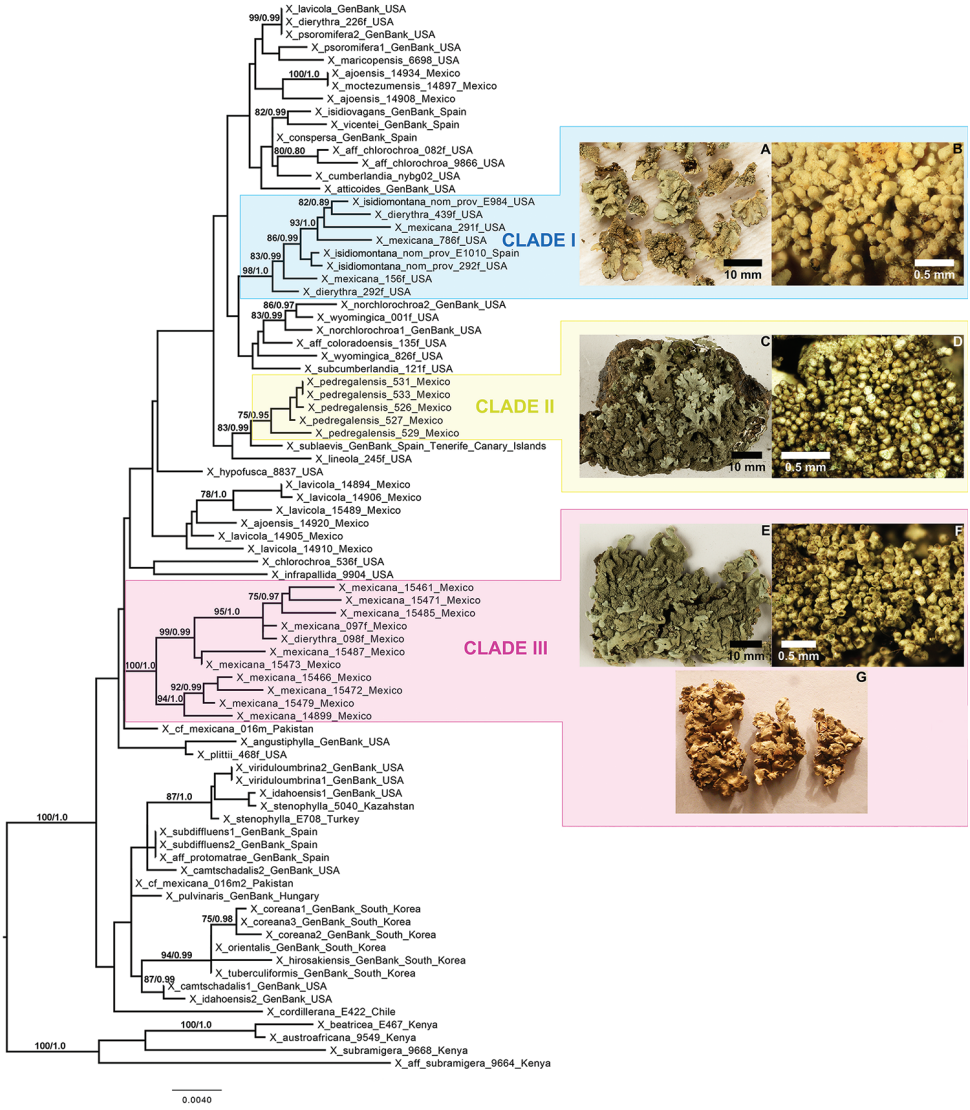

Figure 2. Phylogenetic relationships of the *Xanthoparmelia mexicana* group based on a concatenated data set of ITS, mtSSU, nuLSU and MCM7. Topology based on maximum likelihood (ML) analyses. Bootstrap values above 75 and 0.95 posterior probability are indicated on each branch. The clades I, II and III are highlighted in blue, yellow and pink, respectively. Selected specimens representing clades (habit and isidia): I, *X. mexicana* s. lat. (**A, B**); II, X. *pedregalensis* (**C, D**) and III, *X. mexicana* s. str. (**E, F**), a picture of the *X. mexicana* type specimen from BP is included (**G**).

are different from *X. mexicana* specimens (represented by Clade III in phylogenetic analysis) in having less contiguous lobes, densely isidiate thallus, presence of salazinic acid, norstictic acid and an unknown substance. Since clade 'II' differs phylogenetically and phenotypically from clade 'III' (representing *X. mexicana* s. str. – see below), we describe clade 'II' as a species new to science, *X. pedregalensis* (Figs. 2C and D).

Clade 'III' includes the majority of samples identified as *X. mexicana* collected in different localities of Mexico (Oaxaca, Puebla, San Luis Potosí, Querétaro, Hidalgo). Specimens recovered in this clade were morphologically and chemically similar to the lectotype of *X. mexicana* in BP (Fig. 2G). Therefore, clade 'III' is here recognised as *X. mexicana* s. str. (Gyelnik 1931, Hale 1974) (Figs. 2E and F). So far, we have only been able to confirm the presence of *X. mexicana* s.str. in Mexico. Specimens collected in other areas and previously identified as *X. mexicana* likely represent different species. For example, none of the samples from Asia or those reported in Leavitt et al. (2013) from western United States belongs to *X. mexicana* s. str. Further studies are needed to evaluate the occurrence of this species in other parts of the world, including North America and Europe.

Underestimates of species diversity is common amongst under-studied organismal groups (Pawar 2003, Chiarucci et al. 2011, Lücking 2012, Coleman 2015, Troia and McManamay 2016, Troudet et al. 2017), which is particularly evident in lichenised fungi (Crespo and Perez-Ortega 2009, Crespo and Lumbsch 2010, Leavitt et al. 2011, Lumbsch and Leavitt 2011, Leavitt et al. 2013, Leavitt et al. 2016, Lücking et al. 2016, Leavitt et al. 2018). Previous studies concluded that the species delimitation in lichenised ascomycetes with traditional morphological and chemical characters are apparently misleading with respect to species diversity. In the study of Leavitt et al. (2016), several new taxa were described primarily based on evidence from genetic data, but it does not preclude the possibility that additional studies investigating morphological and chemical characters may identify additional independent characters or combinations of characters, supporting the species circumscribed using molecular data. Our results corroborate findings from the previous studies by showing the need of an integrative approach using not only conventional (i.e. morphology and TLC data), but also new sets of data (e.g. DNA sequence data) to better understand the pattern of species diversity. Our study shows that, by incorporating molecular data, the taxonomic status of a conventionally difficult group based on morphology can be resolved: the three main clades belonging to the *X. mexicana* complex do not form a monophyletic group based on our newly reconstructed phylogeny (Fig. 1). In this context, the species diversity in the *X. mexicana* complex is likely under-estimated and morphologically cryptic species may be identified in the future.

Taxonomy

Xanthoparmelia pedregalensis **Barcenas-Peña, Lumbsch & Leavitt, sp. nov.**
Mycobank: MB826958
Figs. 2C and D

Type. MEXICO. Ciudad de México: Coyoacán, Pedregal de San Angel, 19°19'8.3"N, 99°11'25.93"W, 2321 m elev., xerophytic scrub, on rocks, November, 2017, Ruiz Cazares 1553 (MEXU-holotype), same locality and date Ruiz Cazares 1559 (MEXU-paratype).

Diagnosis. Thallus moderately adnate to adnate, imbricate, upper surface yellow-green, lower surface tan-brown, abundant isidia subglobose to cylindrical, simple to branched and medulla containing salazinic and norstictic acids as major compounds and an unknown substance. Differing from the phenotypically similar *X. mexicana* by nucleotide position characters in the ITS sequence as shown in Table 2.

Etymology. The taxon name is based on its occurrence in the Pedregal de San Angel region of Mexico.

Description. Thallus foliose, moderately adnate to adnate, 2–7 cm in diam., irregularly lobate; lobes subirregular, elongate, plane to subconvex, 1.5–3 mm wide, not lobulate; apices subrotund, smooth, eciliate. Upper surface yellow-green, smooth, shiny, epruinose and emaculate, densely isidiate; isidia initially subglobose, becoming cylindrical to coralloid branched with age, 0.1–0.2 mm in diam., 0.1–0.9 mm tall; tips syncorticate, brown to dark brown, sometimes weakly erumpent; soralia and pustulae absent. Medulla white, with continuous algal layer. Lower surface tan to brown, plane, moderately rhizinate; rhizines pale to dark brown, simple, 0.5–0.9 mm long. Apothecia rare, sessile, 1–2 mm wide, laminal on thallus; disc cinnamon-brown to dark brown; margin smooth, pruina absent; asci: clavate, 8-spored; ascospores hyaline, simple, ellipsoid, 9–10 × 4–5 µm. Pycnidia rare, immersed conidia bifusiform, 5–7 × 1 µm.

Secondary metabolites. Upper cortex K–, C–, KC–, P–; medulla K+ yellow then dark red, KC–, C–, P+ yellow-orange. Upper cortex with usnic acid (major); medulla with salazinic (major) and norstictic acids (submajor) and an unknown substance (minor) (Rf 28–30, brown in daylight after heating, UV brown-dark, yellow halo after heating).

Distribution and ecology. The new species was found in xerophytic scrub vegetation, in Pedregal de San Angel south of Mexico City, growing on volcanic rocks. It is currently known only from the type locality.

Notes. *Xanthoparmelia pedregalensis* is morphological and chemically similar to *X. mexicana.* However, the latter has more contiguous lobes and is less isidiate than *X. pedregalensis*. In addition *X. mexicana* has salazinic (major) and consalazinic acid (minor) and usually norstictic and protocetraric acids (trace) in the medulla, whereas *X. pedregalensis* contains salazinic (major) and norstictic acids (submajor) and an unknown substance. Distinguishing the two species is supported by molecular data.

Additional specimens examined. Mexico. Ciudad de México: Coyoacán, Pedregal de San Angel, 19°19'8.3"N, 99°11'25.93"W, 2321 m elev., xerophytic scrub, on rocks, November, 2017, Ruiz Cazares 1552 (MEXU); 19°19'15.19"N, 99°11'15.22"W, 2311 m, Ruiz Cazares 1555, 1557 (F).

Table 2. Differences of nucleotide positions in the ITS marker between *X. mexicana* and *X. pedregalensis*.

Species	Aligned nucleotide position characters in the ITS marker							
	36	**115**	**379**	**425**	**450**	**466**	**488**	**496**
X. mexicana	G	C	A	C	T	C/T	G	A
X. pedregalensis	A	T	G	G	C	A	C	G

New state records

***Xanthoparmelia ajoensis* (Nash) Egan, 1975: 217.**

Parmelia ajoensis Nash, 1974: 234. [Type collection: Organ Pipe Cactus National Monument, Pima Co., Arizona, USA, Nash 5999 (ASU, holotype; DUKE, US, isotypes).] New to Oaxaca, *X. ajoensis* is distributed across western USA and Mexico where it has previously been reported from Baja California Sur, Durango, Morelos, Puebla, Sinaloa and Sonora on acidic rocks, often in open, arid habitats at relatively low elevations (Hale 1990, Nash and Elix 2004, Nash et al. 2016).

Specimens Examined: Mexico. Oaxaca: Quiotepec, 17°54'18.9"N, 96°58'01.8"W, 696 m elev., xerophytic scrub, on rock, October, 2016, Barcenas-Peña 5906, 5908, 5913, 5915 (MEXU).

***Xanthoparmelia moctezumensis* Nash in C. Culberson, Nash & Johnson, 1979: 155. [Type collection: 28 km E of Moctezuma, Sonora, Mexico, Nash 12548 (ASU, holotype; DUKE, US, isotypes).]**

New to Puebla. *Xanthoparmelia moctezumensis* is distributed throughout south-western USA and Mexico where it has been reported from Baja California Sur, Durango, Sinaloa and Sonora on acidic rocks, often in open, arid to woodland habitats (Nash and Elix 2004, Nash et al. 2016).

Specimens Examined: Mexico. Puebla: San Rafael Coxcatlán, 18°13'16.6"N, 97°07'22.4"W, 1148 m elev., xerophytic scrub, on rock, October, 2016, Barcenas-Peña 5887, 5890, 5891, 5893 (MEXU).

***Xanthoparmelia mexicana* (Gyelnik) Hale, 1974: 488.**

New to Querétaro, San Luis Potosí and Zacatecas. *Xanthoparmelia mexicana* has been reported from Baja California, Baja California Sur, Chihuahua, Coahuila, Distrito Federal, Durango, Guanajuato, Hidalgo, Jalisco, Michoacán, Nuevo León, Oaxaca, Puebla, Sonora and Veracruz, on acidic rocks, often on soil near the coast in open, arid habitats (Nash et al. 2004, 2016).

Specimens Examined: Mexico: Querétaro. Tequisquiapan, Rancho Las Fuentes, 20°33'51.0"N, 100°01'54.6"W W, 1942 m elev., xerophytic scrub, on rock, August, 2017, Barcenas-Peña 7516; San Luis Potosí, Mexquitic de Carmona, La Campana, 22°15'28.9"N, 101°05'26.8"W, 2012 m elev., xerophytic scrub, on rock, August, 2017, Barcenas-Peña 7441; Zacatecas, Fresnillo, El Poleo, 23°06'16.4"N, 102°54'24.3"W, 2227 m elev., xerophytic scrub, on rock, August, 2017, Barcenas-Peña 7356 (all MEXU).

Acknowledgements

The first author thanks the National Council of Science and Technology (CONACYT) by grants for supporting her research stay to the Field Museum. We are grateful to Dr. Tom Nash III, Biol. Alin Ruiz and José Vladimir Rodríguez for sending us the specimens. We are grateful to Dr. Armando Burgos and Biol. Maricarmen Altamirano for their assistance in the field work. We are grateful to Dra. Silke Cram for logistical support at Reserva Ecológica del Pedregal de San Angel. The authors are thankful to the Pritzker Laboratory for Molecular Systematics at the Field Museum. We thank to Negaunee Foundation for financial support.

References

Arup U, Ekman S, Lindblom L, Mattsson J-E (1993) High performance thin layer chromatography (HPTLC), an improved technique for screening lichen substances. Lichenologist 25: 61–71. https://doi.org/10.1006/lich.1993.1018

Blanco O, Crespo A, Elix JA, Hawksworth DL, Lumbsch HT (2004) A molecular phylogeny and a new classification of parmelioid lichens containing *Xanthoparmelia*-type lichenan (Ascomycota: Lecanorales). Taxon 53: 959–975. https://doi.org/10.2307/4135563

Castresana J (2000) Selection of Conserved Blocks from Multiple Alignments for Their Use in Phylogenetic Analysis. Molecular Biology and Evolution 17: 540–552. https://doi.org/10.1093/oxfordjournals.molbev.a026334

Chiarucci A, Bacaro G, Scheiner SM (2011) Old and new challenges in using species diversity for assessing biodiversity. Philosophical Transactions of the Royal Society B 366: 2426–2437. https://doi.org/10.1098/rstb.2011.0065

Coleman CO (2015) Taxonomy in times of the taxonomic impediment – examples from the community of experts on amphipod crustaceans. Journal of Crustacean Biology: 35: 729–740. https://doi.org/10.1163/1937240X-00002381

Crespo A, Pérez-Ortega S (2009) Cryptic species and species pairs in lichens: A discussion on the relationship between molecular phylogenies and morphological characters. Anales del Jardín Botánico de Madrid 66: 71–81. https://doi.org/10.3989/ajbm.2225

Crespo A, Lumbsch HT (2010) Cryptic species in lichen-forming fungi. IMA Fungus 1: 167–170. https://doi.org/10.5598/imafungus.2010.01.02.09

Crespo A, Kauff F, Divakar PK, Prado RD, Pérez-Ortega S, Amo G, Ferencova Z, Blanco O, Roca-Valiente B, Núñez-Zapata J, Cubas P, Argüello A, Elix JA, Esslinger TL, Hawksworth DL, Millanes A, Molina MC, Wedin M, Ahti T, Aptroot A, Barreno E, Bungartz F, Calvelo S, Candan M, Cole M, Ertz D, Goffinet B, Lindblom L, Lücking R, Lutzoni F, Mattsson JE, Messuti MI, Miadlikowska J, Piercey-Normore M, Rico VJ, Sipman HJM, Schmitt I, Spribille T, Thell A, Thor G, Upreti DK, Lumbsch HT (2010) Phylogenetic generic classification of parmelioid lichens (Parmeliaceae, Ascomycota) based on molecular, morphological and chemical evidence. Taxon 59: 1735–1753.

Culberson C, Johnson A (1982) Substitution of methyl tert.-butyl ether for diethyl ether in standardized thin layer chromatographic method for lichen products. Journal of Chromatography B 238: 438–487.

Culberson CF, Nash III TH, Johnson A (1979) 3-a-Hydroxybarbatic Acid, a New Depside in Chemosyndromes of Some *Xanthoparmeliae* with ß-Orcinol Depsides. Bryologist 82: 154–161. https://doi.org/10.2307/3242074

Darriba D, Taboada GL, Doallo R, Posada D (2012) jModelTest 2: more models, new heuristics and parallel computing. Nature Methods 9(8): 772. https://doi.org/10.1038/nmeth.2109

Divakar PK, Crespo A, Kraichak E, Leavitt SD, Singh G, Schmitt I, Lumbsch HT (2017) Using a temporal phylogenetic method to harmonize family- and genus-level classification in the largest clade of lichen-forming fungi. Fungal Diversity 84: 101–117. https://doi.org/10.1007/s13225-017-0379-z

Egan RS (1975) New *Xanthoparmelia* (Lichenes: Parmeliaceae) Records from New Mexico. Mycotaxon 2: 217–222.

Elix JA (1994) *Xanthoparmelia*. Flora of Australia 55: 201–308.

Eriksson OE, Baral HO, Currah RS, Hansen K, Kurtzman CP, Rambold G, Laessøe T (2004) Outline of Ascomycota–2004. Myconet 10: 1–99.

Gardes M, Bruns T (1993) ITS primers with enhanced specificityfor basidiomycetes—Application to the identification of mycorrhizae and rusts. Molecular Ecology 2: 113–118. https://doi.org/10.1111/j.1365-294X.1993.tb00005.x

Guindon S, Gascuel O (2003) A simple, fast and accurate method to estimate large phylogenies by maximum-likelihood. Systematic Biology 52: 696–704. https://doi.org/10.1080/10635150390235520

Gyelnik V (1931) Additamenta ad cognitionem Parmeliarum II. Fedde Repertorium Specierum Novarum Regni Vegetatis 29: 273–291.

Hale ME (1974) *Bulbothrix, Parmelina, Relicina* and *Xanthoparmelia*, Four New Genera in the Parmeliaceae (Lichenes). Phytologia 28: 479–490.

Hale Jr ME (1990) A synopsis of the lichen genus *Xanthoparmelia* (Vainio) Hale (Ascomycotina, Parmeliaceae). Smithsonian Contributions to Botany 74: 1–250. https://doi.org/10.5479/si.0081024X.74

Huelsenbeck JP, Ronquist F (2001) MRBAYES: Bayesian inference of phylogenetic trees. Bioinformatics 17: 754–755. https://doi.org/10.1093/bioinformatics/17.8.754

Jaklitsch WM, Baral HO, Lücking R, Lumbsch HT (2016) Ascomycota. In: Frey W (Ed.) Syllabus of Plant Families - Adolf Engler's Syllabus der Pflanzenfamilien. Gebr. Borntraeger Verlagsbuchhandlung, Stuttgart, 1–150.

Kearse M, Moir R, Wilson A, Stones-Havas S, Cheung M, Sturrock S, Buxton S, Cooper A, Markowitz S, Duran C, Thierer T, Ashton B, Mentjies P, Drummond A (2012) Geneious Basic: an integrated and extendable desktop software platform for the organization and analysis of sequence data. Bioinformatics 28: 1647–1649. https://doi.org/10.1093/bioinformatics/bts199

Leavitt SD, Johnson LA, Goward T, St. Clair LL (2011) Species delimitation in taxonomically difficult lichen-forming fungi: An example from morphologically and chemically diverse

Xanthoparmelia (Parmeliaceae) in North America. Molecular Phylogenetics and Evolution 60: 317–332. https://doi.org/10.1016/j.ympev.2011.05.012

Leavitt SD, Lumbsch HT, Stenroos S, Clair LL (2013) Pleistocene Speciation in North American Lichenized Fungi and the Impact of Alternative Species Circumscriptions and Rates of Molecular Evolution on Divergence Estimates. PLoS ONE 8(12): e85240. https://doi.org/10.1371/journal.pone.0085240

Leavitt SD, Divakar PK, Crespo A, Lumbsch HT (2016) A matter of time – understanding the limits of the power of molecular data for delimiting species boundaries. Herzogia 29: 479–492. https://doi.org/10.13158/heia.29.2.2016.479

Leavitt SD, Kirika PM, Amo de Paz G, Huang JP, Hur JS, Elix JA, Grewe F, Divakar PK, Lumbsch HT (2018) Assessing phylogeny and historical biogeography of the largest genus in lichen-forming fungi, *Xanthoparmelia* (Parmeliaceae, Ascomycota). Lichenologist 50: 299–312. https://doi.org/10.1017/S0024282918000233

Lücking R (2012) Predicting species richness in tropical lichenized fungi with 'modular' combinations of character states. Biodiversity and Conservation 21: 2341–2360. https://doi.org/10.1007/s10531-011-0217-7

Lücking R, Hodkinson BP, Leavitt SD (2016) The 2016 classification of lichenized fungi in the Ascomycota and Basidiomycota – Approaching one thousand genera. Bryologist 119: 361–416. https://doi.org/10.1639/0007-2745-119.4.361

Lumbsch HT (2002) Analysis of phenolic products in lichens for identication and taxonomy. In: Kranner I, Beckett R, Varma A (Eds) Protocols in Lichenology Culturing, biochemistry, ecophysiology and use in biomonitoring. Springer, Berlin, 281–295.

Lumbsch HT, Huhndorf SM (2010) Myconet Volume 14. Part one. Outline of Ascomycota – 2009. Fieldiana Life and Earth Sciences 1: 1–42. https://doi.org/10.3158/1557.1

Lumbsch HT, Leavitt S (2011) Goodbye morphology? A paradigm shift in the delimitation of species in lichenized fungi. Fungal Diversity 50: 59–72. https://doi.org/10.1007/s13225-011-0123-z

Mangold A, Martín MP, Lücking R, Lumbsch HT (2008) Molecular phylogeny suggests synonymy of Thelotremataceae within Graphidaceae (Ascomycota: Ostropales). Taxon 57: 476–486.

Miller MA, Pfeiffer W, Schwartz T (2010) CIPRES Science Gateway survey. http://www.phylo.org

Nash III TH (1974) Two New Species of *Xanthoparmelia* with Diffractaic Acid. Bryologist 72: 234–235.

Nash III TH, Elix JA (2004) *Xanthoparmelia*. In: Nash III TH, Ryan BD, Diederich P, Gries C, Bungartz F (Eds) Lichen Flora of the Greater Sonoran Desert Region. Vol. II. Lichens Unlimited, Arizona State University. Tempe, Arizona, 566–605.

Nash III TH, Herrera-Campos MA, Elix JA (2016) *Xanthoparmelia* in Mexico. Bibliotheca Lichenologica 110: 621–641.

Orange A, James PW, White FJ (2010) Microchemical methods for the identification of lichens, second edition with additions and corrections. British Lichen Society, London, 1–101.

Pawar S (2003) Taxonomic Chauvinism and the Methodologically Challenged. BioScience 53: 861–864. https://doi.org/10.1641/0006-3568(2003)053[0861:TCATMC]2.0.CO;2

Rambaut A (2014) FigTree 1.2.2. http://tree.bio.ed.ac.uk/software/figtree/

Ronquist F, Huelsenbeck JP (2003) MrBayes 3: Bayesian phylogenetic inference under mixed models. Bioinformatics 19: 1572–1574. https://doi.org/10.1093/bioinformatics/btg180

Schmitt I, Crespo A, Divakar PK, Fankhauser JD, Herman-Sackett E, Kalb K, Nelsen MP, Nelson NA, Rivas-Plata E, Shimp AD, Widhelm T, Lumbsch HT (2009) New primers for promising single-copy genes in fungal phylogenetics and systematics. Persoonia 23: 35–40. https://doi.org/10.3767/003158509X470602

Stamatakis A (2014) RAxML Version 8: A tool for phylogenetic analysis and post-analysis of large phylogenies. Bioinformatics 30: 1312–1313. https://doi.org/10.1093/bioinformatics/btu033

Thell A, Crespo A, Divakar PK, Kärnefelt I, Leavitt SD, Lumbsch HT, Seaward MRD (2012) A review of the lichen family Parmeliaceae – history, phylogeny and current taxonomy. Nordic Journal of Botany 30: 641–664. https://doi.org/10.1111/j.1756-1051.2012.00008.x

Troia MJ, McManamay RA (2016) Filling in the GAPS: evaluating completeness and coverage of open-access biodiversity databases in the United States. Ecology and Evolution 6: 4654–4669. https://doi.org/10.1002/ece3.2225

Troudet J, Grandcolas P, Blin A, Vignes-Lebbe R, Legendre F (2017) Taxonomic bias in biodiversity data and societal preferences. Scientific Reports 7(1): 1–14. https://doi.org/10.1038/s41598-017-09084-6

Vaidya G, Lohman DJ, Meier R (2011) SequenceMatrix: concatenation software for the fast assembly of multi-gene datasets with character set and codon information. Cladistics 27: 171–180. https://doi.org/10.1111/j.1096-0031.2010.00329.x

Vilgalys R, Hester M (1990) Rapid genetic identification and mapping of enzymatically amplified ribosomal DNA from several *Cryptococcus* species. Journal of Bacteriology 172: 4238–4246. https://doi.org/10.1128/jb.172.8.4238-4246.1990

White TJ, Bruns TD, Lee S, Taylor J (1990) Amplification and direct sequencing of fungal ribosomal RNA genes for phylogenetics. In: Innis MA, Gelfand DH, Sninsky JJ, White TJ (Eds) PCR Protocols. Academic Press, San Diego, 315–322.

Zoller S, Scheidegger C, Sperisen C (1999) PCR primers for the amplification of mitochondrial small subunit ribosomal DNA of lichen-forming ascomycetes. Lichenologist 31: 511–516 https://doi.org/10.1006/lich.1999.0220

MycoKeys 40: 29–51 (2018)
doi: 10.3897/mycokeys.40.28636
http://mycokeys.pensoft.net

RESEARCH ARTICLE

A peer-reviewed open-access journal
MycoKeys
Launched to accelerate biodiversity research

Liberomyces pistaciae sp. nov., the causal agent of pistachio cankers and decline in Italy

Salvatore Vitale[1,*], Dalia Aiello[2,*], Vladimiro Guarnaccia[3,4], Laura Luongo[1], Massimo Galli[1], Pedro W. Crous[3,4], Giancarlo Polizzi[2], Alessandra Belisario[1], Hermann Voglmayr[5]

1 *Consiglio per la Ricerca in Agricoltura e l'Analisi dell'Economia Agraria (CREA)- Centro di Ricerca Difesa e Certificazione (DC), Via C. G. Bertero 22, 00156 Roma, Italy* **2** *Dipartimento di Agricoltura, Alimentazione e Ambiente, sezione Patologia Vegetale, University of Catania, Via S. Sofia 100, 95123 Catania, Italy* **3** *Westerdijk Fungal Biodiversity Institute, Uppsalalaan 8, 3584 CT Utrecht, The Netherlands* **4** *Department of Plant Pathology, University of Stellenbosch, Matieland 7602, South Africa* **5** *Division of Systematic and Evolutionary Botany, Department of Botany and Biodiversity Research, University of Vienna, Rennweg 14, 1030 Wien, Austria*

Corresponding author: *Hermann Voglmayr* (hermann.voglmayr@univie.ac.at)

Academic editor: *C. Gueidan* | Received 25 July 2018 | Accepted 3 September 2018 | Published 18 September 2018

Citation: Vitale S, Aiello D, Guarnaccia V, Luongo L, Galli M, Crous PW, Polizzi G, Belisario A, Voglmayr H (2018) *Liberomyces pistaciae* sp. nov., the causal agent of pistachio cankers and decline in Italy. MycoKeys 40: 29–51. https://doi.org/10.3897/mycokeys.40.28636

Abstract

A new canker and decline disease of pistachio (*Pistacia vera*) is described from Sicily (Italy). Observations of the disease and sampling of the causal agent started in spring 2010, in the area where this crop is typically cultivated, Bronte and Adrano (Catania province) and later extended to the Agrigento and Caltanissetta provinces. Isolations from the margins of twig, branch and stem cankers of declining plants resulted in fungal colonies with the same morphology. Pathogenicity tests on 5-year-old potted plants of *Pistacia vera* grafted on *P. terebinthus* reproduced similar symptoms to those observed in nature and the pathogen was confirmed to be a coloniser of woody plant tissue. Comparison of our isolates with the type of the apparently similar *Asteromella pistaciarum* showed that our isolates are morphologically and ecologically different from *A. pistaciarum*, the latter being a typical member of Mycosphaerellaceae. *Asteromella pistaciarum* is lectotypified, described and illustrated and it is considered to represent a

* Both authors contributed equally to the manuscript.

spermatial morph of *Septoria pistaciarum*. Multi-locus phylogenies based on two (ITS and LSU rDNA) and three (ITS, *rpb2* and *tub2*) genomic loci revealed isolates of the canker pathogen to represent a new species of *Liberomyces* within the Delonicicolaceae (Xylariales), which is here described as *Liberomyces pistaciae* **sp. nov.** (Delonicicolaceae, Xylariales). The presence of this fungus in asymptomatic plants with apparently healthy woody tissues indicates that it also has a latent growth phase. This study improves the understanding of pistachio decline, but further studies are needed for planning effective disease management strategies and ensuring that the pathogen is not introduced into new areas with apparently healthy, but infected plants.

Keywords
Delonicicolaceae, nut disease, pathogenicity, *Pistacia vera*, Xylariales, 1 new species

Introduction

Cases of pistachio tree decline with gummosis, leaf canopy thinning and fruit losses have been observed for several years in the area of Bronte (Catania province, Sicily, Italy), which is considered the most typical area where high-quality pistachios are produced in Italy (http://www.dibartolosrl.it/bronte-pistachios/). Although pistachio is characterised by good rusticity, it is subject to several fungal diseases known to afflict pistachio trees in the Mediterranean area. Of these, the most commonly reported are phylloptosis, leaf spots mainly caused by *Septoria pistaciae*, *S. pistaciarum* and *Pseudocercospora pistacina*, gum cankers by *Cytospora terebenthi* and branch and twig cankers by *Botryosphaeria dothidea* (Chitzanidis 1995, Teviotdale et al. 2002, Vitale et al. 2007, Crous et al. 2013). The latter is widespread and already present as a latent pathogen in numerous plant communities in various parts of the world (Marsberg et al. 2017). Amongst soil-borne pathogens, *Verticillium dahliae* and *Phytophthora* spp. are reported to be particularly damaging in California (Holtz 2008). Moreover, recently a new blight was reported on pistachio fruit caused by *Arthrinium xenocordella* in the Agrigento province, southern Italy (Aiello et al. 2018).

From spring 2010 onwards, surveys have been carried out in 15 pistachio orchards of Catania, Agrigento and Caltanissetta provinces, Sicily, where declining trees were present. Declining plants showed twig, branch and stem cankers associated with vascular necrosis and tree decline. Abundant gummosis often occurred in association with cankered lesions. The cankered area resulted in localised, sunken lesions with several central cracks. After removing the bark, discolouration and necrotic tissue were evident and lesions deepened into the woody tissue. A coelomycetous fungus with pycnidial conidiomata was consistently isolated from these lesions.

The aims of this study were thus to investigate the aetiology of the decline syndrome observed in Bronte and to provide morphological, taxonomic, phylogenetic and pathogenic evidence of the causal organism which proved to be an undescribed species of *Liberomyces*, which was initially misidentified as *Asteromella pistaciarum*.

Materials and methods

Field survey and isolation

Surveys of 15 pistachio orchards were conducted from 2010 to 2017 in Bronte and Adrano (Catania province, eastern Sicily) and Agrigento and Caltanissetta provinces (western Sicily). Approximately 10 samples per orchard showing cankered twigs and branches from declining pistachio plants were randomly collected for analysis (Fig. 1). Sub-cortical and wood fragments (about 5 × 5 mm) were cut from the lesion margins between affected and healthy tissues. In addition, from one orchard in Bronte, twigs were also sampled from asymptomatic pistachio plants. Subsequently, tissue pieces were disinfected by soaking in 70% ethanol for 5 s, 4% sodium hypochlorite for 90 s, rinsed in sterile water for 60 s and dried on sterile filter paper in a laminar flow cabinet. The fragments were placed on to 1.5% (w/v) malt extract agar (MEA, Oxoid, Basingstoke, UK) and 2% potato dextrose agar (PDA, Oxoid), incubated at room temperature (25 ± 5 °C) and examined for fungal growth. Numerous slow-growing cultures were obtained and single-conidial isolations were performed with conidia collected from pycnidia produced on those cultures within one month of incubation at room temperature under natural light conditions. More than 80 single-spore isolates were obtained from symptomatic and asymptomatic tissue isolations. Amongst these, 71 isolates were characterised by molecular and phylogenetic analysis (Table 1) and the four isolates ISPaVe1958, ISPaVe2105, ISPaVe2106 and ISPaVe2148 were considered for morphological, taxonomic and pathogenic studies. For a summary of sampling information of these isolates, see Suppl. Material 1.

Morphological characterisation

For morphological investigations, cultures were grown on MEA, PDA and 2% corn meal agar (CMA, Sigma-Aldrich) supplemented with 2% w/v dextrose (CMD). Moreover, pycnidial formation was assessed on artificially inoculated sterilised pistachio twigs incubated in a moist chamber. The isolates used in this study are maintained in the culture collections of the Dipartimento di Agricoltura, Alimentazione e Ambiente, University of Catania (PV) and of the CREA-DC (ex CREA-PAV), the extype isolate ISPaVe1958 of the new pistachio pathogen was deposited at the Westerdijk Fungal Biodiversity Institute (CBS), Utrecht, The Netherlands and the holotype specimen in the Fungarium of the Department of Botany and Biodiversity Research, University of Vienna (WU).

For investigations of temperature-growth relationships of the new pistachio pathogen, the holotype isolate ISPaVe1958 and the more recent isolate ISPaVe2148 were used. Agar plugs (5 mm diam.) were taken from the edge of actively growing cultures on MEA and transferred on to the centre of 9 cm diam. Petri dishes containing 1.5%

MEA. Three replicate plates were incubated at 10, 15, 20, 25, 30 and 35 °C in the dark and measurements were taken after 21 d at right angles along two lines intersecting the centre of the inoculum and the mean growth rates plus and minus the standard deviation were calculated.

The holotype isolate ISPaVe1958 (CBS 128196) of the new pistachio pathogen and the type specimens of *Asteromella pistaciarum* deposited in the Natural History Museum of Vienna (W) were morphologically examined. For light microscopy, squash mounts and hand sections of pycnidia were made using a razor blade and observed in tap water or in 3% KOH. Methods of microscopy included stereomicroscopy using a Nikon SMZ 1500 equipped with a Nikon DS-U2 digital camera and light microscopy with Nomarski differential interference contrast (DIC) using the compound microscope Zeiss Axio Imager.A1 equipped with a Zeiss Axiocam 506 colour digital camera. Images were captured and measured with NIS-Elements D v. 3.0 or with the Zeiss ZEN Blue Edition software. For certain images of pycnidia, the stacking software Zerene Stacker v. 1.04 (Zerene Systems LLC, Richland, WA, USA) was used. Measurements are reported as maximum and minimum in parentheses and the range representing the mean plus and minus the standard deviation of a number of measurements given in parentheses.

Pathogenicity

Pathogenicity tests with four fungal strains of the undescribed pistachio pathogen were performed to satisfy Koch's postulates. Trials were carried out outdoors and in a growth chamber at 25 ± 1 °C. Potted 5-yr-old plants of *Pistacia vera* grafted on to *P. terebinthus* were used for artificial inoculations. Three plants for each isolate and six inoculation sites for each plant were considered.

Inoculations were made on stems and twigs after removing a 5 mm diam. bark disc with a cork borer, replacing it with a 5 mm plug from a 14-d-old PDA culture and covering it with sterile wet cotton, wrapped with parafilm (Pechney Plastic Packaging Inc., Chicago, USA) and aluminium foil to prevent contamination and desiccation. An equivalent number of plants and inoculation sites were inoculated with sterile PDA plugs as controls. The inoculated plants were observed every week. Symptom typology and the length of lesions were assessed after 12 months. To fulfil Koch's postulates, re-isolation was conducted following the same procedure as described above for isolations. Tissue fragments were plated on MEA or PDA and morphological and molecular identifications by sequencing the ITS rDNA were performed.

DNA extraction, PCR amplification and sequencing

The extraction of genomic DNA from pure cultures was performed as reported in previous studies (Voglmayr and Jaklitsch 2011, Jaklitsch et al. 2012, Guarnaccia and

Crous 2017) by using the DNeasy Plant Mini Kit (QIAgen GmbH, Hilden, Germany) or the Wizard Genomic DNA Purification Kit (Promega Corporation, WI, USA). For the ex-type strain of the new species, the complete internal transcribed spacer region (ITS1-5.8S-ITS2) and a ca. 0.9 kb fragment of the large subunit nuclear ribosomal DNA (nLSU rDNA) were amplified and sequenced as a single fragment with primers V9G (de Hoog and Gerrits van den Ende 1998) and LR5 (Vilgalys and Hester 1990); the complete ITS region of the other strains was amplified with primers ITS5 and ITS4 (White et al. 1990); the RNA polymerase II subunit 2 (*rpb2*) gene was amplified with primers fRPB2-5F2 and fRPB2-7cR (Liu et al. 1999, Sung et al. 2007) or dRPB2-5f and dRPB2-7r (Voglmayr et al. 2016); and the beta-tubulin (*tub2*) gene with primer pairs T1 and T22 or Tub2Fd and Bt-2b (O'Donnell and Cigelnik 1997, Aveskamp et al. 2009). The PCR product was purified using an enzymatic PCR cleanup (Werle et al. 1994) as described in Voglmayr and Jaklitsch (2008). DNA was cycle-sequenced using the ABI PRISM Big Dye Terminator Cycle Sequencing Ready Reaction Kit v. 3.1 (Applied Biosystems, Warrington, UK) with the same primers as in PCR; in addition, primers ITS4, LR2R-A (Voglmayr et al. 2012) and LR3 (Vilgalys and Hester 1990) were used for the ITS-LSU fragment. Sequencing was performed on an automated DNA sequencer (3730xl Genetic Analyser, Applied Biosystems).

Phylogenetic analyses

NCBI BLASTn searches of the ITS and LSU of the undescribed pistachio pathogen revealed members of Xylariales as closest matches. For phylogenetic analyses, two combined matrices were produced; GenBank accession numbers of the sequences used in the phylogenetic analyses are given in Table 1. A combined ITS-LSU matrix was generated to reveal the phylogenetic position of the undescribed pistachio pathogen within Xylariales. For this, representative GenBank sequences of Xylariales were selected from Jaklitsch et al. (2016) and supplemented with some additional GenBank sequences; six taxa of Sordariomycetes were added as outgroup. The second combined matrix contained three loci (ITS, *rpb2*, *tub2*) sequenced for 68 isolates of the undescribed pistachio pathogen; in addition, GenBank sequences of four accessions of Delonicicolaceae and of six additional members of Xylariales were added and two species of Diaporthales were used as outgroup (Guarnaccia and Crous 2017, Voglmayr et al. 2017).

All alignments were produced with the server version of MAFFT (www.ebi.ac.uk/Tools/mafft), checked and refined using BioEdit v. 7.0.9.0 (Hall 1999). After exclusion of ambiguously aligned regions and long gaps, the final ITS-LSU matrix contained 1340 nucleotide characters and the three loci matrix 1941 nucleotide characters (660 from ITS, 781 from *rpb2* and 500 from *tub2*). The alignment and phylogenetic trees were deposited in TreeBASE (http://purl.org/phylo/treebase/phylows/study/TB2:S23059).

Maximum Likelihood (ML) analyses were performed with RAxML (Stamatakis 2006) as implemented in raxmlGUI v. 1.3 (Silvestro and Michalak 2012), using the

ML + rapid bootstrap setting and the GTRGAMMAI substitution model with 1000 bootstrap replicates.

Maximum Parsimony (MP) analyses were performed with PAUP v. 4.0a161 (Swofford 2002), using 1000 replicates of heuristic search with random addition of sequences and subsequent TBR branch swapping (MULTREES option in effect, steepest descent option not in effect, COLLAPSE command set to MINBRLEN). Molecular characters were unordered and given equal weight; gaps were treated as missing data. Bootstrap analyses with 1000 replicates were performed in the same way, with 5 rounds of replicates of heuristic search with random addition of sequences and subsequent TBR branch swapping during each bootstrap replicate, with each replicate limited to 1 million rearrangements in the analysis of the three-loci matrix.

Results

Field survey and isolation

Cankers and decline symptoms caused by the undescribed pistachio pathogen were detected in 10 orchards amongst the 15 investigated. The disease was primarily observed in the winter period and during late spring.

In the Bronte and Adrano areas (Catania province), symptoms were observed during the dormant season. Symptomatic plants showed gum exudation and often bark scaling on trunk and/or branches. When bark scaling occurred, it appeared as cracking and peeling of the bark. On trunks and large branches, cankers first appeared as visible dead circular areas that developed in the bark, which subsequently became dark and sunken. From that point onwards, infected areas expanded in all directions but much faster along the main axis of the stem, branch or twig. Under some environmental conditions, the host produced callus tissue around dead areas limiting the canker. Under the bark, cankers were characterised by discolouration and necrotic tissues and, in some cases, these extended to the vascular tissues and pith (Figs 1, 2).

During the active growing season, the symptomatic plants also showed canopy decline. Inflorescences and shoots, originating from infected branches or twigs, wilted and died. When the trunk was girdled by a canker, a collapse of the entire plant occurred (Fig. 1).

More than 80 single-spore isolates were obtained from symptomatic and a few also from asymptomatic pistachio plants. Amongst these, 71 isolates were characterised by molecular phylogenetic analyses and 68 deposited at the Westerdijk Fungal Biodiversity Institute, Utrecht, Netherlands (Table 1).

Pathogenicity

The initial symptom, observed 3 weeks after artificial fungal inoculation, was gum exudation produced around the point inoculated. After removing the bark, a dark

Table 1. Isolates and accession numbers used in the phylogenetic analyses.

Taxon	Strain[1,2,3]	ITS[3]	LSU[3]	*tub2*[3]	*rpb2*[3]
Acrocordiella occulta	CBS 140500^{ET}	KT949893	KT949893		
Alnecium auctum	CBS 124263^{ET}	KF570154	KF570154		
Amphibambusa bambusicola	MFLUCC 11-0617^{HT}	KP744433	KP744474		
Amphisphaeria umbrina	HKUCC 994	AF009805	AF452029		
Anthostoma decipiens	CBS 133221	KC774565	KC774565		
Arthrinium phragmites	CBS 135458^{HT}	KF144909	KF144956		
Arthrinium saccharicola	CBS 831.71	KF144922	KF144969		
Barrmaelia macrospora	CBS 142768^{ET}	KC774566	KC774566		
Bartalinia robillardoides	CBS 122705^{ET}	KJ710460	KJ710438	LT853252	LT853152
Basiseptospora fallax	CBS 129020^{ET}	JF440983	JF440983		
Beltrania rhombica	CBS 141507	KX306749	KX306778		
Beltraniella odinae	NBRC 6774	00677401[4]	00677401[4]		
Beltraniopsis neolitseae	CBS 137974^{HT}	KJ869126	KJ869183		
Biscogniauxia nummularia	MUCL 51395^{ET}	JX658444	KT281894		
Broomella vitalbae	CBS 140412	KT949895	KT949895		
Cainia graminis	CBS 136.62	KR092793	AF431949		
Calosphaeria pulchella	CCTU 316	JX876610	JX876611		
Camillea obularia	ATCC 28093	KY610384	KY610429		
Chaetosphaeria innumera	MR 1175	AF178551	AF178551		
Coniocessia maxima	CBS 593.74^{HT}	GU553332	GU553344		
Coniocessia nodulisporioides	CBS 281.77^{IT}	GU553333	GU553352		
Creosphaeria sassafras	CBS 127876	KT949900	KT949900		
Cryptovalsa rabenhorstii	CBS 125574	KC774567	KC774567		
Daldinia concentrica	CBS 113277	AY616683	KT281895	KC977274	KY624243
Delonicicola siamense	MFLUCC 15-0670^{HT}	MF167586	MF158345	–	MF158346
Diaporthe eres	CBS 109767	KC343075	AF408350		
Diaporthe limonicola	CBS 142549^{HT}	MF418422		MF418582	**MH797629**
Diatrype disciformis	CBS 197.49	-	DQ470964		
Discosia artocreas	NBRC 8975	AB594773	AB593705		
Eutypa lata	CBS 208.87^{NT}	DQ006927	DQ836903		
Graphostroma platystoma	CBS 270.87	JX658535	AY083827		
Hymenopleella hippophaeicola	CBS 140410^{ET}	KT949901	KT949901		
Hyponectria buxi	UME 31430	-	AY083834		
Hypoxylon fragiforme	MUCL 51264^{ET}	KC477229	KM186295		
Idriella lunata	MUCL 7551	KC775735	KC775710		
Immersidiscosia eucalypti	MAFF 242781	AB594793	AB593725		
Juglanconis juglandina	CBS 133343	KY427149		KY427234	KY427199
Kretzschmaria deusta	CBS 163.93	KC477237	KT281896		
Leiosphaerella praeclara	CBS 125586^{ET}	JF440976	JF440976		
Lepteutypa fuckelii	CBS 140409^{NT}	KT949902	KT949902		
Liberomyces macrosporus	CCF 4028^{HT}	FR715522	FR715522	FR715498	FR715509
Liberomyces pistaciae	**CPC 31292 = CBS 144225**	**MH797562**		**MH797697**	**MH797630**
Liberomyces pistaciae	**CPC 31293**	**MH797563**		**MH797698**	**MH797631**
Liberomyces pistaciae	**CPC 31294**	**MH797564**		**MH797699**	**MH797632**
Liberomyces pistaciae	**CPC 31295**	**MH797565**		**MH797700**	**MH797633**
Liberomyces pistaciae	**CPC 31296**	**MH797566**		**MH797701**	**MH797634**
Liberomyces pistaciae	**CPC 31297**	**MH797567**		**MH797702**	**MH797635**
Liberomyces pistaciae	**CPC 31298**	**MH797568**		**MH797703**	**MH797636**
Liberomyces pistaciae	**CPC 31299**	**MH797569**		**MH797704**	**MH797637**
Liberomyces pistaciae	**CPC 31300**	**MH797570**		**MH797705**	**MH797638**
Liberomyces pistaciae	**CPC 31301**	**MH797571**		**MH797706**	**MH797639**
Liberomyces pistaciae	**CPC 31302**	**MH797572**		**MH797707**	**MH797640**
Liberomyces pistaciae	**CPC 31303**	**MH797573**		**MH797708**	**MH797641**
Liberomyces pistaciae	**CPC 31304**	**MH797574**		**MH797709**	**MH797642**

Taxon	Strain[1,2,3]	ITS[3]	LSU[3]	*tub2*[3]	*rpb2*[3]
Liberomyces pistaciae	**CPC 31305**	**MH797575**		**MH797710**	**MH797643**
Liberomyces pistaciae	**CPC 31315**	**MH797576**		**MH797711**	**MH797644**
Liberomyces pistaciae	**CPC 31316**	**MH797577**		**MH797712**	**MH797645**
Liberomyces pistaciae	**CPC 31317**	**MH797578**		**MH797713**	**MH797646**
Liberomyces pistaciae	**CPC 31318**	**MH797579**		**MH797714**	**MH797647**
Liberomyces pistaciae	**CPC 31319**	**MH797580**		**MH797715**	**MH797648**
Liberomyces pistaciae	**CPC 31320**	**MH797581**		**MH797716**	**MH797649**
Liberomyces pistaciae	**CPC 31321**	**MH797582**		**MH797717**	**MH797650**
Liberomyces pistaciae	**CPC 31322**	**MH797583**		**MH797718**	**MH797651**
Liberomyces pistaciae	**CPC 31323**	**MH797584**		**MH797719**	**MH797652**
Liberomyces pistaciae	**CPC 31324**	**MH797585**		**MH797720**	**MH797653**
Liberomyces pistaciae	**CPC 31325**	**MH797586**		**MH797721**	**MH797654**
Liberomyces pistaciae	**CPC 31326**	**MH797587**		**MH797722**	**MH797655**
Liberomyces pistaciae	**CPC 31327**	**MH797588**		**MH797723**	**MH797656**
Liberomyces pistaciae	**CPC 31328**	**MH797589**		**MH797724**	**MH797657**
Liberomyces pistaciae	**CPC 31329**	**MH797590**		**MH797725**	**MH797658**
Liberomyces pistaciae	**CPC 31330**	**MH797591**		**MH797726**	**MH797659**
Liberomyces pistaciae	**CPC 31332**	**MH797592**		**MH797727**	**MH797660**
Liberomyces pistaciae	**CPC 31333**	**MH797593**		**MH797728**	**MH797661**
Liberomyces pistaciae	**CPC 33611**	**MH797594**		**MH797729**	**MH797662**
Liberomyces pistaciae	**CPC 33612**	**MH797595**		**MH797730**	**MH797663**
Liberomyces pistaciae	**CPC 33613**	**MH797596**		**MH797731**	**MH797664**
Liberomyces pistaciae	**CPC 33614**	**MH797597**		**MH797732**	**MH797665**
Liberomyces pistaciae	**CPC 33629**	**MH797598**		**MH797733**	**MH797666**
Liberomyces pistaciae	**CPC 33630**	**MH797599**		**MH797734**	**MH797667**
Liberomyces pistaciae	**CPC 33848**	**MH797600**		**MH797735**	**MH797668**
Liberomyces pistaciae	**CPC 33849**	**MH797601**		**MH797736**	**MH797669**
Liberomyces pistaciae	**CPC 33850**	**MH797602**		**MH797737**	**MH797670**
Liberomyces pistaciae	**CPC 33851**	**MH797603**		**MH797738**	**MH797671**
Liberomyces pistaciae	**CPC 33852**	**MH797604**		**MH797739**	**MH797672**
Liberomyces pistaciae	**CPC 33853**	**MH797605**		**MH797740**	**MH797673**
Liberomyces pistaciae	**CPC 33854**	**MH797606**		**MH797741**	**MH797674**
Liberomyces pistaciae	**CPC 33855**	**MH797607**		**MH797742**	**MH797675**
Liberomyces pistaciae	**CPC 33856**	**MH797608**		**MH797743**	**MH797676**
Liberomyces pistaciae	**CPC 33857**	**MH797609**		**MH797744**	**MH797677**
Liberomyces pistaciae	**CPC 33858**	**MH797610**		**MH797745**	**MH797678**
Liberomyces pistaciae	**CPC 33859**	**MH797611**		**MH797746**	**MH797679**
Liberomyces pistaciae	**CPC 33860**	**MH797612**		**MH797747**	**MH797680**
Liberomyces pistaciae	**CPC 33861**	**MH797613**		**MH797748**	**MH797681**
Liberomyces pistaciae	**CPC 33862**	**MH797614**		**MH797749**	**MH797682**
Liberomyces pistaciae	**CPC 33863**	**MH797615**		**MH797750**	**MH797683**
Liberomyces pistaciae	**CPC 33866**	**MH797616**		**MH797751**	**MH797684**
Liberomyces pistaciae	**CPC 33867**	**MH797617**		**MH797752**	**MH797685**
Liberomyces pistaciae	**CPC 33868**	**MH797618**		**MH797753**	**MH797686**
Liberomyces pistaciae	**CPC 33869**	**MH797619**		**MH797754**	**MH797687**
Liberomyces pistaciae	**CPC 33870**	**MH797620**		**MH797755**	**MH797688**
Liberomyces pistaciae	**CPC 33871**	**MH797621**		**MH797756**	**MH797689**
Liberomyces pistaciae	**CPC 33872**	**MH797622**		**MH797757**	**MH797690**
Liberomyces pistaciae	**CPC 33873**	**MH797623**		**MH797758**	**MH797691**
Liberomyces pistaciae	**CPC 33874**	**MH797624**		**MH797759**	**MH797692**
Liberomyces pistaciae	**CPC 34204**	**MH797625**		**MH797760**	**MH797693**
Liberomyces pistaciae	**CPC 34205**	**MH797626**		**MH797761**	**MH797694**
Liberomyces pistaciae	**CPC 34206**	**MH797627**		**MH797762**	**MH797695**
Liberomyces pistaciae	**CPC 34207**	**MH797628**		**MH797763**	**MH797696**
Liberomyces pistaciae	**ISPaVe1958[HT] = CBS 128196**	**MH798901**	**MH798901**	**MH791335**	**MH791334**
Liberomyces pistaciae	**ISPaVe2105**	**FR681904**	–		

Taxon	Strain[1,2,3]	ITS[3]	LSU[3]	*tub2*[3]	*rpb2*[3]
Liberomyces pistaciae	**ISPaVe2106**	**FR681905**	–		
Liberomyces pistaciae	**ISPaVe2148**	**MH798902**	–		
Liberomyces saliciphilus	H041	FR715510		FR715496	FR715507
Liberomyces saliciphilus	H077	FR715511		FR715497	FR715508
Liberomyces saliciphilus	CCF 4020[HT]	FR715515	FR715515		
Lopadostoma turgidum	CBS 133207[ET]	KC774618	KC774618		
Melanconis stilbostoma	CBS 121894	JQ926229	JQ926229		
Melogramma campylosporum	CBS 141086	JF440978	JF440978		
Microdochium lycopodinum	CBS 122885[HT]	JF440979	JF440979		
Microdochium phragmitis	CBS 285.71[ET]	AJ279449	EU926218	KP859076	KP859122
Nectria cinnabarina	CBS 125165[ET]	HM484548	HM484562		
Neopestalotiopsis protearum	CBS 114178[HT]	LT853103		LT853251	LT853151
Pestalotiopsis knightiae	CBS 114138[HT]	KM199310	KM116227		
Phlogicylindrium eucalyptorum	CBS 111689	KF251205	KF251708		
Phlogicylindrium uniforme	CBS 131312[HT]	JQ044426	JQ044445		
Polyancora globosa	CBS 118182[HT]	DQ396469	DQ396466		
Poronia punctata	CBS 656.78	KT281904	KY610496		
Pseudapiospora corni	CBS 140736[NT]	KT949907	KT949907		
Pseudomassaria chondrospora	CBS 125600	JF440981	JF440981		
Pseudomassariella vexata	CBS 129022[ET]	JF440977	JF440977		
Requienella fraxini	CBS 140475[HT]	KT949910	KT949910		
Requienella seminuda	CBS 140502[ET]	KT949912	KT949912		
Robillarda sessilis	CBS 114312[ET]	KR873256	KR873284		
Sarcostroma restionis	CBS 118154[HT]	DQ278922	DQ278924		
Seimatosporium cupressi	CBS 224.55[ET]	LT853083		LT853230	LT853131
Seimatosporium rosae	CBS 139823[ET]	KT198726	KT198727	LT853253	LT853153
Seiridium marginatum	CBS 140403[ET]	KT949914	KT949914		
Seynesia erumpens	SMH 1291	-	AF279410		
Strickeria kochii	CBS 140411[ET]	KT949918	KT949918		
Truncatella angustata	ICMP 7062	AF405306	AF382383		
Vialaea insculpta	DAOM 240257	JX139726	JX139726		
Vialaea minutella	BRIP 56959	KC181926	KC181924		
Xylaria hypoxylon	CBS 122620[ET]	KY610407	KY610495		
Zetiasplozna acaciae	CBS 137994[HT]	KJ869149	KJ869206		

[1] Abbreviations: **ATCC**: American Type Culture Collection, Manassas, VA, USA; **BRIP**: Queensland Plant Pathology Herbarium, Brisbane, Australia; **CBS**: Culture collection of the Westerdijk Fungal Biodiversity Institute, Utrecht, The Netherlands; **CCF**: Culture collection of the Dept. of Botany, Charles University, Prague, Czech Republic; **CCTU**: Culture Collection of Tabriz University, Iran; **CPC**: Culture collection of Pedro Crous, housed at CBS; H: Isolates from Pažoutová et al. (2012); **DAOM**: Canadian National Mycological Herbarium, Ottawa, Canada; **H**: Isolates from Pažoutová et al. (2012); **HKUCC**: The University of Hong Kong Culture Collection, Hong Kong, China; **ICMP**: International Collection of Microorganisms from Plants, Auckland, New Zealand; **ISPaVe**: Culture collection of the Consiglio per la Ricerca in Agricoltura e l'Analisi dell'Economia Agraria, Roma, Italy (CREA-DC); **MAFF**: MAFF Genbank, National Institute of Agrobiological Sciences, Ibaraki, Japan; **MFLUCC**: Mae Fah Luang University Culture Collection, Chiang Rai, Thailand; **MR**: Culture collection of Martina Réblová, Department of Taxonomy, Institute of Botany of the Czech Academy of Sciences, Průhonice, Czech Republic; **MUCL**: BCCM/MUCL Agro-food & Environmental Fungal Collection, Louvain-la-Neuve, Belgium; **SMH**: Culture collection of Sabine Huhndorf, Field Museum of Natural History, Chicago, USA; **UME**: Herbarium of the Department of Ecology and Environmental Science, Umeå University, Umeå, Sweden.

[2] **ET** Ex-epitype strain; **HT** Ex-holotype strain; **IT** Ex-isotype strain; **NT** Ex-neotype strain.

[3] Isolates/sequences in bold were isolated/sequenced in the present study.

[4] Sequence downloaded from NBRC (http://www.nbrc.nite.go.jp/).

Figure 1. Symptoms caused by *Liberomyces pistaciae* on *Pistacia vera in vivo*. **a** Plant killed by canker on trunk **b** Twigs dieback **c, d** Shoots wilted on infected twig **e** Gum and cracking of the trunk **f, g** Internal tissue of trunk cankers **h** Gum exudation on branch **i** Internal dark discolouration in cross section of branch **j** Necrotic tissue in longitudinal section of twig **k, l** External and internal cankers on twigs.

Figure 2. Symptoms reproduced from mycelial plug inoculation with *Liberomyces pistaciae* on 5-year-old potted plants of *Pistacia vera*. Stem symptoms after **a, b** 3 wks **c** 6 months **d, e** 12 months **f, g** Cankers on twigs.

discolouration and necrotic tissue were visible (Figs 2a, b). After 6 months, external cankers were observed in correspondence with the inoculated sites and small cracks were present in the sunken central area (Fig. 2c). After 12 months, symptoms were very obvious and similar to the cracked cankers observed in nature. Long and deep cracks were evident on the sunken area that defined the cankered lesion. After removing the bark, it was evident that the pathogen was able to colonise the wood and long discolourations were present (Figs 2d, e). After 12 months from inoculation, the length of lesions ranged from 12 to 45 mm. For ISPaVe1958 and ISPaVe2105,

length lesions averaged 16.7 ± 3.0 and 31 ± 1.0 mm, respectively, while for ISPaVe2106 and ISPaVe2148, 18 ± 0.0 mm and 29.7 ± 2.0 mm. Controls measured 4.0 ±1.0 mm in average. Cultures, morphologically identical with the new pistachio pathogen, were re-isolated from these cankers, fulfilling Koch's postulates. Moreover, ITS sequence comparison of these re-isolated cultures confirmed the species identity.

Growth rates

The growth rate experiments revealed 30 °C as optimal temperature for both isolates with an evidently better growth of the holotype ISPaVe1958 at this temperature in comparison to ISPaVe2148 (Fig. 3).

Phylogenetic analyses

Of the 1340 nucleotide characters of the ITS-LSU matrix, 519 are parsimony informative. The best ML tree (-lnL = 19486.775), revealed by RAxML, is shown as a phylogram in Fig. 4. Maximum parsimony analyses revealed 14 MP trees 4008 steps long (not shown). The backbone of the MP trees differs in several deeper unsupported nodes from the ML tree (not shown); notably in the MP tree, the *Liberomyces* clade was not the most basal node of Xylariales, although without support (not shown).

In the ML and MP analyses of the ITS-LSU matrix (Fig. 4), the Xylariales received maximum support, but backbone support within Xylariales was low to absent. The new species clustered within the *Liberomyces* clade, which was sister to *Delonicicola siamense* (Delonicicolaceae, Xylariales). The Delonicicolaceae received high support (100% ML and 99% MP bootstrap support), but their closest relatives remained unclear due to lack of significant backbone support in all deeper nodes (Fig. 4). The sister-group relationship of *L. saliciphilus* and *L. macrosporus* received moderate support (81% ML and 89% MP bootstrap support).

Of the 1941 nucleotide characters of the ITS-*rpb2-tub2* matrix, 743 are parsimony informative (201 from ITS, 343 from *rpb2*, 199 from *tub2*). The best ML tree (-lnL = 12820.324), revealed by RAxML, is shown as a phylogram in Fig. 5. Maximum parsimony analyses revealed 6 MP trees 2669 steps long, with a tree backbone identical to that of the ML tree (not shown).

The analyses of the ITS-*rpb2-tub2* matrix (Fig. 5) revealed similar topologies to the analyses of the ITS-LSU matrix. The Xylariales and Delonicicolaceae received high support in ML and MP analyses. The new pistachio pathogen formed a genetically homogeneous clade with high to maximum support, confirming that all isolates sequenced belong to the same species. As in the ITS-LSU analyses, it was placed as sister to the highly supported *Liberomyces saliciphilus-L. macrosporus* clade with moderate support.

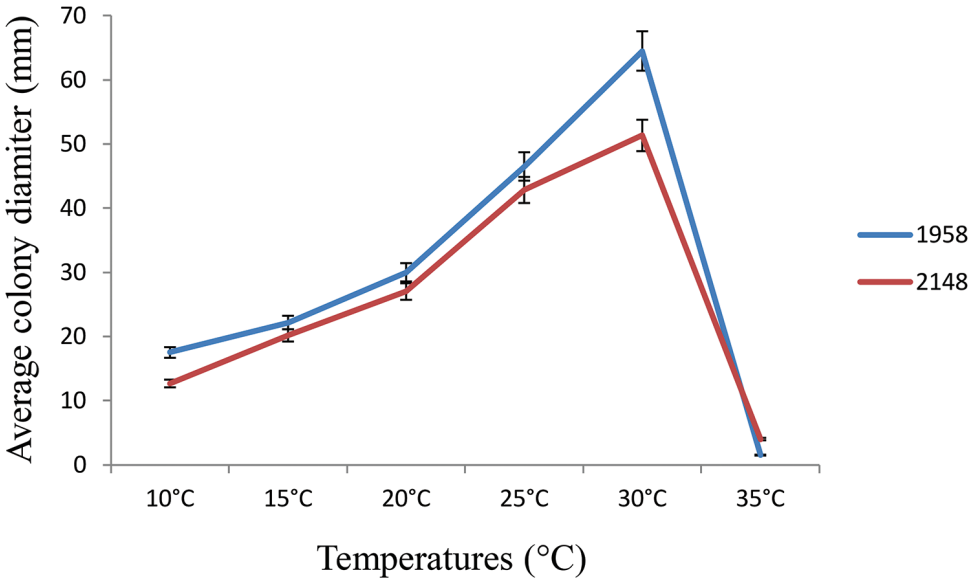

Figure 3. Temperature-growth relationships of the holotype isolate ISPaVe1958 compared to the more recent isolate ISPaVe2148 of *Liberomyces pistaciae* on 1.5% MEA. Mean growth rates (mm) plus and minus the standard deviation, calculated on three replicates after 21 d of incubation, are shown.

Taxonomy

As a result of the morphological and molecular phylogenetic investigations, the undescribed pistachio pathogen is described as a new species, *Liberomyces pistaciae*. In addition, for comparison, a morphological re-description and illustrations are also provided for the apparently similar, little known pistachio pathogen, *Asteromella pistaciarum*, based on type material and it is recognised as a synonym of *Septoria pistaciarum*.

Liberomyces pistaciae **Voglmayr, S. Vitale, D. Aiello, Guarnaccia, Luongo & Belisario, sp. nov.**
MycoBank: MB827682
Fig. 6

Diagnosis. Species with distinctly smaller conidia (3.2–5.0 × 1.0–2.0 µm) than in *Liberomyces saliciphilus* Pažoutová, M. Kolařík & Kubátová and *L. macrosporus* Pažoutová, M. Kolařík & Kubátová.

Type. ITALY. Sicily: Bronte (Catania province), on cankered twig of *Pistacia vera*, June 2010, A. Belisario (holotype: WU 39967; ex-type culture CBS 128196 = ISPaVe1958).

Etymology. Named after its host genus, *Pistacia*.

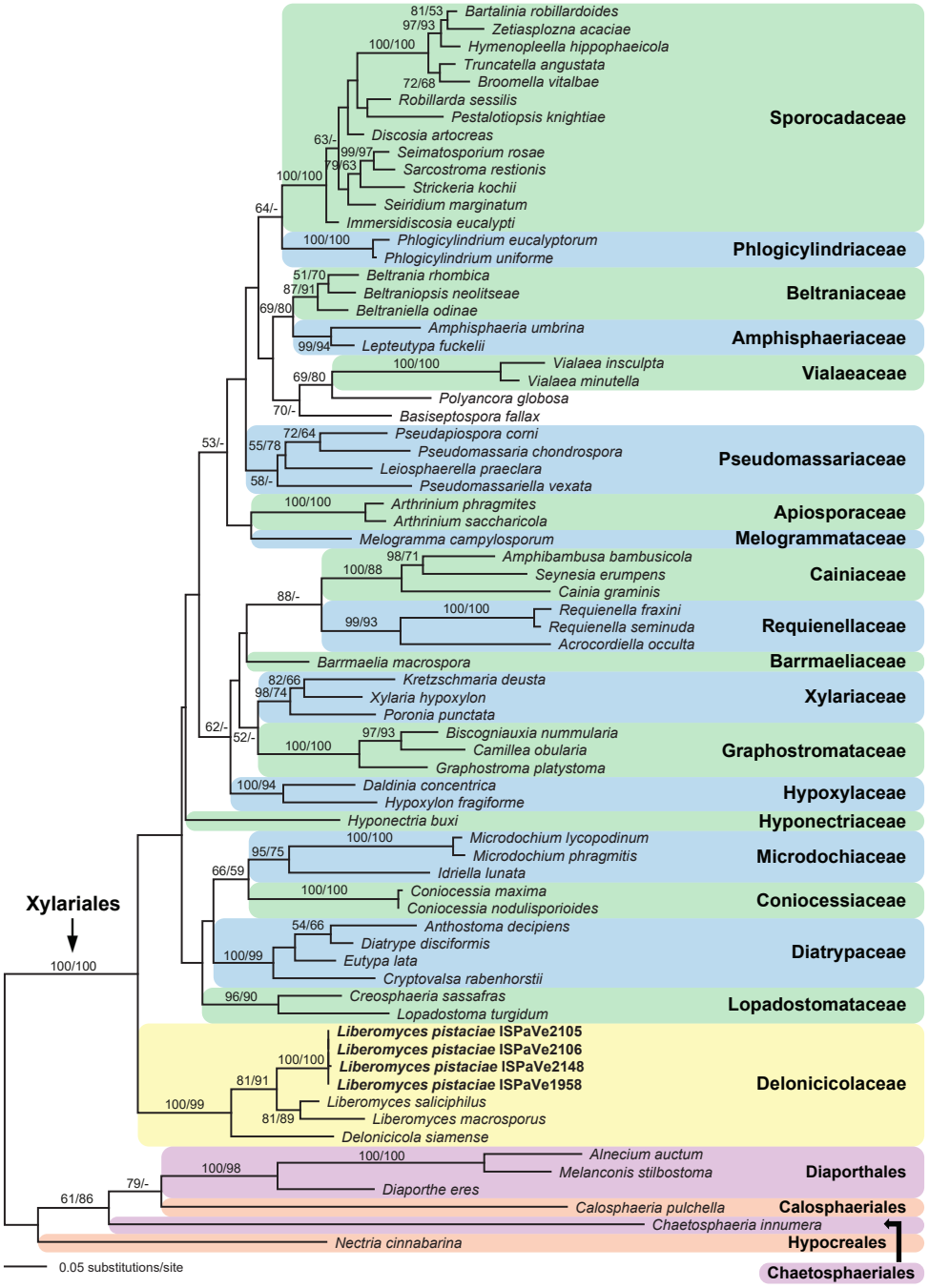

Figure 4. Phylogram of the best ML tree (-lnL = 19486.775) revealed by RAxML from an analysis of the combined ITS-LSU matrix of selected Xylariales, showing the phylogenetic position of *Liberomyces pistaciae* (bold) within Delonicicolaceae. ML and MP bootstrap support above 50% are given above or below the branches.

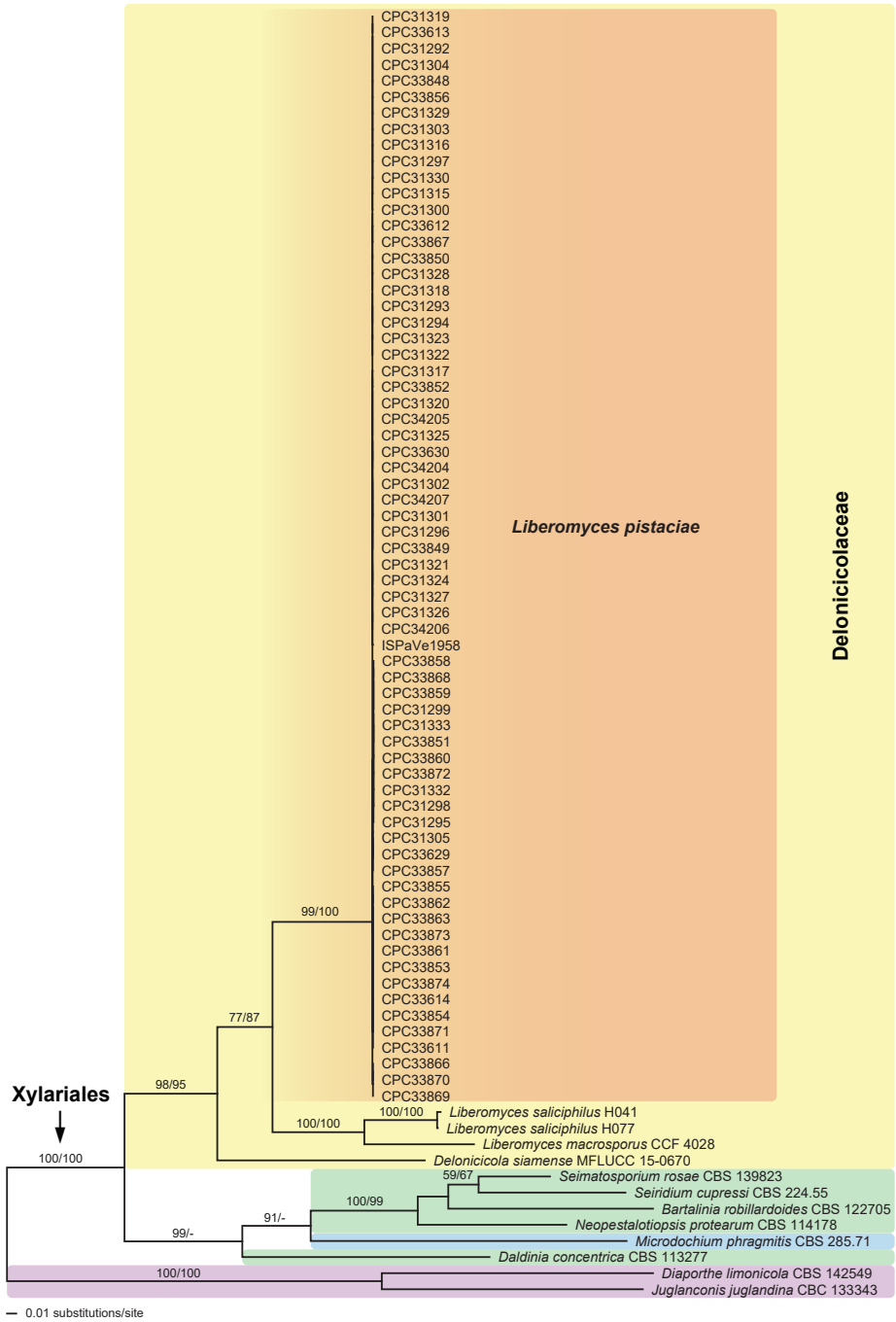

Figure 5. Phylogram of the best ML tree (-lnL = 12820.324) revealed by RAxML from an analysis of the combined ITS-*rpb2*-*tub2* matrix of selected Xylariales, showing the phylogenetic position of *Liberomyces pistaciae* (bold) within Delonicicolaceae. The tree was rooted with two species of Diaporthales (*Diaporthe limonicola*, *Juglanconis juglandina*). ML and MP bootstrap support above 50% are given above the branches.

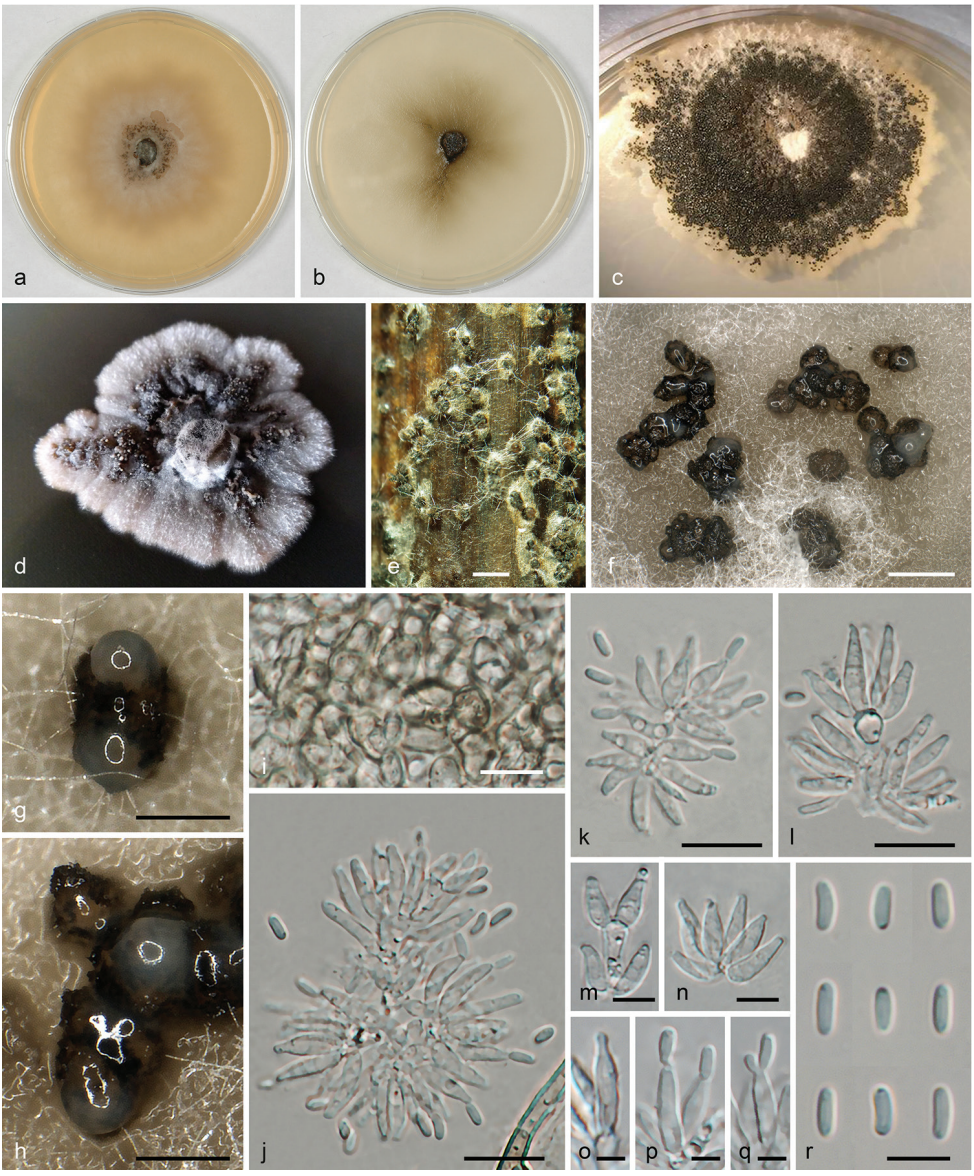

Figure 6. *Liberomyces pistaciae*. **a–d** Cultures (**a** MEA, 6 weeks, 22 °C **b** CMD, 6 weeks, 22 °C **c** PDA, 3 weeks, 25 °C **d** PDA, 2 weeks, 25 °C) **e** Pycnidia produced on artificially inoculated sterilised pistachio twigs **f–h** Pycnidia in face view on MEA **i** Pycnidial wall in face view **j–n** Conidiophores and conidiogenous cells **o–q** Conidiogenous cells (**o** young **p, q** showing sympodial conidiation) **r** Conidia. All in water. Sources: **a–c, f–r** ex-holotype strain ISPaVe1958 = CBS 128196 **d, e** PV1= CPC 31292. Scale bars: 500 µm (**e, f**); 200 µm (**g, h**); 10 µm (**i–l**); 5 µm (**m–r**).

Description. *Conidiomata* pycnidial, superficial or immersed, single to densely aggregated, subglobose or cupular, uni- or irregularly plurilocular, first hyaline to pale brown, turning dark brown to blackish, without ostiole, irregularly rupturing at the

apex and exuding a pale whitish conidial drop at maturity, (100–)170–260(–330) µm diam. (n=40). *Pycnidial wall* thin, of pale brown cells, (2.0–)3.5–6.3(–10.0) µm diam. (n=162) forming a *textura angularis*, outside darker, thicker-walled and more rounded, inside lined by a layer of angular hyaline cells giving rise to conidiophores. *Conidiophores* short, densely fasciculate, up to three times branched, hyaline, smooth, arising from the inner wall of the entire conidioma, 10–28 µm long. *Conidiogenous cells* holoblastic with sympodial proliferation, lageniform to cylindrical, (5.5–)6.5–8.5(–10.0) × 1.7–2.5(–2.7) µm (n=52), in dense intercalary or terminal whorls of 2–9. *Conidia* straight to allantoid, hyaline, smooth, 1-celled, (3.2–)3.8–4.5(–5.0) × (1.0–)1.2–1.5(–2.0) µm, l/w = (2.0–)2.7–3.5(–4.7) µm (n=182).

Culture characteristics. Colonies slow-growing (about 4 cm in diam. in 1 month on MEA, 4 cm in 2 weeks on CMD at 22 °C), initially white, turning pale to dark brown with age, with a whitish slightly lobed margin (Fig. 6a and b), surface mycelium sparse. Red to brown pigments diffusing in growth medium. Densely aggregated pycnidia formed after 7 d on the inoculum plug, successively also on the colony surface.

Notes. Morphologically, *Liberomyces pistaciae* is similar to the other two species of the genus, *L. macrosporus* and *L. saliciphilus*, but the latter have distinctly longer conidia (5–7.5 µm in *L. saliciphilus*, 8–13 µm in *L. macrosporus*).

***Septoria pistaciarum* Caracc., Boll. Stud. Inform. R. Giard Colon Palermo 13: 10 [extr.] (1934).**
Fig. 7

Asteromella pistaciarum Bremer & Petr., Sydowia 1(4–6): 253 (1947). For additional synonymy and a description of the *Septoria* morph, see Crous et al. (2013). **Syn.**

Type of *Asteromella pistaciarum*. TURKEY. Ankara, on leaves of *Pistacia vera*, 29 Oct. 1944, *H. Bremer* (lectotype of *Asteromella pistaciarum* designated here: W 1973-15537, MBT383208; isotype: W 1979-11134).

Description of the asteromella-like spermatial morph. *Infection* localised, producing distinct, brown, irregularly polyangular lesions of 0.5–1.5 mm diam., successively confluent, sharply delimited by leaf veins, visible on both sides of the leaf. *Pycnidia* (57–)69–101(–106) µm wide, (99–)107–134(–143) µm high (n=12), subepidermal, gregarious, solitary or in small groups, ellipsoid to pyriform, dark brown to black, with a central, circular, well-visible apical ostiole; peridium 8–19 µm wide, pseudoparenchymatous, of dark brown cells (3.0–)3.8–7.0(–10.3) µm diam. (n=50). Inner side lined with hyaline cells giving rise to phialides and short conidiophores. *Conidiophores* 1–3-celled, cells more or less square-shaped, bearing intercalary and terminal phialides. *Conidiogenous cells* enteroblastic, phialidic, hyaline, (3.7–)5.0–8.5(–10.5) × (2.5–)3.0–4.0(–4.7) µm (n=30), ampulliform to broadly lageniform, straight or curved. *Conidia* (3.4–)4.3–5.4(–6.6) × (0.9–)1.0–1.3(–1.5) µm, l/w = (2.8–)3.5–4.8(–6.1) (n=67), oblong, 1-celled, hyaline, with 1–2 subterminal guttules.

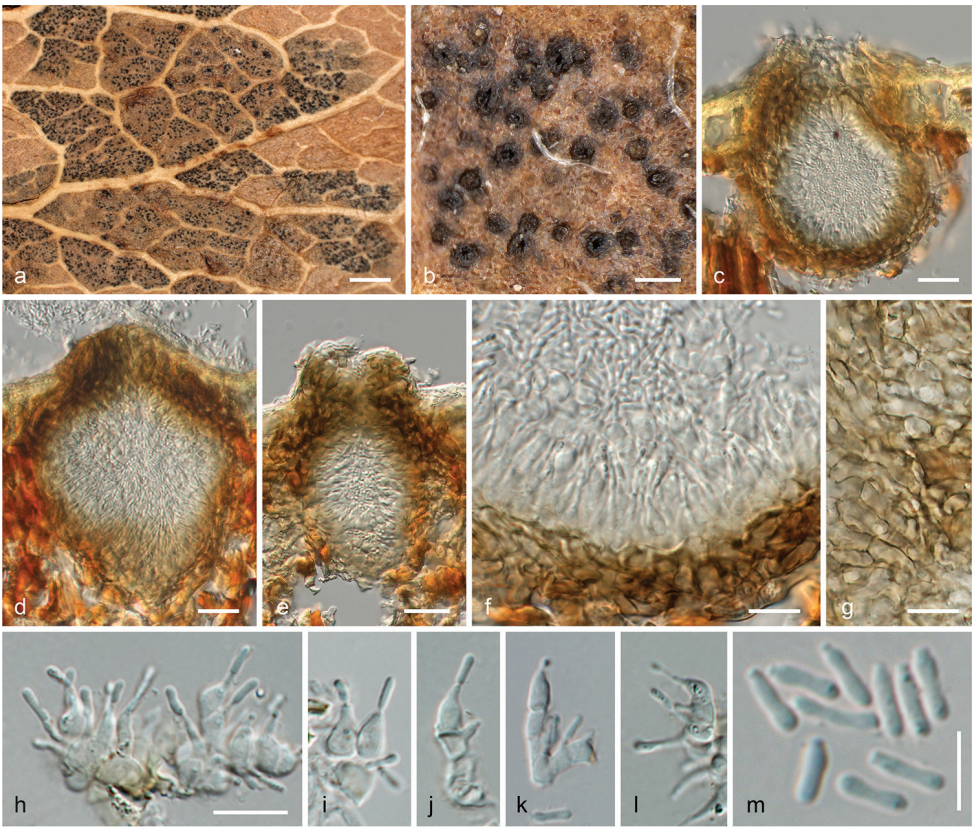

Figure 7. *Asteromella pistaciarum* W 1973-15537 (lectotype). **a, b** Pycnidia in leaf in face view **c–e** Pycnidia embedded in leaf in vertical section **f** Pycnidial wall with phialides and conidia in vertical section **g** Pycnidial wall in tangential section **h–l** Conidiophores and conidiogenous cells **m** Conidia. Scale bars: 10 mm (**a**); 100 µm (**b**); 20 µm (**c–e**); 10 µm (**f–l**); 5 µm (**m**).

Notes. The classification and description of the lectotype of *Asteromella pistaciarum* is here added as it is morphologically similar to *Liberomyces pistaciae* and the latter had therefore initially been misidentified as the former (see e.g. Pažoutová et al. 2012, who included a sequence of *Liberomyces pistaciae* as *Asteromella pistaciarum* in their phylogenies). In addition, *Asteromella pistaciarum* has not been addressed in previous taxonomic accounts. Two isotype specimens are located in the Natural History Museum of Vienna (W) from which W 1973-15537 is here selected as the lectotype based on preservation and abundance of the specimens. In the original description, Bremer and Petrak (1947) reported a close association of *Asteromella pistaciarum* with *Septoria pistaciarum* and an immature mycosphaerella-like sexual morph, which they consider to represent the same species. We agree with this treatment and consider *Asteromella pistaciarum* to be the spermatial morph of *Septoria pistaciarum*, the former therefore becoming a synonym of the latter based on priority.

Discussion

This study represents the first work determining the causal agent of cankers and decline of pistachio trees in Sicily, the major production area of Italy. In the field, severe symptoms of canker were observed on branches, shoots and trunks. In some cases, decline and death of host plants also occurred. The fungus almost exclusively isolated from these symptoms was *Liberomyces pistaciae* and the decline syndrome was strictly reproduced by artificial inoculation experiments. Seventy-one isolates recovered from different orchards over a 7-yr period were identified by molecular analysis. The molecular phylogenetic analyses (Figs 4, 5) clearly demonstrate that the genus *Liberomyces* is affiliated with the Xylariales, which confirms the results of previous analyses (Pažoutová et al. 2012, Perera et al. 2017). In both of our analyses, the genus *Liberomyces* is a sister group to *Delonicicola siamense* with moderate to high support, for which Perera et al. (2017) established a new family and order, Delonicicolaceae and Delonicicolales. However, if the order Delonicicolales is accepted, the Xylariales are unsupported in Perera et al. (2017) as well as in our phylogenetic analyses of the ITS-LSU matrix (Fig. 4). In the order Xylariales, insufficient backbone resolution and support of phylogenies based on ITS-LSU rDNA has been commonly observed (e.g. Jaklitsch and Voglmayr 2012, Jaklitsch et al. 2016), which often significantly increases if protein-coding genes like *rpb2* and *tub2* are considered (e.g. Voglmayr et al. 2018, Wendt et al. 2018). However, for most lineages of Xylariales, only ITS-LSU rDNA data are currently available. Remarkably, also in the phylogenetic analyses of Perera et al. (2017), which were inferred from a combined SSU, ITS, LSU and *rpb2* matrix, internal support of Xylariales is absent if Delonicicolales are classified as a separate order. This fact may be due to lack of *rpb2* sequence data for many lineages within Xylariales. Therefore, we consider the establishment of a separate order Delonicicolales premature and presently we propose the classification of Delonicicolaceae within Xylariales in which this family also fits morphologically, given its conidiomatal morphology and conidiogenesis.

Due to the pycnidial conidiomata and conidia of similar sizes, the current pistachio pathogen, here described as *Liberomyces pistaciae*, was initially identified as *Asteromella pistaciarum*, the true identity of which was unclear at that time. No sequence data are available for authentic material of the latter. However, a re-investigation of the type specimen of *A. pistaciarum* revealed substantial differences between both species, providing a clear distinction between the two organisms. While the type of *A. pistaciarum* has short reduced conidiophores with intercalary and terminal ampulliform phialides (Fig. 7h–l), *L. pistaciae* has densely fasciculate conidiophores with verticillately arranged holoblastic, lageniform to cylindrical conidiogenous cells with sympodial conidial proliferation (Fig. 6j–q). In addition, the type of *A. pistaciarum* has distinctly more elongate conidia with a l/w of (2.8–)3.5–4.8(–6.1), compared to (2.0–) 2.7–3.5(–4.7) in *L. pistaciae*. Moreover, the disease symptoms are markedly different. The type collection of *A. pistaciarum* represents a foliar pathogen causing clearly delimited polyangular leaf lesions with gregarious subepidermal pycnidia on both sides of the leaf

(Fig. 7a), whereas *L. pistaciae* causes a canker disease of stems and branches. Although no recent collections, sequence data or cultures are available for *A. pistaciarum*, its close association with *Septoria pistaciarum* and an immature mycosphaerella-like sexual morph on the holotype specimen, which was already noted in the original description (Bremer and Petrak 1947), provides strong evidence that *A. pistaciarum* represents the spermatial morph of *Septoria pistaciarum* and it is therefore here considered to be a synonym of the latter.

There are many fungal genera which can act as plant pathogens, but may behave also as latent pathogens, while closely related species are symptomless endophytes (Carroll 1988). This is apparently also the case in the pathogen *Liberomyces pistaciae*, which might have a latent phase within the host tissues since it was also isolated from asymptomatic pistachio plants. A latent phase represents a specific condition where the fungus can either develop symptoms or induce changes in the physiology of the host plant (Romero et al. 2001, Crous et al. 2015, 2016). Furthermore, Millar (1980) and Andrews et al. (1985) observed that certain latent pathogens become pathogenic when the host is stressed and this may be the case in *L. pistaciae* on pistachio trees in Bronte. In this regard, the ecology of its closest relatives, *L. macrosporus* and *L. saliciphilus*, is of interest, as they were isolated as bark and wood endophytes from several woody hosts (Pažoutová et al. 2012), indicating that the primary ecology of the genus *Liberomyces* may be endophytic, from which the pathogenic *L. pistaciae* may have evolved. However, detailed studies are necessary to evaluate the influence of stress on pathogenicity of *L. pistaciae*.

On the basis of the high disease incidence and the frequency of this species observed in several orchards in the last years, we believe that *L. pistaciae* represents a menace to pistachio production in Sicily. As no epidemiological data are yet available, it is not possible to suggest any control strategies to avoid *L. pistaciae* infections. Nevertheless, the use and distribution of infected propagation material taken from nurseries and mechanical injuries or pruning wounds could play an important role in promoting the infections. The recent increase in importance of this and other diseases of pistachio in Sicily has stimulated further research and studies are in progress to extend the survey to other areas and to obtain important information to formulate effective disease management strategies.

Acknowledgements

This study was financially supported by the research project “Ricerche per il miglioramento della frutticoltura meridionale” (FRUMED) financed by the National Ministry of Agriculture (MiPAAF). The financial support by the Austrian Science Fund (FWF; project P27645-B16) to H. Voglmayr is gratefully acknowledged. Cordial thanks are due to A. Igersheim (W) for the loan of specimens and to W. Till (WU) for managing the herbarium loans.

References

Aiello D, Gulisano S, Gusella G, Polizzi G, Guarnaccia V (2018) First report of fruit blight caused by *Arthrinium xenocordella* on *Pistacia vera* in Italy. Plant Disease 102: 1853. https://doi.org/10.1094/PDIS-02-18-0290-PDN

Andrews JH, Hecht EP, Bashirian S (1985) Association between the fungus *Acremonium curvulum* and Eurasian water milfoil, *Myriophyllum spicatum*. Canadian Journal of Botany 60: 1216–1221. https://doi.org/10.1139/b82-154

Aveskamp MM, Verkley GJ, de Gruyter J, Murace MA, Perelló A, Woudenberg JH, Groenewald JZ, Crous PW (2009) DNA phylogeny reveals polyphyly of *Phoma* section *Peyronellaea* and multiple taxonomic novelties. Mycologia 10: 363–382. https://doi.org/10.3852/08-199

Bremer H, Petrak F (1947) Neue Kleinpilze aus der Türkei. Sydowia 1: 248–263. http://www.zobodat.at/pdf/Sydowia_1_0248-0263.pdf

Carroll G (1988) Fungal endophytes in stems and leaves: from latent pathogen to mutualistic symbiont. Ecology 69: 2–9. https://doi.org/10.2307/1943154

Chitzanidis A (1995) Pistachio diseases in Greece. Acta Horticulturae 419: 345–348. https://doi.org/10.17660/ActaHortic.1995.419.57

Crous PW, Groenewald JZ, Slippers B, Wingfield MJ (2016) Global food and fibre security threatened by current inefficiencies in fungal identification. Philosophical Transactions of the Royal Society B 371: 20160024. https://doi.org/10.1098/rstb.2016.0024

Crous PW, Hawksworth DL, Wingfield MJ (2015) Identifying and naming plant-pathogenic fungi: past, present, and future. Annual Review of Phytopathology 53: 247–267. https://doi.org/10.1146/annurev-phyto-080614-120245

Crous PW, Quaedvlieg W, Sarpkaya K, Can C, Erkiliç A (2013) Septoria-like pathogens causing leaf and fruit spot of pistachio. IMA Fungus 4: 187–199. https://doi.org/10.5598/imafungus.2013.04.02.04

de Hoog GS, Gerrits van den Ende AHG (1998) Molecular diagnostics of clinical strains of filamentous basidiomycetes. Mycoses 41: 183–189. https://doi.org/10.1111/j.1439-0507.1998.tb00321.x

Guarnaccia V, Crous PW (2017) Emerging citrus diseases in Europe caused by species of *Diaporthe*. IMA Fungus 8: 317–334. https://doi.org/10.5598/imafungus.2017.08.02.07

Guarnaccia V, Groenewald JZ, Polizzi G, Crous PW (2017) High species diversity in *Colletotrichum* associated with citrus diseases in Europe. Persoonia 39: 32–50. https://doi.org/10.3767/persoonia.2017.39.02

Hall TA (1999) BioEdit: a user-friendly biological sequence alignment editor and analysis program for Windows 95/98/NT. Nucleic Acids Symposium Series 41: 95–98.

Holtz BA (2008) Soilborne diseases of pistachio. Pistachio 5th Short Course 2008. University of California, Davis. http://fruitsandnuts.ucdavis.edu/files/74185.pdf

Jaklitsch WM, Gardiennet A, Voglmayr H (2016) Resolution of morphology-based taxonomic delusions: *Acrocordiella*, *Basiseptospora*, *Blogiascospora*, *Clypeosphaeria*, *Hymenopleella*, *Lepteutypa*, *Pseudapiospora*, *Requienella*, *Seiridium* and *Strickeria*. Persoonia 37: 82–105. https://doi.org/10.3767/003158516X690475

Jaklitsch WM, Stadler M, Voglmayr H (2012) Blue pigment in *Hypocrea caerulescens* sp. nov. and two additional new species in sect. *Trichoderma*. Mycologia 104: 925–941. https://doi.org/10.3852/11-327

Jaklitsch WM, Voglmayr H (2012) Phylogenetic relationships of five genera of *Xylariales* and *Rosasphaeria* gen. nov. (Hypocreales). Fungal Diversity 52: 75–98. https://doi.org/10.1007/s13225-011-0104-2

Liu YL, Whelen S, Hall BD (1999) Phylogenetic relationships among ascomycetes: evidence from an RNA polymerase II subunit. Molecular Biology and Evolution 16: 1799–1808. https://doi.org/10.1093/oxfordjournals.molbev.a026092

Marsberg A, Kemler M, Jami F, Nagel JH, Postma-Smidt A, Naidoo S, Wingfield MJ, Crous PW2, Spatafora JW, Hesse CN, Robbertse B, Slippers B (2017) *Botryosphaeria dothidea*: a latent pathogen of global importance to woody plant health. Molecular Plant Pathology 18: 477–488. https://doi.org/10.1111/mpp.12495

Millar CS (1980) Infection processes on conifer needles. In Blakeman JP (Ed.) Microbial ecology of the phylloplane. Academic Press, London, 185–209.

O'Donnell K, Cigelnik E (1997) Two divergent intragenomic rDNA ITS2 types within a monophyletic lineage of the fungus *Fusarium* are nonorthologous. Molecular Phylogenetics and Evolution 7: 103–116. https://doi.org/10.1006/mpev.1996.0376

Pažoutová S, Šrůtka P, Holuša J, Chudíčková M, Kubátová A, Kolařík M (2012) *Liberomyces* gen. nov. with two new species of endophytic coelomycetes from broadleaf trees. Mycologia 104: 198–210. https://doi.org/10.3852/11-081

Perera RH, Maharachchikumbura SS, Jones EG, Bahkali AH, Elgorban AM, Liu J-K, Liu Z-Y, Hyde KD (2017) *Delonicicola siamense* gen. & sp. nov. (Delonicicolaceae fam. nov., Delonicicolales ord. nov.), a saprobic species from *Delonix regia* seed pods. Cryptogamie, Mycologie 38: 321–340. https://doi.org/10.7872/crym/v38.iss3.2017.321

Romero A, Carrión G, Rico-Gray V (2001) Fungal latent pathogens and endophytes from leaves of *Parthenium hysterophorus* (Asteraceae). Fungal Diversity 7: 81–87. http://www.fungaldiversity.org/fdp/sfdp/FD_7_81-87.pdf

Silvestro D, Michalak I (2012) raxmlGUI: a graphical front-end for RAxML. Organisms Diversity & Evolution 12: 335–337. https://doi.org/10.1007/s13127-011-0056-0

Stamatakis E (2006) RAxML-VI-HPC: maximum likelihood-based phylogenetic analyses with thousands of taxa and mixed models. Bioinformatics 22: 2688–2690. https://doi.org/10.1093/bioinformatics/btl446

Sung GH, Sung JM, Hywel-Jones NL, Spatafora JW (2007) A multi-gene phylogeny of Clavicipitaceae (Ascomycota, Fungi): identification of localized incongruence using a combinational bootstrap approach. Molecular Phylogenetics and Evolution 44: 1204–1223. https://doi.org/10.1016/j.ympev.2007.03.011

Swofford DL (2002) PAUP* 4.0b10: phylogenetic analysis using parsimony (*and other methods). Sinauer Associates, Sunderland, Mass.

Teviotdale BL, Michailides TJ, Pscheidt JW (2002) Compendium of nut crop diseases in temperate zones. APS Press, St Paul, Minn.

Vilgalys R, Hester M (1990) Rapid genetic identification and mapping of enzymatically amplified ribosomal DNA from several *Cryptococcus* species. Journal of Bacteriology 172: 4238–4246. https://doi.org/10.1128/jb.172.8.4238-4246.1990

Vitale S, Avanzato D, Belisario A (2007) Malattie fungine del pistacchio, possibile ostacolo allo sviluppo della coltivazione nell'Italia centrale. Frutticoltura 69: 68–71.

Voglmayr H, Akulov OY, Jaklitsch WM (2016) Reassessment of *Allantonectria*, phylogenetic position of *Thyronectroidea*, and *Thyronectria caraganae* sp. nov. Mycological Progress 15: 921–937. https://doi.org/10.1007/s11557-016-1218-4

Voglmayr H, Castlebury LA, Jaklitsch WM (2017) *Juglanconis* gen. nov. on Juglandaceae, and the new family Juglanconidaceae (Diaporthales). Persoonia 38: 136–155. https://doi.org/10.3767/003158517X694768

Voglmayr H, Friebes G, Gardiennet A, Jaklitsch WM (2018) *Barrmaelia* and *Entosordaria* in Barrmaeliaceae (fam. nov., Xylariales) and critical notes on *Anthostomella*-like genera based on multi-gene phylogenies. Mycological Progress 17: 155–177. https://doi.org/10.1007/s11557-017-1329-6

Voglmayr H, Jaklitsch WM (2008) *Prosthecium* species with *Stegonsporium* anamorphs on *Acer*. Mycological Research 112: 885–905. https://doi.org/10.1016/j.mycres.2008.01.020

Voglmayr H, Jaklitsch WM (2011) Molecular data reveal high host specificity in the phylogenetically isolated genus *Massaria* (Ascomycota, Massariaceae). Fungal Diversity 46: 133–170. https://doi.org/10.1007/s13225-010-0078-5

Voglmayr H, Rossman AY, Castlebury LA, Jaklitsch WM (2012) Multigene phylogeny and taxonomy of the genus *Melanconiella* (Diaporthales). Fungal Diversity 57: 1–44. https://doi.org/10.1007/s13225-012-0175-8

Wendt L, Sir EB, Kuhnert E, Heitkämper S, Lambert C, Hladki AI, Romero AI, Luangsa-ard JJ, Srikitikulchai P, Peršoh D, Stadler M (2018) Resurrection and emendation of the Hypoxylaceae, recognised from a multigene phylogeny of the Xylariales. Mycological Progress 17: 115–154. https://doi.org/10.1007/s11557-017-1311-3

Werle E, Schneider C, Renner M, Völker M, Fiehn W (1994) Convenient single-step, one tube purification of PCR products for direct sequencing. Nucleic Acids Research 22: 4354–4355. https://doi.org/10.1093/nar/22.20.4354

White TJ, Bruns T, Lee S, Taylor J (1990) Amplification and direct sequencing of fungal ribosomal RNA genes for phylogenetics. In: Innis MA, Gelfand DH, Sninsky JJ, White TJ (Eds) PCR protocols: A guide to methods and applications: 315–322. [Academic Press, San Diego]

Supplementary material 1

Information on *Liberomyces pistaciae* isolates used in this study

Authors: Salvatore Vitale, Dalia Aiello, Vladimiro Guarnaccia, Laura Luongo, Massimo Galli, Pedro W. Crous, Giancarlo Polizzi, Alessandra Belisario, Hermann Voglmayr

Data type: species data

Link: https://doi.org/10.3897/mycokeys.40.28636.suppl1

MycoKeys 40: 53–67 (2018)
doi: 10.3897/mycokeys.40.26918
http://mycokeys.pensoft.net

RESEARCH ARTICLE

A peer-reviewed open-access journal
MycoKeys
Launched to accelerate biodiversity research

A new section and species of *Agaricus* subgenus *Pseudochitonia* from Thailand

Mao-Qiang He[1,2,3], Boontiya Chuankid[3], Kevin D. Hyde[3], Ratchadawan Cheewangkoon[1], Rui-Lin Zhao[2,4]

1 *Department of Entomology and Plant Pathology, Faculty of Agriculture, Chiang Mai University, Chiang Mai, 50200, Thailand* **2** *State key laboratory of Mycology, Institute of Microbiology, Chinese Academy of Sciences, Beijing, 100101, China* **3** *Center of Excellence in Fungal Research, Mae Fah Luang University, Chiang Rai, 57100, Thailand* **4** *College of Life Sciences, University of Chinese Academy of Sciences, Huairou District, Beijing, 100408, China*

Corresponding authors: *R. Cheewangkoon* (ratchadawan.c@cmu.ac.th); *R.-L. Zhao* (zhaorl@im.ac.cn)

Academic editor: *Zai-Wei Ge* | Received 29 June 2018 | Accepted 7 September 2018 | Published 20 September 2018

Citation: He M-Q, Chuankid B, Hyde KD, Cheewangkoon R, Zhao R-L (2018) A new section and species of *Agaricus* subgenus *Pseudochitonia* from Thailand. MycoKeys 40: 53–67. https://doi.org/10.3897/mycokeys.40.26918

Abstract

A large species diversity has recently been discovered in the genus *Agaricus*. Six subgenera and 23 sections are now recognised. In this study, three specimens collected from Thailand, formed a monophyletic clade in subgenus *Pseudochitonia*, based on analyses of ITS sequence data. Further analyses, based on multi-gene sequence data (ITS, LSU, tef1-α), using BEAST, revealed that this clade originated 26.7 Ma. According to their distinct morphological characteristics, phylogenetic position and relatively old divergence time, a new section *Cymbiformes* is proposed and this section is represented by a new species *A. angusticystidiatus*. This new section is characterised by the strong iodoform odour of basidiomes and cymbiform basidiospores. Descriptions, colour photographs and illustrations are presented.

Keywords

New taxa, Agaricaceae, Phylogeny, Taxonomy

Introduction

Agaricus L. 1753 (Agaricaceae, Agaricales) is a well-known genus. Many species in this genus are commercially cultivated and served as food. One of the popular edible mushrooms is *A. bisporus* (J.E. Lange) Imbach, which is the most extensively cultivated mushroom in the world, accounting for 38% of world production (ISMS Edible mushrooms 2017, http://www.isms.biz/edible-mushrooms/). Another popular edible mushroom, *A. subrufescens* Peck, is also a medicinal mushroom and contains abundant bioactive compounds, for example, some compounds extracted from the basidiomes can be used as antioxidant (De Silva et al. 2012, 2013a, b, Llarena-Hernández et al. 2017). In the field, *Agaricus* is easily recognised by its white or brown caps with fibrillose scales on the surface, free lamellae, brown spore print and annulate stipe. Under the microscope, it is characterised by brown basidiospores, single or multiseptate cheilocystidia and often lacks pleurocystidia. Habitats of *Agaricus* are various, the most common being forests and grasslands, such as *A. campestris* L. of section *Agaricus*, which can be found gregariously in small groups or in fairy rings in grasslands. *Agaricus* also exists in arid habitats, for example, *A. colpeteorum* T. Lebel and *A. lamelliperditus* T. Lebel & M.D. Barrett of section *Minores*, which were discovered in arid zones of Australia (Lebel 2013).

The taxonomic, systematic and species delimitation of *Agaricus* inferred by morphology are variable (Cappelli 1984, Singer 1986). In the 1990s, the application of molecular techniques brought new perspectives to fungal taxonomic research including the genus *Agaricus* (White et al. 1990). Using phylogenetic analyses, the taxonomy of *Agaricus* is becoming more and more stable. Zhao et al. (2011) used ITS sequence data from *Agaricus* specimens from temperate and tropical areas to build a phylogenetic topology for the genus, which revealed eleven new clades and indicated phylogenetic relationships between temperate and tropical species. Zhao et al. (2016) carried out multi-gene phylogenetic and evolutionary molecular clock analyses. In that study, *Agaricus* was segregated into five subgenera and 20 sections, according to the phylogenetic position and divergence time of each clade. With the recent discovery of an American subgenus and a new clade found in the Caribbean area, *Agaricus* now contains six subgenera and 23 sections (Zhao et al. 2016, Chen et al. 2017, Parra et al. 2018).

In this study three interesting specimens found near Chiang Mai, Thailand were analysed morphologically and molecularly. We provide a full description and analyses are presented to support the distinction of this material as a new species and section in subgenus *Pseudochitonia*.

Materials and methods

Morphological examination

Photographs were taken immediately *in situ*, in the field in Thailand. Basidiomes were wrapped in aluminium foil or kept in plastic boxes separately. Macro morphological

characteristics were recorded when specimens were fresh. Every specimen was completely dried in an electrical food drier at 60 °C, then kept in a plastic ziplock bag and deposited in Herbarium Mycologicum Academiae Sinicae (HMAS), Mae Fah Luang University Herbarium (MFLU), Biotec Bandkok Herbarium (BBH) and the Thiers Herbarium at San Francisco State University (SFSU). Colour terms and notations in parentheses are those of Kornerup and Wanscher (1978). Anatomical and cytological characteristics including basidiospores, basidia, cystidia and pileipellis were observed using an Olympus CX31 microscope. Scanning electron microscope (SEM) photos for basidiospores were captured through a Hitachi SU8010 Field Emission SEM (Tokyo, Japan). Measurements were analysed and recorded as X = the mean of length by width ± SD, Q = the quotient of basidiospore length to width and Q_m = the mean of Q values ± SD. All the protocols of morphological studies followed Largent's methodology (Largent 1986).

DNA extraction and PCR

At the Institute of Microbiology Chinese Academy of Science, genomic DNA was extracted from dry specimens by using an E.Z.N.A. Forensic DNA Extraction Kit (D3591-01, Omega Bio-Tek) following the manufacturer's protocol. PCR amplification was performed following He et al. (2017). Primers for the internal transcribed spacer (ITS), large ribosomal subunit (LSU) and translation elongation factor (tef1-α) were ITS4/ITS5, LR5/LROR and 983f/1567r, respectively (White et al. 1990, Moncalvo et al. 2000, 2002, Morehouse et al. 2003). PCR products were sent to a commercial company for sequencing and both directions were sequenced to ensure accuracy. At the Botanic Garden Meise (BR), genomic DNA was extracted from dry specimens using a CTAB isolation procedure adapted from Doyle (1990). Ca. 10 mg of tissue was ground with a Retsch 300 beadmill. ß-mercaptoethanol (0.2%) was added to the CTAB lysis buffer just prior to extraction; samples were lysed for 1 hour at 60 °C; proteins and polysaccharides were removed by two consecutive extractions with chloroform: isoamylalcohol (24:1), after which DNA was precipitated by the addition of 0.8 volume isopropanol to the aqueous phase. The pellet was washed once in 600 µl 70% ethanol, air-dried and suspended in 100 µl TE pH 8.0. RNA was then digested with RNase A. For PCR amplification of the ITS1-5.8S-ITS2 region of rDNA, ITS1-F (Gardes and Bruns 1993) and ITS4 (White et al. 1990) primers were used. Amplifications were performed in 20 µl reactions containing 2 µl 10× polymerase buffer, 0.2 µM of each dNTP, 200 µg $µl^{-1}$ bovine serum albumin (BSA), 0.25 µM of forward and reverse primers and 0.5 U Taq polymerase (DreamTaq, Thermo Scientific, St. Leon-Rot, Germany). Cycling was carried out using the following programme: 3 min at 94 °C; 35 cycles of 30 s at 94 °C, 30 s at 52 °C, 60 s at 72 °C; 5 min at 72 °C. PCR products were purified by adding 1 U of Exonuclease I and 0.5 U FastAP Alkaline Phosphatase (Thermo Scientific, St. Leon-Rot, Germany) and incubated at 37 °C for 1 h, followed by inactivation at 80 °C for 15 min. Sequencing was performed by Macrogen Inc. (The Netherlands) with PCR primers.

Table 1. Taxa information used in the phylogenetic analyses, new taxa are in bold, "T" refers to type.

Species Name	Collection Number	LSU	ITS	tef1-α	Origin
Agaricus abruptibulbus	ZRL2012005	KT951460	KT951356	KT951626	Yunnan, China
A. albosquamosus T	LD2012192	KT951520	KT951394	KT951636	Thailand
A. amoenus T	ZRL2010072	KT951524	KT951348	KT951638	Yunnan, China
A. angusticystidiatus	**BC088**	–	**MG888054**	–	**Thailand**
A. angusticystidiatus	**ZRL2085**	**MG835413**	**KT951434**	–	**Thailand**
***A. angusticystidiatus* T**	**ZRL2043**	**MG835412**	**JF691553**	–	**Thailand**
A. atrodiscus	LD2012185	KT951473	KT284912	KT951653	Thailand
A. benesii	LAPAG283	–	JF797179	–	Burgos, Spain
A. bernardiformis	CA433	KT951467	KT951321	KT951577	–
A. biannulatus	LAPAG611	–	JF896229	–	Sardinia, Italy
A. biberi	LAPAG687	KR006614	KM657919	KR006642	Hungary
A. bingensis	ADK1992	–	KJ540954	–	Atakora, Benin
A. bisporiticus	LD2012111	KT951507	KJ575611	KT951650	Thailand
A. bisporiticus	MCR25	–	KJ575608	–	Pakistan
A. bisporus	LAPAG446	KR006611	KM657920	KR006640	Burgos, Spain
A. bitorquis	CA427	KT951491	KT951320	KT951646	
A. bitorquis	WZR2012827	KT951492	KM657916	KT951647	Xingjiang, China
A. bohusii	LAPAG562	KR006613	KM657928	KR006641	Madrid, Spain
A. boisseletii	CA123	–	DQ182531	–	–
A. brunneopictus	ADK2564	–	JF514518	–	Plateau Atlantique, Bénin
A. brunneopileatus T	ZRL2012115	KT951489	KT951404	KT951587	Yunnan, China
A. brunneosquamulosus	LD2012105	–	KJ540968	–	Thailand
A. brunneosquamulosus	ZRL4017	–	JF691549	–	Thailand
A. caballeroi	AH44503	–	KJ575605	–	Spain
A. campestris	LAPAG370	KR006607	KM657927	KR006636	Madrid, Spain
A. campestroides	LAPAF2	–	JF727842	–	Plateaux, Togo
A. candidolutescens T	LD2012129	KT951525	KT951335	KT951616	Thailand
A. cf. *bernardi*	CA383	KT951469	KT951319	KT951576	
A. cf. *goossensiae*	ADK2171	–	JF514517	–	Borgou, Benin
A. chiangmaiensis	NTS113	–	JF514531	–	Thailand
A. comtulus	LAPAG724	KT951448	KT951332	KT951593	Burgos, Spain
A. crassisquamosus T	ZRL2012607	KT951510	KT951376	KT951645	Tibet, China
A. cupressicola	LAPAG889	KT951465	KT951334	KT951649	Roma, Italy
A. desjardinii	WZR2012907	KT951474	KM657901	KT951644	Xinjiang, China
A. dilutibrunneus T	ZRL2012010	KT951512	KT951358	KT951569	Yunnan, China
A. dolichopus	ZRL2012715	KT951502	KT951382	KT951573	Tibet, China
A. dolichopus	ZRL2014120	–	KT951433	–	–
A. duplocingulatus	ZRL3064	–	KJ540966	–	Thailand
A. erectosquamosus T	LD2012165	KT951509	KT951338	KT951565	Thailand
A. erythrosarx	MURU6080	–	JF495068	–	–
A. freirei	CA186	–	DQ185553	–	–
A. fuscofibrillosus	WC913	–	AY484684	–	–
A. fuscopunctatus	LD2012115	–	KJ575612	–	Thailand
A. fuscovelatus	RWK2100	–	KJ577973	–	–

Species Name	Collection Number	LSU	ITS	tef1-α	Origin
A. gennadii	CA339	–	KT951318	KT951575	–
A. grandiomyces T	ZRL2012611	KR006624	KM657879	KR006652	Tibet, China
A. gratolens	ZRL3093	KT951488	JF691548	–	Thailand
A. haematinus	ZRL2109	–	KT951435	–	Thailand
A. haematinus	ZRL2136	–	JF691552	–	Thailand
A. hondensis	RWK1938	–	DQ182513	–	USA
A. huijsmanii	LAPAG639	KT951444	KF447889	KT951571	Navarra, Spain
A. kunmingensis	ZRL2012015	KT951506	KT951361	KT951642	Yunnan, China
A. kunmingensis	ZRL2012007	–	KT951427	–	Yunnan, China
A. lamellidistans T	ZRL3099	–	JF691556	–	Thailand
A. laskibarii	LAPAG115	–	AY943975	–	Landes, France
A. leucocarpus T	LD2012159	KX083981	KU975101	KX198048	Thailand
A. leucolepidotus T	LD201214	KT951519	KT951336	KT951635	Thailand
A. linzhiensis T	ZRL2012618	KT951503	KT951378	KT951582	Tibet, China
A. litoralis	LAPAG420	KT951483	KT951327	KT951572	Burgos, Spain
A. litoraloides	ZRL2011249	KT951523	KT951353	KT951580	Yunnan, China
A. magnivelaris	F2389	–	JF727851	–	–
A. martinicensis	F2815	KX084032	JF727855	KX198038	MartiniqueFrance
A. megacystidiatus	LD2012179	–	KF305946	–	Thailand
A. microvolvatulus	LD201271	KT951508	KJ575614	KT951651	Thailand
A. murinocephalus	ZRL3044	–	JF691555	–	Thailand
A. nevoi	LAPAG257	KR006606	KM657922	KR006635	Burgos, Spain
A. nevoi	LAPAG535	–	KT951330	KT951574	Teruel, Spain
A. nigrobrunnescens	DEH632	–	JX308267	–	Hawaii, USA
A. nigrogracilis T	ZRL2012014	KR006621	KM657882	KR006647	Yunnan, China
A. niveogranulatus	LD201124	–	KJ540959	–	Thailand
A. padanus	WZR2012903	KR006616	KM657903	KR006644	Xingjiang, China
A. pallidobrunneus T	ZRL2012358	KT951471	KT951370	KT951566	Yunnan, China
A. parvitigrinus	CA158	–	AY899267	–	–
A. pattersoniae	RWK1415	–	AY943974	–	–
A. phaeolepidotus	CA217	–	DQ185552	–	–
A. pilosporus	LAPAG227	–	KT951425	–	Burgos, Spain
A. pseudolangei	ZRL3012	–	JF691551	–	Thailand
A. rufoaurantiacus	LAPAM15	KX671708	KT951313	KT951641	Dominican Republic
A. silvaticus	ALG07 213		KT951307	KT951567	Algonquin, ON, Canada
A. sinodeliciosus	WZR2012822	KT951518	KM657907	KT951648	Xingjiang, China
A. sordidocarpus	LD201237	–	KJ540946	–	Thailand
A. subrufescens	ZRL2012722	KT951451	KT951383	KT951632	Yunnan, China
A. subsaharianus	ADK4732	–	JF440300	–	Ouagadougou, Burkina Faso
A. sylvaticus	LAPAG382	KR006608	KM657929	KR006637	Burgos, Spain
A. sylvaticus	ZRL2012013	KT951500	KT951360	KT951570	Thailand
A. sylvaticus	ZRL2012568	KT951501	KT951371	KT951568	Tibet, China
A. tibetensis	ZRL2012585	KR006633	KM657895	KR006658	Tibet, China
A. tollocanensis	CA235	–	AY703913	–	–

Species Name	Collection Number	LSU	ITS	tef1-α	Origin
A. toluenolens	CA911	–	KJ540947	–	–
A. trisulphuratus complex	LAPAF7	KR006605	KM657924	KR006634	Plateaux, Togo
A. trisulphuratus complex	Swk079	KT951472	KT951343	KT951561	Lanjak-Entimau, Malaysia
A. trisulphuratus complex	ZRL2014023	–	KT951428	–	China
A. trisulphuratus complex	ZRL2014024	–	KT951429	–	China
A. trisulphuratus complex	ZRL2014030	–	KT951432	–	China
A. trisulphuratus complex	ZRL2132	–	JF691558	–	Thailand
A. tytthocarpus	ZRLWXH3077	KR006618	KM657889	KR006645	Fujian, China
A. variabilicolor	ZRL4002	–	KT951438	–	Thailand
A. variabilicolor	ZRL4007	–	KT951439	–	Thailand
A. variabilicolor	ZRL4012	–	KT951440	–	Thailand
A. variicystis	LD201228	–	KT951426	–	Thailand
A. variicystis T	LD201234	KT951517	KT951339	KT951562	Thailand
A. xanthodermulus	CA160	–	AY899273	–	–
A. xanthodermus	CA15	–	AY899271	–	–
A. xanthodermus	LAPAG387	KR006609	KM657923	KR006638	Soria, Spain
A. xanthosarcus	Goossens5415	–	JF514523	–	–
A. sp.	CA486	–	JF797189	–	–
A. sp.	CA820	–	JF727861	–	–
A. sp.	LD2012162	KT951493	KT951337	KT951563	Thailand
A. sp.	NT020	–	JF797197	–	Thailand
A. sp.	Swk014	KT951482	KT951342	KT951654	Lanjak-Entimau, Malaysia
A. sp.	ZRL133	KT951505	KT951344	KT951656	Thailand
A. sp.	ZRL2010010	KT951511	KT951347	KT951639	Thailand
A. sp.	ZRL2010099	KT951479	KT951349	KT951564	Yunnan, China
A. sp.	ZRL2012267	KT951504	KT951368	KT951655	Yunnan, China
A. sp.	ZRL2012629	KR006627	KM657890	KR006656	Tibet, China
A. sp.	ZRLWXH3078	KT951464	KT951464	KT951643	Fujian, China
A. sp.	ZRLWXH3161	KT951526	KT951391	KT951615	Guangdong, China
A. sp.	ZRLWXH3140	–	KT951441	–	Guangdong, China
Heinemannomyces sp.	ZRL185	KT951527	KT951346	KT951657	Thailand

Sequence alignment, phylogenetic analyses and divergence time estimation

A total of 119 specimens representing 87 species were incorporated in phylogenetic analyses. Three new sequences representing *A. angusticystidiatus* were generated from this study. They are one ITS sequence from specimen BC088 and two LSU sequences from ZRL2085 and ZRL2043 separately. Details of all sequences

are listed in Table 1. Sequences were checked in BioEdit V.7.0.4 first (Hall 2007). Alignments were made by Muscle (Edgar 2004) for each region separately, then adjusted by hand and ambiguous regions removed. Alignments were submitted to TreeBase (Submission ID: 22231). Two data matrices were made for different analyses. The first one is an ITS sequence dataset which contains 84 specimens, all belonging to subgenus *Pseudochitonia* and an outgroup *A. campestris.* This dataset was used for Bayesian and Maximum Likelihood analyses. Phylogenetic trees generated by Bayesian Inference (BI) analysis were performed in MrBayes 3.1.2. (Ronquist and Huelsenbeck 2003). Best model is GTR + I + G which was indicated by MrModeltest 2.2 (Nylander 2004). Ten million generations were run for six Markov chains and sampled every 100th generation resulting in 100,000 trees. Burn-in was determined in Tracer v1.6 with effective sample sizes (ESS) higher than 200 (http://tree.bio.ed.ac.uk/software/tracer). Remaining trees were used to calculate Bayesian posterior probabilities (PP). Maximum Likelihood (ML) analysis and bootstrap values calculation were performed in raxmlGUI 1.5b1 using GTRGAMMA model with 1000 replicates (Silvestro and Michalak 2012). The second dataset included 63 ITS, 61 LSU and 59 tef1-α gene sequences from specimens representing the six subgenera of *Agaricus*. The second multi-gene dataset was used for divergence time estimation. Model selections were performed in jModel Test v. 2 (Darriba et al. 2012) for each gene separately. An XML file was generated in BEAUTI v. 1.8. Priors were set according to the previous fossil-calibrated analysis of Zhao et al. (2016). An independent Monte Carlo Markov Chain of 50 million generations was run and log states every 5,000 generations by BEAST v1.8 (Drummond et al. 2012). The log file was checked in Tracer v. 1.6 (Rambaut et al. 2014) to ensure ESS (Effective Sample Sizes) value higher than 200. An ultrametric maximum-clade-credibility (MCC) tree was summarised using TreeAnnotator 1.8, discarding 10% of states as burn-in and annotating clades with ≥ 0.8 posterior probability.

Results

The Bayesian tree from ITS sequences is shown in Figure 1. A total of 84 sequences are represented from 12 sections of subg. *Pseudochitonia* and *A. campestris* was used as outgroup. All sections are well supported both by posterior probabilities (PP) and bootstrap (BS). Phylogenetic trees generated from Bayesian and ML analyses showed identical topologies and are also almost identical with those of Zhao et al. (2016) with the exception of *A. dilutibrunneus* R.L. Zhao, which clustered with two unknown specimens (*A.* sp./CA486 and *A*. cf. *goossensiae*/ADK2171) and formed a monophyletic clade in our analyses, isolated from all other species in the previous study (Zhao et al. 2016). Our three specimens (*ZRL2043*, *ZRL2085* and *BC088*) formed a monophyletic clade in subg. *Pseudochitonia* which is fully supported both in PP and BS values and located at an isolated position (Fig.1).

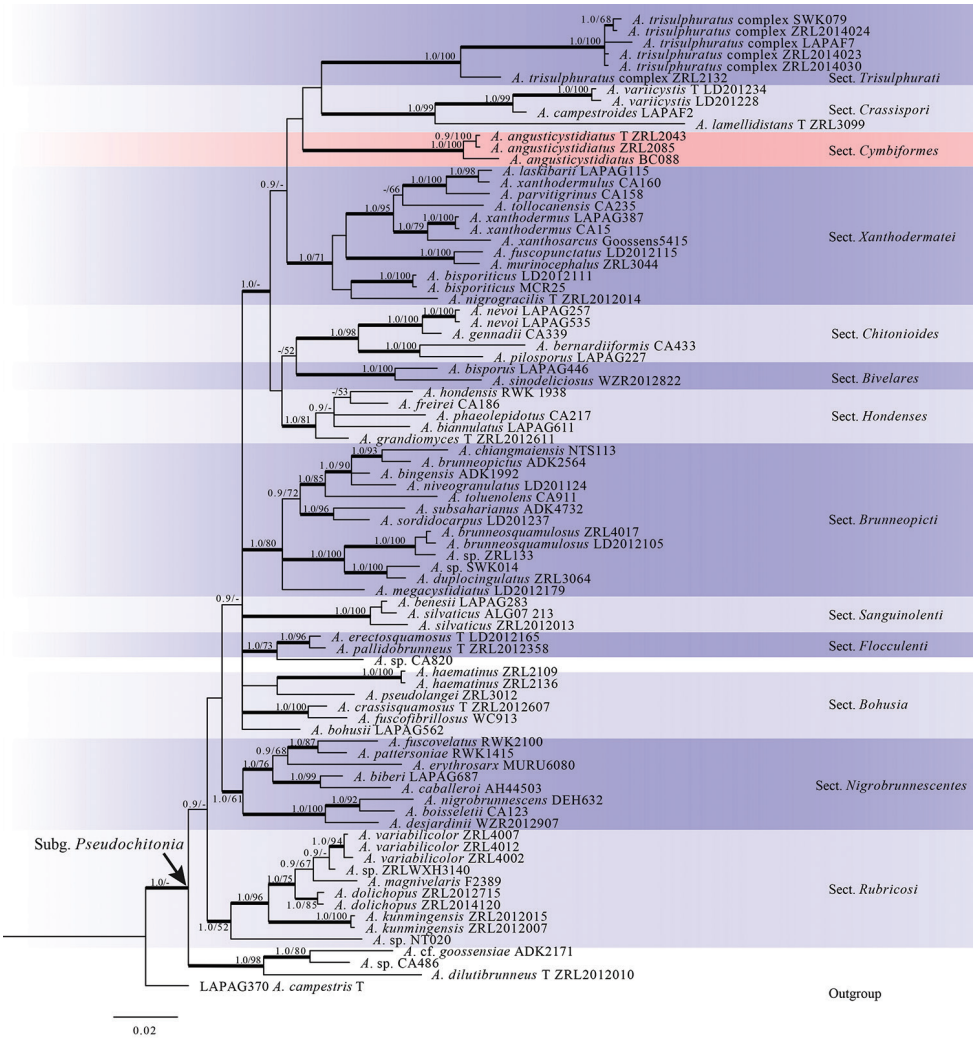

Figure 1. Phylogenetic tree of *Agaricus* subgenus *Pseudochitonia* generated from Bayesian analysis of ITS sequences, rooted with *A. campestris*. Bayesian posterior probability (PP) values ≥ 0.9 or Bootstrap support (BS) values ≥ 50% are indicated at the internodes (PP/BS). The branches in bold mean the related PP > 0.95, "T" refers to sequences from type specimen.

The multi-gene MCC tree is shown in Figure 2. It was conducted based on the dataset of multi-gene sequences. A total of 63 specimens were included, comprising 43 specimens used in ITS analysis, 19 specimens from five subgenera and an outgroup *Heinemannomyces* sp. All subgenera and sections are well-supported statistically. *Agaricus* diverged at the stem age 66 Ma (million years ago), all subgenera diverged between 29.2–33.9 Ma and sections diverged between 20–26.9 Ma. Our three specimens formed a new monophyletic clade in subg. *Pseudochitonia* with strong PP support and this clade diverged at 26.7 Ma.

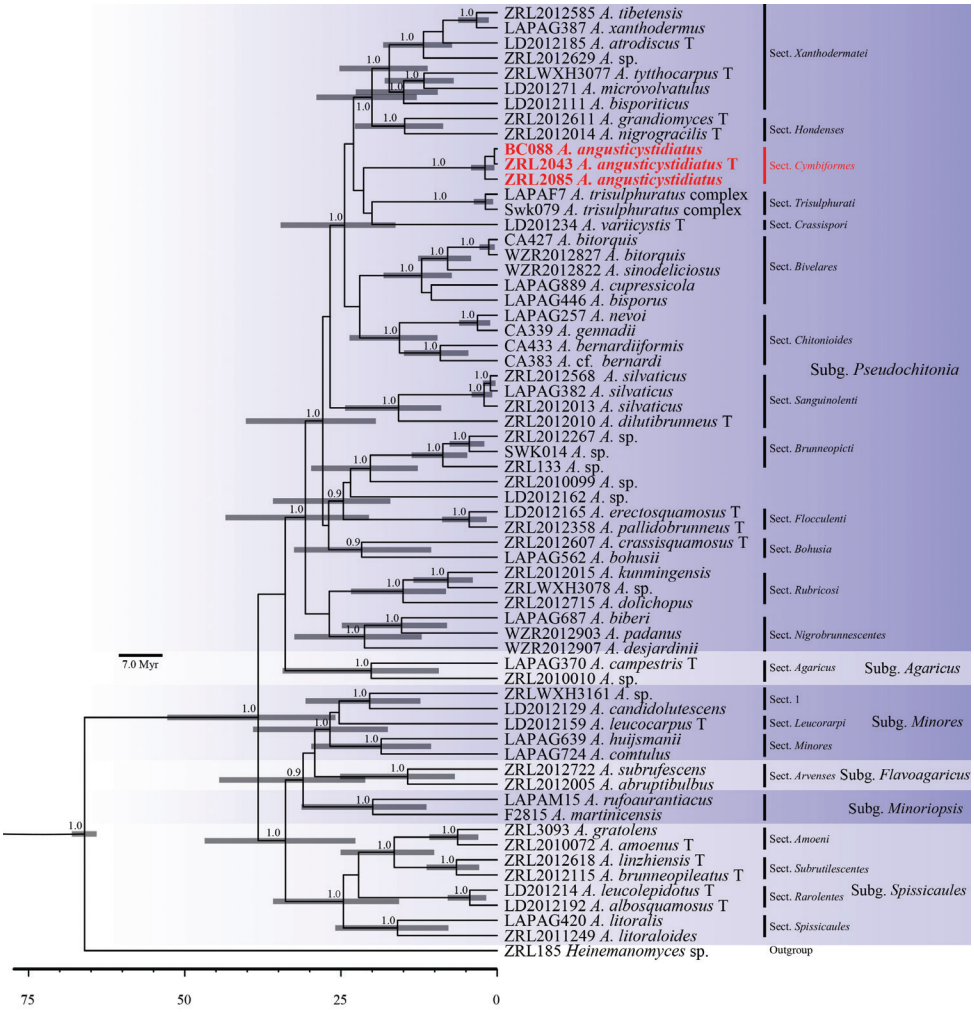

Figure 2. Maximium Clade Credibility tree of genus *Agaricus* based on ITS, LSU and tef1-α gene sequences with the outgroup *Heinemannomyces* sp. Posterior probability values equal or above 0.9 are annotated at the internodes. The 95% highest posterior density of divergence time estimation are marked by horizontal bars.

Taxonomy

***Agaricus* (*Pseudochitonia*) section *Cymbiformes* M.Q. He & R.L. Zhao, sect. nov.**
Mycobank Number: MB824147
Faceoffungi Number: FoF04104

Type species. *Agaricus angusticystidiatus* M.Q. He, Desjardin., K.D. Hyde & R.L. Zhao

Etymology. In reference to the cymbiform basidiospores.

Original description. KOH reaction negative, Schäffer's reaction negative on dry specimens. No discolouration on touching, but discolouration reddish-brown on cutting. Annulus membranous. Smell strong iodoform. Basidiospores cymbiform and cheilocystidia narrow with variable shapes.

Agaricus angusticystidiatus **M.Q. He, Desjardin, K.D. Hyde & R.L. Zhao, sp. nov.**
Mycobank Number: MB825177
Faceoffungi Number: FoF04105
Figure 3

Etymology. refers to the narrow clavate cheilocystidia.

Type. Thailand, Chiang Mai Province, Mae Taeng, Baan Mae Sae village, on Hwy 1095 near 50 km marker, 19°14.599'N, 98°39.456'E, alt. 960 m. In rain forest dominated by *Castanopsis armata*, *Castanopsis* sp., *Pinus* sp., *Lithocarpus* sp., 26 June 2005, collected by Jennifer Kerekes. **Holotype**: *ZRL2043* (HMAS279593); **Isotype**: and SFSUZRL2043,

Original description. *Pileus* 40–80 mm diam., plano-convex, applanate, broadly umbonate; surface concentric squamulose with small skull-cup at disc, appressed, slightly fissured, light brown (6D8), brown (7E3), greyish-brown (5D5), dark brown (6D6) against the grey (8E3) background. Context 4–5 mm thick at disc, fragile, white to grey (8E3) in age. *Lamellae* free, crowded, lamellulae with 3–4 lengths, 3–4 mm broad, normal to slightly ventricose, brown (7E5) to dark brown (7F7-8), edge colour similar to the gill itself. *Stipe* 55–100 × 5–8 (base 8–15) mm, cylindrical bulbous, with rhizomorphs in most cases, hollow, surface glabrous to silky, white to dark brown (6D6). *Annulus* pendent or percurrent; single; upper side membranous, white; lower side surface powdery, light yellow (4B2) grain-like dots in circulate; superior, persistent, edge entire, up to 5 mm broad. Smell of iodoform. No colour change on touching; light dull red, greyish brown (7D4) on cutting.

KOH reaction: negative. Schäffer's reaction: negative on dry specimens.

Basidiospores 5–6.5 × 3–4 (–4.5) µm [X = 5.6 ± 0.5 × 3.8 ± 0.4, Q = 1.1–2.2, Q_m = 1.52 ± 0.7, n = 20], cymbiform, some endosporium, no germ pore, brown. *Basidia* 10–15 × 5.5–7 µm, clavate, hyaline, smooth, 4-spored. *Pleurocystidia* absent. *Cheilocystidia* 20–30 (–45) × 5–8 µm, occasionally one septum, narrowly clavate to clavate, some with elongated top, rarely subcapitate, hyaline, smooth. *Pileipellis* cutis consisting of 3–5 µm diam. hyphae, hyaline, smooth, non-constricted at septa. Annulus hyphae same as pileipellis.

Habit. Gregarious on soil in rain forest which is mainly dominated by *Castanopsis armata*, *Castanopsis* sp., *Pinus* sp., *Lithocarpus* sp.

Distribution. Thailand, Chiang Mai Province (type distribution).

Other materials examined. Thailand, Chiang Mai Province, Mae Taeng, Ban Mae Sae Village, on Hwy 1095 near 50 km marker, 19°14.599'N, 98°39.456'E, elev. ca. 960 m, 3 July 2004, collected by Thitiya Boonpratuang, *ZRL2085* (HMAS279594, and

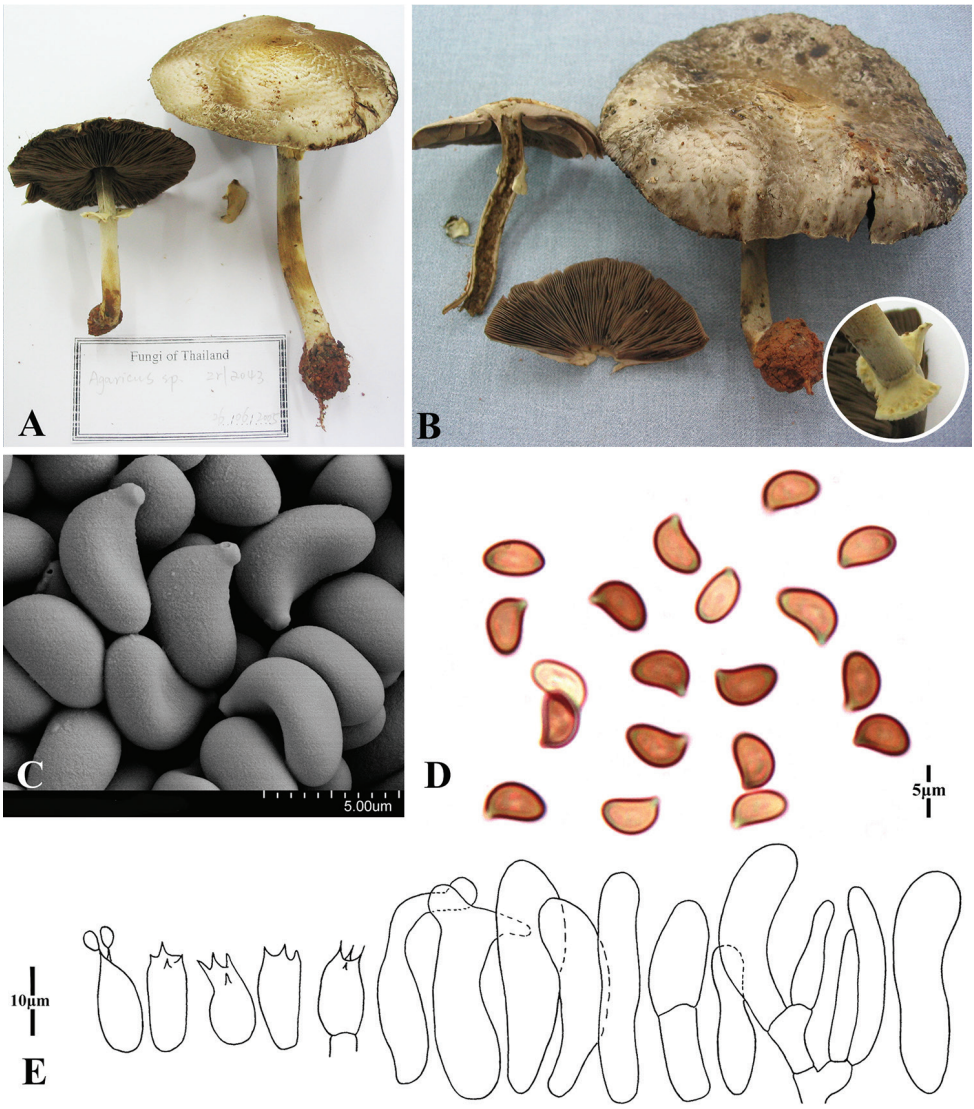

Figure 3. Morphology of *Agaricus angusticystidiatus* **A, B** basidiomes **C, D** basidiospores **E** basidia and cheilocystidia.

SFSUZRL2085); Thailand, Chiang Mai Province, Mae Taeng, Mushrooms research center, 30 July 2014, collected by Boontiya Chuankid, *BC088* (MFLU 14-0903).

Notes. This new species is morphologically distinguished from other *Agaricus* species by its strong iodoform smell, context reddish-brown discolouration on cutting, cymbiform basidiospores and narrow cheilocystidia with variable shapes. Phylogenetic analyses confirmed it is a member of the subgenus *Pseudochitonia* with an isolated phylogenetic position in *Agaricus*. This new species is similar to *A. iodolens* Heinem. & Gooss.-Font. of section *Xanthodermatei*, because both have relatively slender basidiomes and odour of iodine (Naritsada et al. 2014). However, this new species has

cymbiform basidiospores and a bulbous stipe, while those of *A. iodolens* are ellipsoid and an equal stipe (Zoberi 1972). *Agaricus lamellidistans* R.L. Zhao and *A. variicystis* L.J. Chen, K. D. Hyde & R. L. Zhao of section *Crassispori* resemble this new species, because all have greyish-brown pilei and cymbiform basidiospores. These species lack discolouration on cutting, while those of *A. angusticystidiatus* have dull red discolouration on cutting (Zhao et al. 2016).

Discussion

Based on phylogenetic and morphological studies, we propose *A. angusticystidiatus* as a new species in subgenus *Pseudochitonia*. Furthermore, the dating analysis, based on multi-gene sequences, indicated that *A. angusticystidiatus* diverged at 26.7 Ma which is slightly older than other sections in *Agaricus* (18–26 Ma, in Zhao et al. 2016). Therefore, a new section *Cymbiformes* is proposed, which presently only contains species *A. angusticystidiatus*. Thus up to now, there are six subgenera and 24 sections in the genus *Agaricus* (Zhao et al. 2016; Chen et al. 2017; Parra et al. 2018).

Zhao et al. 2016 had conducted a reconstruction of the taxonomic system of *Agaricus*. In that study, they used the following criteria to recognise subgenera and sections: "(i) they must be monophyletic and statistically well-supported in the multigene analyses; (ii) their respective stem ages should be roughly equivalent and subgenera stem ages must be older than section stem ages; and (iii) they should be identifiable phenotypically, whenever possible" (Zhao et al. 2016). That means divergence time has been used as an additional criterion to rank taxa of above species level in *Agaricus*. Later, the criterion of divergence time, along with phylogenetic, monophyletic and morphological support, has been accepted in other new subgenus and section recognitions in *Agaricus*, such as a new subgenus *Minoriopsis* (Chen et al. 2017); and a new section *Kerrigania* (Parra et al. 2018).

As mentioned before, this proposed new section *Cymbiformes* has a closely phylogenetic relationship with sections *Trisulphurati* and *Crassispori*. In morphology, all of them differed with other sections of *Agaricus* by the combination of negative Schäffer's reaction, chemical odours such as phenol, ink or carbolic acid and basidiospores endosporium and often cymbiform. However, section *Trisulphurati* has woolly squamules on the surfaces of the pileus and stipe and the other two sections only have appressed squamules at the centre of the pileus. Furthermore, this new section *Cymbiformes* could be separated from section *Crassispori* by its negative KOH reaction and developed annulus (the latter is positive KOH reaction and with fragile annulus) (Zhao et al. 2016).

So far, section *Cymbiformes* is only known from a tropical area. The cymbiform basidiospores are rare in *Agaricus* species. Presently there are three *Agaricus* species from tropical areas which have this kind of basidiospores. They are *A. angusticystidiatus* of section *Cymbiformes* and *A. lamellidistans* and *A. variicystis* of section *Crassispori* (Zhao et al. 2016). In phylogenetic analyses, these two sections also show a close phylogenetic

position, which is similar to previous studies (specimens *ZRL2043* and *ZRL2085* were treated as *A*. sp. in Zhao et al. 2011; Zhao et al. 2016). The presence of cymbiform basidiospores is a common character in another genus *Micropsalliota* of Agaricaceae. In phylogenetic analyses, *Agaricus* is sister to *Hymenagaricus,* then sister to *Chlorophyllum, Heinemannomyces* and *Micropsalliota* (Zhao et al. 2017) and all of them have tropical distribution habitats. Thus we hypothesised that cymbiform basidiospores have formed at least twice in evolutionary events and are associated with tropical environments.

Acknowledgements

This project was conducted under the financial support of the National Key R&D Program of China (Project No. 2018YFD0400200), the National Natural Science Foundation of China (Project ID:31470152 and 31360014) and Beijing Innovative Consortium of Agriculture Research System (Project ID: BAIC05-2018).

References

Capelli A (1984) *Agaricus*, Fungi Europaei. Libreria editrice Biella Giovanna, I – 21047, Saronno, Italy 1, 1–560.

Chen J, Callac P, Parra LA, Karunarathna SC, He MQ, Moinard M, De Kesel A, Raspé O, Wisitrassameewong K, Hyde KD, Zhao RL (2017) Study in *Agaricus* subgenus *Minores* and allied clades reveals a new American subgenus and contrasting phylogenetic patterns in Europe and Greater Mekong Subregion. Persoonia 38: 170–196. https://doi.org/10.3767/003158517X695521

Chen J, Zhao RL, Parra LA, Guelly AK, De Kesel A, Rapior S, Hyde KD, Chukeatirote E, Callac P (2015) *Agaricus* section *Brunneopicti*: a phylogenetic reconstruction with descriptions of four new taxa. Phytotaxa 192(3): 145–168. https://doi.org/10.11646/phytotaxa.192.3.2

Darriba D, Taboada GL, Doallo R, Posada D (2012) jModelTest 2: more models, new heuristics and parallel computing. Nature methods 9: 772. https://doi.org/10.1038/nmeth.2109

De Silva DD, Rapior S, Fons F, Bahkali AH, Hyde KD (2012) Medicinal mushrooms in supportive cancer therapies: an approach to anti-cancer effects and putative mechanisms of action. Fungal Diversity 55(1): 1–35. https://doi.org/10.1007/s13225-012-0151-3

De Silva DD, Rapior S, Hyde KD, Bahkali AH (2013a) Medicinal mushrooms in prevention and control of diabetes mellitus. Fingal Diversity 56(1): 1–29. https://doi.org/10.1007/s13225-012-0187-4

De Silva DD, Rapior S, Sudarman E, Stadler M, Xu JC, Alias SA, Hyde KD (2013b) Bioactive metabolites from macrofungi: ethnopharmacology, biological activities and chemistry. Fungal Diversity 62(1): 1–40. https://doi.org/10.1007/s13225-013-0265-2

Doyle JJ (1990) Isolation of plant DNA from fresh tissue. Focus 12: 13–15.

Drummond AJ, Suchard MA, Xie D, Rambaut A (2012) Bayesian phylogenetics with BEAUti and BEAST 1.7. Molecular Biology and Evolution 29(8): 1969–1973. https://doi.org/10.1093/molbev/mss075

Edgar RC (2004) MUSCLE: multiple sequence alignment with high accuracy and high throughput. Nucleic Acids Research 32(5): 1792–1797. https://doi.org/10.1093/nar/gkh340

Gardes M, Bruns TD (1993) ITS primers with enhanced specificity for basidiomycetes—application to the identification of mycorrhizae and rusts. Molecular ecology 2(2): 113–118. https://doi.org/10.1111/j.1365-294X.1993.tb00005.x

Hall T (2007) BioEdit v7. Ibis Biosciences, Carlsbad Available from: http://www.mbio.ncsu.edu/BioEdit/BioEdit.html

He MQ, Chen J, Zhou JL, Ratchadawan C, Hyde KD, Zhao RL (2017) Tropic origins, a dispersal model for saprotrophic mushrooms in *Agaricus* section *Minores* with descriptions of sixteen new species. Scientific Reports 7(1): 5122. https://doi.org/10.1038/s41598-017-05203-5

Kornerup A, Wanscher JH (1978) Methuen handbook of colour (3rd edn). Eyre Methuen, London.

Largent DL (1986) How to identify mushrooms to genus vol. I–V. Mad River Press Eureka.

Lebel T (2013) Two new species of sequestrate *Agaricus* (section *Minores*) from Australia. Mycological Progress 12(4): 699–707. https://doi.org/10.1007/s11557-012-0879-x

Llarena-Hernández RC, Renouf E, Vitrac X, Mérillon JM, Savoie JM (2017) Antioxidant Activities and Metabolites in Edible Fungi, a Focus on the Almond Mushroom *Agaricus subrufescens*. In: Mérillon J-M, Ramawat KG (Eds) Fungal Metabolites. Springer International Publishing AG, Cham, 739–760.

Moncalvo JM, Lutzoni FM, Rehner SA, Johnson J, Vilgalys R (2000) Phylogenetic relationships of Agaric fungi based on nuclear large subunit ribosomal DNA sequences. Systematic biology 49(2): 278–305. https://doi.org/10.1093/sysbio/49.2.278

Moncalvo JM, Vilgalys R, Redhead SA, Johnson JE, James TY, Aime MC, Hofstetter V, Verduin SJW, Larsson E, Baroni TJ, Thorn RG, Jacobsson S, Clémençon H, Miller Jr OK (2002) One Hundred and Seventeen Clades of Euagarics. Molecular phylogenetics and evolution 23(3): 357–400. https://doi.org/10.1016/S1055-7903(02)00027-1

Morehouse EA, James TY, Ganley ARD, Vilgalys R, Berger L, Murphy PJ, Longcore JE (2003) Multilocus sequence typing suggests that the chytrid pathogen of amphibians is a recently emerged clone. Molecular Ecology 12(2): 395–403. https://doi.org/10.1046/j.1365-294X.2003.01732.x

Naritsada T, Nawaz R, Khalid AN, Chen J, Hyde KD, Zhao R, Parra LA, Hanif M, Moinard M, Callac P (2014) Morphological and molecular characterization of three *Agaricus* species from tropical Asia (Pakistan, Thailand) reveals a new group in section *Xanthodermatei*. Mycologia 106(6): 1220–1232. https://doi.org/10.3852/14-076

Nylander J (2004) MrModeltest v2. Program distributed by the author. Evolutionary Biology Centre, Uppsala University.

Parra LA, Angelini C, Ortiz-Santana B, Mata G, Billette C, Rojo C, Chen J, Callac P (2018) The genus *Agaricus* in the Caribbean. Nine new taxa mostly based on collections from the Dominican Republic. Phytotaxa 345(3): 219–271. https://doi.org/10.11646/phytotaxa.345.3.2

Rambaut A, Suchard MA, Xie D, Drummond AJ (2014) Tracer v1.6. Available from http://beast.bio.ed.ac.uk/Tracer [accessed on 24 July 2015]

Ronquist F, Huelsenbeck JP (2003) MrBayes 3: Bayesian phylogenetic inference under mixed models. Bioinformatics 19(12): 1572–1574. https://doi.org/10.1093/bioinformatics/btg180

Silvestro D, Michalak I (2012) raxmlGUI: a graphical front-end for RAxML. Organisms Diversity & Evolution 12(4): 335–337. https://doi.org/10.1007/s13127-011-0056-0

Singer R (1986) The Agaricales in modern taxonomy. ed. 4. J. Cramer, Vaduz.

White TJ, Bruns T, Lee SJ, Taylor JL (1990) Amplification and direct sequencing of fungal ribosomal RNA genes for phylogenetics. In: Innis MA, Gelfand DH, Sninsky J, White TJ (Eds) PCR Protocols: a Guide to Methods and Applications. Academic Press, San Diego, 315–322.

Zhao RL, Karunarathna SC, Raspé O, Parra LA, Guinberteau J, Moinard M, De Kesel A, Barroso G, Courtecuisse R, Hyde KD, Guelly AK (2011) Major clades in tropical *Agaricus*. Fungal Diversity 51(1): 279–296. https://doi.org/10.1007/s13225-011-0136-7

Zhao RL, Zhou JL, Chen J, Margaritescu S, Sánchez-Ramírez S, Hyde KD, Callac P, Parra LA, Li GJ, Moncalvo JM (2016) Towards standardizing taxonomic ranks using divergence times–a case study for reconstruction of the *Agaricus* taxonomic system. Fungal Diversity 78(1): 239–292. https://doi.org/10.1007/s13225-016-0357-x

Zhao RL, Li GJ, Sánchez-Ramírez S, Stata M, Yang ZL, Wu G, Dai YC, He SH, Cui BK, Zhou JL, Wu F (2017) A six-gene phylogenetic overview of Basidiomycota and allied phyla with estimated divergence times of higher taxa and a phyloproteomics perspective. Fungal Diversity 84(1): 43–74. https://doi.org/10.1007/s13225-017-0381-5

Zoberi MH (1972) Tropical Macrofungi: some common species. Palgrave Macmillan, London, 99–108. https://doi.org/10.1007/978-1-349-01618-1_20

MycoKeys 40: 69–88 (2018)
doi: 10.3897/mycokeys.40.26025
http://mycokeys.pensoft.net

RESEARCH ARTICLE

A peer-reviewed open-access journal
MycoKeys
Launched to accelerate biodiversity research

Three new species of *Krogia* (Ramalinaceae, lichenised Ascomycota) from the Paleotropics

Sonja Kistenich[1], Jouko K. Rikkinen[2,3], Holger Thüs[4,5], Charles S. Vairappan[6], Patricia A. Wolseley[4], Einar Timdal[1]

1 *Natural History Museum, University of Oslo, 0318 Oslo, Norway* **2** *Finnish Museum of Natural History, University of Helsinki, 00014 Helsinki, Finland* **3** *Department of Biosciences, University of Helsinki, 00014 Finland* **4** *Department of Life Sciences, The Natural History Museum, London SW75BD, UK* **5** *State Museum of Natural History Stuttgart, Rosenstein 1, 70191 Stuttgart, Germany (current address)* **6** *Institute for Tropical Biology and Conservation, Universiti Malaysia Sabah, 88400 Kota Kinabalu, Sabah, Malaysia*

Corresponding author: *S. Kistenich* (s.d.kistenich@nhm.uio.no)

Academic editor: *Imke Schmitt* | Received 20 April 2018 | Accepted 10 September 2018 | Published 26 September 2018

Citation: Kistenich S, Rikkinen JK, Thüs H, Vairappan CS, Wolseley PA, Timdal E (2018) Three new species of *Krogia* (Ramalinaceae, lichenised Ascomycota) from the Paleotropics. MycoKeys 40: 69–88. https://doi.org/10.3897/mycokeys.40.26025

Abstract

Krogia borneensis Kistenich & Timdal, *K. isidiata* Kistenich & Timdal and *K. macrophylla* Kistenich & Timdal are described as new species, the first from Borneo and the two latter from New Caledonia. The new species are supported by morphology, secondary chemistry and DNA sequence data. *Krogia borneensis* and *K. isidiata* contain sekikaic and homosekikaic acid, both compounds reported here for the first time from the genus. *Krogia macrophylla* contains an unknown compound apparently related to boninic acid as the major compound. DNA sequences (mtSSU and nrITS) are provided for the first time for *Krogia* and a phylogeny of the genus based on 15 accessions of five of the six accepted species is presented. *Krogia antillarum* is reported as new to Brazil, Guatemala and Mexico.

Keywords

Borneo, New Caledonia, lichens, *Phyllopsora*, phylogeny, rainforest, TLC

Introduction

Krogia Timdal is a corticolous genus occurring in tropical humid forests and rainforests. It closely resembles the much more common genus *Phyllopsora* Müll. Arg. in thallus morphology, but differs mainly in having a weak or absent amyloid reaction in the tholus of the asci and filiform, curved ascospores that are spirally arranged in the ascus (Timdal 2002). In *Phyllopsora*, the tholus shows a deeply amyloid conical structure (*Bacidia*-type) and the ascospores vary from ellipsoid to acicular, but are never spirally arranged. Nearly every examined specimen of *Krogia* has at least some scattered red or purple patches on the thallus or apothecia caused by non-crystalline, acetone-insoluble pigment(s).

Three species of *Krogia* are known: *K. antillarum* Timdal (the West Indies; Timdal 2009), *K. coralloides* Timdal (Mauritius; Timdal 2002) and *K. microphylla* Timdal (the Dominican Republic; Lumbsch et al. 2011). All species are recently discovered and known from only a few collections.

During revision of material of *Phyllopsora* from Southeast Asia and Oceania, we have come across material of three apparently undescribed *Krogia* species. There are no published sequences of *Krogia*, but we have provided sequences of the mitochondrial small subunit (mtSSU) and of the nuclear ribosomal transcribed spacer region (ITS) from the three putative new species and from two of the three previously described species. The sequences, some of which were taken from an unpublished paper on the phylogeny of the Ramalinaceae (Kistenich et al. in press), were used to infer a phylogeny.

Material and methods

The specimens

The specimens of the three new species were discovered during ongoing global studies of *Phyllopsora* by Kistenich and Timdal in material provided by Rikkinen (New Caledonia) and Thüs, Vairappan and Wolseley (Borneo), with additional specimens provided by A. Elvebakk (New Caledonia) and A. Paukov (Borneo). The specimens are deposited in B, BM, BORH, H, O and PC. DNA sequences of the two previously described *Krogia* species were generated from specimens in B and O and from a specimen provided by P. Diederich (hb Diederich). Additionally, we included 14 mtSSU and 12 ITS sequences (Table 1) from nine species in six genera known to be closely related to *Krogia* as well as from the holotype of the genus *Krogia*, *K. coralloides*, from a previous molecular study on the family Ramalinaceae (Kistenich et al. in press).

Anatomy

Microscope sections were cut using a freezing microtome and mounted in water, 10% KOH (K), lactophenol cotton blue and a modified Lugol's solution, in which water

Table 1. Specimens used in this study with voucher information, major lichen substances and GenBank accession numbers. New sequences are indicated by accession numbers in bold.

Species and sequence ID	Voucher	Major lichen substances	mtSSU	ITS
Aciculopsora salmonea	Costa Rica, 2004, Lücking 17543 (BR), **isotype**	–	MG925842	MG925948
Bacidia rosella	Sweden, 1997, Ekman 3117 (BG)	–	AY300877	AF282086
Bacidia rubella	Switzerland, van den Boom 41103 (LG DNA 578)	–	JQ796830	JQ796852
Bacidia sipmanii	Tenerife, Sérusiaux s.n. (LG DNA 361)	–	JQ796832	JQ796853
Bacidina brittoniana	USA, 1999, Ekman 3657 (BG)	–	–	MG925954
Bacidina delicata	France, Sérusiaux s. n. (LG DNA 369)	–	JQ796834	JQ796854
Bacidina neosquamulosa	Netherlands, van den Boom 41056 (LG DNA 490)	–	JQ796837	JQ796855
Bacidina phacodes	Sweden, 1998, Ekman 3414 (UPS)	–	AY567725	AF282100
Eschatogonia prolifera I	Peru, 2006, Timdal 10207 (O)	didymic acid	MG925870	MG925969
Eschatogonia prolifera II	Peru, 2006, Timdal 10429 (O)	didymic acid	MG925871	MG925970
Krogia antillarum I	Trinidad And Tobago, 2008, Rui & Timdal 10844 (O), **paratype**	4-O-methylcrypto-chlorophaeic acid	**MH174271**	**MH174281**
Krogia antillarum II	Guatemala, 2002, Andersohn s.n. (B)	4-O-methylcrypto-chlorophaeic acid	**MH174272**	–
Krogia antillarum III	Mexico, 1994, Wolf & Sipman 2052 (B)	4-O-methylcrypto-chlorophaeic acid	**MH174273**	**MH174282**
Krogia antillarum IV	Brazil, 2015, Dahl, Kistenich, Timdal & Toreskaas AM-39 (O)	4-O-methylcrypto-chlorophaeic acid	**MH174274**	**MH174283**
Krogia borneensis I	Malaysia, 2013, Vairappan & Thüs L291 (BORH), **holotype**	sekikaic acid, homosekikaic acid	**MH174275**	–
Krogia borneensis II	Malaysia, 2012, Wolseley, Thüs & Vairappan D-3-10-2 (BM)	sekikaic acid, homosekikaic acid	**MH174276**	–
Krogia borneensis III	Malaysia, 2014, Paukov 2234 (B)	sekikaic acid, homosekikaic acid	**MH174277**	–
Krogia borneensis	Malaysia, 1997, Wolseley Q21 p.p. (BM)	sekikaic acid, homosekikaic acid	–	–
Krogia borneensis	Malaysia, 2013, Vairappan & Thüs L229 (BM)	sekikaic acid, homosekikaic acid	–	–
Krogia coralloides I	Mauritius, 1991, Krog & Timdal MAU51/83 (O), **holotype**	boninic acid, unknown	MG925875	MG925977
Krogia coralloides II	Mauritius, 2016, Diederich 18455 (hb. Diederich)	boninic acid, unknown	**MH174278**	**MH174284**
Krogia isidiata I	New Caledonia, 2005, Elvebakk 05:633 (O), **holotype**	sekikaic acid, homosekikaic acid	–	**MH174285**
Krogia isidiata II	New Caledonia, 2016, Rikkinen 34385 (H)	sekikaic acid, homosekikaic acid	**MH174279**	**MH174286**
Krogia isidiata	New Caledonia, 2016, Rikkinen 35034 (H)	sekikaic acid, homosekikaic acid	–	–
Krogia isidiata	New Caledonia, 2016, Rikkinen 35688 (H)	sekikaic acid, homosekikaic acid	–	–
Krogia macrophylla I	New Caledonia, 2016, Rikkinen 36047 (H)	unknown	–	**MH174287**
Krogia macrophylla II	New Caledonia, 2016, Rikkinen 36077 (H), **holotype**	unknown	–	**MH174288**
Krogia macrophylla III	New Caledonia, 2016, Rikkinen 35037 (H)	unknown	–	**MH174289**
Krogia macrophylla IV	New Caledonia, 2011, Rikkinen 38565 (H)	unknown	**MH174280**	**MH174290**
Physcidia wrightii I	Mauritius, 1991, Krog & Timdal MAU14/14 (O)	sekikaic acid, divaricatic acid	MG925911	–
Physcidia wrightii II	Mauritius, 1991, Krog & Timdal MAU13/10 (O)	sekikaic acid, divaricatic acid	MG925912	–
Toninia cinereovirens	Norway, 1994, Haugan & Timdal 7953 (O)	–	AY567724	AF282104
Waynea californica	USA, 1995, Ekman L1486 (UPS)	–	MG925947	–

was replaced by 50% lactic acid. Amyloid reactions were observed in the modified Lugol's solution after pretreatment in K and crystals of lichen substances were observed using polarised light.

Secondary chemistry

Thin-layer chromatography (TLC) was performed in accordance with the methods of Culberson (1972), modified by Menlove (1974) and Culberson and Johnson (1982). Examinations were made in the three standard solvent systems A, B' and C.

DNA extraction, PCR and sequencing

We extracted DNA from apothecia and/or thallus tissue of 14 *Krogia* specimens. The DNA extraction followed the protocol described by Bendiksby and Timdal (2013). We selected the two genetic markers mtSSU and nrITS (including ITS1, 5.8S and ITS2) for molecular analyses. Polymerase chain reactions (PCR) were performed with the primer pairs mtSSU1 and mtSSU3R (Zoller et al. 1999) for mtSSU as well as ITS1-F (Gardes and Bruns 1993) and ITS4 (White et al. 1990) for ITS. In case of poor amplification success, internal primers were used: mtSSUF (5'-ACCAGTAGTGAAGTATGTTGTT-3') and mtSSUR (5'-AACAACATACTTCACTACTGGT-3') for mtSSU and ITS_lichF and ITS_lichR (Bendiksby and Timdal 2013) for ITS. We used the following cycling conditions: 95 °C for 7 min, 35 cycles of 95 °C for 30 s, 60 °C for 30 s, 72 °C for 30 s, followed by 72 °C for 7 min. We used Illustra PuReTaq Ready-To-Go PCR Beads (GE Healthcare, Buckinghamshire, UK) with half-sized reactions, i.e. prior to adding DNA, we transferred 12 µl of the mixture to a new PCR tube. To this, we added 0.5 µl of template DNA and 1 µl of each primer (10 µM). The PCR products were purified with the Illustra ExoProStar Clean-Up Kit (GE Healthcare, Buckinghamshire, UK) following the manufacturer's instructions, but with a 10-fold enzyme dilution. We sent the purified PCR products to Macrogen Europe (Amsterdam, The Netherlands) for Sanger sequencing according to the company's instructions for sample preparation.

DNA sequence analysis

We assembled and edited the resulting sequences using the software Geneious R9 (Kearse et al. 2012). For the separate alignment of the variable ITS1 and ITS2 sequences, we used PASTA version 1.7 (Mirarab et al. 2015) with OPAL as aligner and merger, the maximum subproblem set to 50%, RAxML as the tree estimator under a GTR+Γ model and a maximum of 500 iterations. We also used PASTA for the mtSSU alignment with the same settings except that we used a GTR+I+Γ model. As the 5.8S alignment contains mainly conserved regions, the online version of MAFFT version

7.313 (http://mafft.cbrc.jp/alignment/software/; Katoh and Standley 2013) was used (G-INS-i) with default settings except that the scoring matrix was set to 2PAM. Alignments were concatenated for subsequent analyses.

We used PartitionFinder2 (Lanfear et al. 2016) to infer the best-fitting substitution models and partitioning scheme for the concatenated alignment with the Bayesian Information Criterion (BIC) to select amongst all possible combinations of models implemented in MrBayes (1-, 2- and 6-rate models). Subset rates were treated as proportional ('linked branch lengths'). We defined four potential subsets prior to the analysis: mtSSU, ITS1, 5.8S and ITS2.

Three *Bacidia* De Not. species, *B. rosella* (Pers.) De Not., *B. rubella* (Hoffm.) A. Massal. and *B. sipmanii* M. Brand et al., were used as outgroup in all phylogenetic analyses based on the molecular phylogeny of the Ramalinaceae (Kistenich et al. in press). We checked for incompatibilities amongst gene trees by subjecting each marker to a simple maximum likelihood bootstrap analysis as implemented in RAxML Black Box 8.2.10 (Stamatakis 2014) on the CIPRES webserver (Miller et al. 2010) with default settings. Resulting gene trees were inspected manually for incompatibilities.

The alignment was subjected to maximum likelihood analyses using Garli 2.01 (Zwickl 2006) on the CIPRES webserver (Miller et al. 2010) and on the Abel high performance computing cluster (University of Oslo, Norway) under the models and partitioning scheme suggested by PartitionFinder2. We searched for the best tree using 500 repetitions from a random tree. We ran the nonparametric bootstrapping analysis with 500 replicates, each on 10 search replicates from a random tree.

We analysed the alignment phylogenetically using MrBayes 3.2.6 (Altekar et al. 2004; Ronquist and Huelsenbeck 2003) with BEAGLE (Ayres et al. 2012) on the CIPRES webserver (Miller et al. 2010). We used a (1, 1, 1, 1, 1, 1) Dirichlet for the rate matrix, a (1, 1, 1, 1) Dirichlet for the state frequencies, an exponential (1) distribution for the gamma shape parameter and a uniform (0, 1) distribution for the proportion of invariable sites. Subset rates were assumed proportional with the prior distribution following a (1, 1, 1, 1, 1, 1, 1) Dirichlet. We assumed a compound Dirichlet prior on branch lengths (Rannala et al. 2011; Zhang et al. 2012). For the gamma distribution component of this prior, we set $\alpha = 1$ and $\beta = 0.5$, as the expected tree length α/β (taken from the preceding maximum likelihood analysis) was approximately 1.9. The Dirichlet component of the distribution was set to the default (1, 1). Four parallel Markov chain Monte Carlo (MCMC) runs were performed, each with six chains and the temperature increment parameter set to 0.2 (Altekar et al. 2004). The appropriate degree of heating, adjusted for swap rates in the interval 0.1–0.7, was determined by monitoring cold and hot chains in preliminary runs. We used a burnin of 50% and sampled every 1000th tree. The runs were diagnosed for convergence every 10^6 generations and were set to terminate either at convergence or after having reached 100×10^6 generations. Convergence was defined as an average standard deviation of split frequencies (ASDSF) smaller than 0.01. We projected the bootstrap support (BS) values from the Garli-analysis on to the MrBayes majority rule consensus tree with posterior probabilities (PP) and collapsed branches with BS < 50 and PP < 0.7. The resulting trees were edited in TreeGraph 2 (Stöver and Müller 2010).

Results

Secondary chemistry

The results of the TLC analyses are shown in Table 1. We identified four lichen substances: 4-O-methylcryptochlorophaeic acid (in *K. antillarum*), sekikaic acid and homosekikaic acid (in *K. borneensis* and *K. isidiata*) and boninic acid (in *K. coralloides*). An unidentified major compound, similar to boninic acid in colour and fluorescence on the developed chromatograms, occurred in *K. coralloides* and *K. macrophylla*. On the chromatograms, the two compounds were first pale brown, then after a few days turning greyish-pink, UV_{366}+ blue and occurred in R_f-classes A:5, B':5, C:6; the unknown moved just above boninic acid in all solvent systems.

Molecular data and phylogenetic analyses

We successfully generated DNA sequences for 14 *Krogia* specimens, including 10 mtSSU and 10 ITS sequences (Table 1). The final dataset comprised 29 accessions (Table 1) and resulted in a 1424 bp long alignment counting 28% missing data and 470 parsimony-informative sites. The alignment is available at TreeBase (https://treebase.org – study no. 22518).

Initial RAxML analyses produced congruent gene trees of the mtSSU and ITS datasets; only unsupported (< 0.7) topological differences between the consensus trees were observed. We therefore continued with the subsequent phylogenetic analyses. PartitionFinder2 suggested three subsets and two different substitution models, the GTR+G model for (1) mtSSU, (2) ITS1 and ITS2 and the K80+I model for (3) 5.8S. The likelihood score of the best tree found by Garli was –8023.487881. The Bayesian analysis halted automatically after 3 million generations, when the ASDSF in the last 50% of each run had fallen below 0.01. We used 6004 trees for constructing the final majority-rule consensus tree. The phylogenetic results generated by Garli and MrBayes showed no incongruences. The extended majority-rule consensus tree of our alignment (Fig. 1), based on the Bayesian topology with all compatible groups (BS ≥ 50 and/or PP ≥ 0.7), shows that all *Krogia* accessions group together in five distinct and well-supported clades with short terminal branches. Accessions of *Bacidina* Vězda were resolved as the phylogenetic sister clade to the *Krogia* accessions, albeit only supported by PP. Not all *Bacidina* accessions formed a distinct group, but were split in two clades. Except for accessions of the same species, i.e. *Eschatogonia prolifera* (Mont.) R. Sant. and *Physcidia wrightii* (Tuck.) Tuck., there was poor resolution for the remaining accessions resulting in polytomy for the backbone of the ingroup.

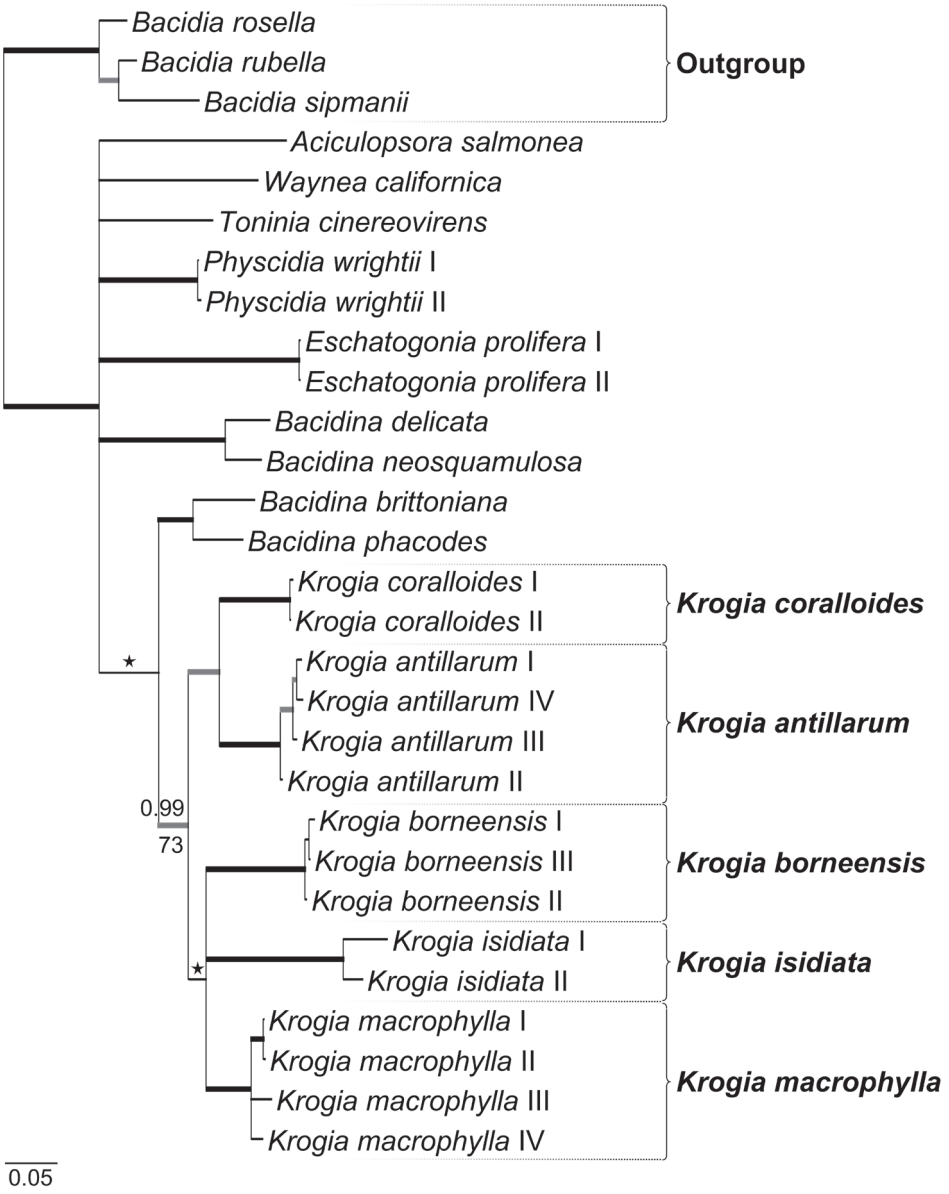

Figure 1. Hypothesis of the phylogenetic relationships and placement of the 15 *Krogia* accessions. It shows the extended majority-rule consensus tree resulting from the Bayesian MCMC analysis with Bayesian PP ≥ 0.7 (above branch) and/or Garli maximum likelihood BS ≥ 50 (below branch) and branch lengths. Strongly supported branches (PP ≥ 0.95 and BS ≥ 95) are marked in bold; branches with PP ≥ 0.95 and BS ≥ 70 are marked in bold grey; branches only supported by PP ≥ 0.7 are marked with an asterisk above the branch. *Bacidia rosella*, *B. rubella* and *B. sipmanii* were used as outgroup. Scale bar indicates 0.05 changes per site.

Discussion

The genus *Krogia* was first described by Timdal in 2002 and only few reports of the genus have been published since (Lumbsch et al. 2011; Timdal 2009). Furthermore, no molecular phylogenetic studies investigating the monophyly of this genus have been conducted. In our study, we present the first multi-locus phylogenetic hypothesis of the genus *Krogia* (Fig. 1) and describe three new species from the Paleotropics based on molecular, morphological and chemical data.

All accessions of *Krogia* included in our molecular phylogeny (Table 1) form a well-supported, monophyletic group (Fig. 1). Five strongly supported clades can be distinguished within the genus. These five clades are delimited by rather long branches in comparison to the short terminal branches, indicating that the five clades correspond to five different species (Fig. 1). Two clades correspond to the two previously described species *K. coralloides* (Timdal 2002) and *K. antillarum* (Timdal 2009), while the remaining three clades correspond to the three new species *K. borneensis*, *K. isidiata* and *K. macrophylla*. The new species are morphologically distinct from one another and from the three known species, *K. antillarum*, *K. coralloides* and *K. microphylla*: *Krogia borneensis* forms more elongated and often linear squamules, *K. isidiata* forms characteristically long and sparingly branched isidia and *K. macrophylla* is a large species with wider squamules than any of the known species. We therefore describe them as new species. All *Krogia* species known contain the characteristic red or purple spots on the thallus and apothecia, consisting of one or more unknown pigments.

Our specimens of the genus *Krogia* were typically found amongst collections of undetermined tropical rainforest lichens, particularly amongst those tentatively named *Phyllopsora*. Timdal (2002) suggested a close relationship between *Krogia* and *Phyllopsora* based on overall morphological similarity. The two genera are anatomically distinct (Timdal 2002), although both form small squamules or lobes on bark. A comprehensive molecular phylogeny of the family Ramalinaceae, however, revealed the type species of the two genera to belong to different major clades within the family (Kistenich et al. in press). They are therefore not as closely related as previously anticipated.

On detailed microscopic examination of specimens of the new species *K. borneensis*, we discovered a thin, unicellular cortex on the upper and lower side of the thallus. This type of cortex, with a single layer of rounded or cuboid cells and a thick cell wall, is characteristic for the tropical genus *Eschatogonia* Trevis. (Timdal 2008). The cellular cortex surrounding the fungal tissue in *K. borneensis* has thinner cell walls and consists of somewhat longer, rather rectangular cells instead of the round and cuboid cells observed in *Eschatogonia* species. Our molecular phylogenetic hypothesis confirms that *Krogia* is not closely related to *Eschatogonia.* This indicates that the characteristic cortex in *Eschatogonia* has evolved independently.

Krogia is resolved as the phylogenetic sister to a clade consisting of the type species of *Bacidina*, *B. phacodes* (Körb.) Vězda and *B. brittoniana* (Riddle) LaGreca & Ekman (Fig. 1). *Krogia* differs from *Bacidina* s.str. (sensu Kistenich et al. in press) in having spirally arranged ascospores and a non- to weakly amyloid ascus tholus.

In recent years, lichenologists have increasingly focused on tropical regions and many new species have been described each year (e.g. Aptroot et al. 2018; Lücking et al. 2014; Masson et al. 2015; Naksuwankul et al. 2016; Sodamuk et al. 2017). It seems that the full diversity of tropical lichens is yet to be discovered. In our study, we report two new species of *Krogia*, *K. isidiata* and *K. macrophylla*, from but one island, the island Grande Terre belonging to New Caledonia. Therefore, further extensive collecting expeditions to remote tropical areas are necessary to explore the total diversity of the genus *Krogia*.

Taxonomy

Krogia borneensis **Kistenich & Timdal, sp. nov.**
Mycobank: MB825078
Fig. 2

Diagnosis. The species differs from *K. isidiata* in forming lacinules as vegetative dispersal units, not isidia, and from the other species in the genus in producing sekikaic and homosekikaic acid.

Type. Malaysia, Borneo, Sabah, Maliau conservation area, trail between Nepenthes Camp and waterfall Takob Akob, 4°43.4'N, 116°52.2'E, 900–1000 m alt., in low (few metres) and open pristine montane "Kerangas" (heath) forest with higher trees mostly along a small stream, on smooth barked tree in the vicinity of the stream, 2013-02-23, C. Vairappan & H. Thüs L291 (BORH, holotype) [TLC: sekikaic and homosekikaic acid; GenBank: MH174275 (mtSSU)].

Description. Thallus effuse, squamulose; squamules up to 1 mm wide, deeply divided into 0.1–0.2 wide lobes, ascending, imbricate, flattened, elongated to partly linear, often slightly laterally constricted, greyish-green with patches of red (K+ purple) spots, epruinose, glabrous; margin concolorous with upper side, not fibrillose; lower side white; lacinules formed by tips of the lobes. Upper cortex composed of a single layer of thick-walled cells with angular to shortly cylindrical lumina (resembling *Eschatogonia*-type), not containing crystals (polarised light!); algal layer 30–40 µm thick, filled with crystals dissolving in K; medulla composed of loosely interwoven hyphae, not containing crystals dissolving in K; lower cortex resembling upper cortex, both continuing over the edge of the squamule; prothallus brownish-black, often well developed. Apothecia (present in the holotype only) up to 0.6 mm diam. when simple, forming aggregates up to 1.5 mm diam., medium brown with red patches or entirely reddish-brown, more or less plane, with an indistinct, slightly paler, often flexuose margin; excipulum pale brown to colourless, composed of radiating, closely conglutinated hyphae, in inner part containing colourless crystals dissolving in K; hypothecium partly to entirely stained by a blood red pigment which dissolves in K with a purple effusion; epithecium colourless, not containing crystals. Ascospores filiform, curved, non-septate, spirally arranged in ascus, 20–31 × ca. 1.0 µm (n=10, from holotype). Conidiomata not seen.

Figure 2. *Krogia borneensis*. **A** Field photograph of the holotype **B** habitat at type locality **C** herbarium photograph of holotype. Scale bar: 1 mm. Photo: H. Thüs (**A, B**), E. Timdal (**C**).

Chemistry. Sekikaic acid (major), homosekikaic acid (major). Spot tests: all negative, except for red patches being K+ purple.

Distribution. The species is known from five localities in Borneo.

Ecology. The species occurred in rather low "Kerangas" (heath) forest vegetation or on transition vegetation between the heath and oak/conifer (particularly *Agathis*) forest at higher elevations (ca. 1000 m) on very poor soils on sandstone (Fig. 2B). The species always grew on the rather smooth barked, middle-sized trees together with various Pyrenulaceae and Graphidaceae.

Etymology. The specific epithet refers to its occurrence in Borneo.

Remarks. The medium-sized, flattened squamules make the species morphologically most similar to the neotropical *K. antillarum*. The squamules are more elongated, often linear and with more lateral constrictions in *K. borneensis* than in *K. antillarum*, which has more fan-shaped squamules. The former species has a thin, unicellular cortex on both upper and lower side, whereas the latter has a multicellular (20–30 µm thick) upper cortex and lacks a lower cortex (Timdal 2009). Chemically, the latter species differs in forming 4-O-methylcryptochlorophaeic acid.

Krogia isidiata shares the secondary chemistry (sekikaic and homosekikaic acid) with *K. borneensis*, but they differ in their vegetative dispersal units, the former producing cylindrical isidia, the latter flat lacinules (fragmenting squamules). The upper cortex of *K. isidiata* is multicellular (15–30 µm thick) and the lower cortex is absent.

Additional specimens examined. Malaysia, Borneo. *Sabah*: Danum, plot 88, dipterocarp forest logged in 1988, 4°58'N, 117°50'E, 131 m alt., 1997-04-30, P. Wolseley Q21 p.p. (BM 001104020); Danum valley, pristine lowland dipterocarp forest 4°57.96'N, 117°47.32'E, 200–400 m alt., 2012, P. Wolseley, H. Thüs & C. Vairappan D-3-10-2 (BORH); Maliau conservation area, trail between Nepenthes Camp and waterfall Takob Akob, transition between pristine montane "Kerangas" (heath forest) and montane oak-conifer (*Agathis*) forest, 4°42.6'N, 116°52.5'E, 900–1000 m alt., 2013, C. Vairappan & H. Thüs L229 (BM); Ranau district, Kinabalu park, Musang camp on the Tambuyukon trail (loc. T98), 6°12.720'N, 116°40.891' E, 1429 m alt., epiphytic, 2014-12-09, A. Paukov 2234 (B).

Krogia isidiata **Kistenich & Timdal, sp. nov.**
Mycobank: MB825079
Fig. 3

Diagnosis. The species differs from *K. borneensis* in forming isidia as vegetative dispersal units, not lacinules, and from the other species in the genus in producing sekikaic and homosekikaic acid.

Type. New Caledonia, Province Sud, 20 km NNE of Nouméa, along dirt mountain road to Mt Dzumac, 3–400 m S of Seismic Station, ca. 22°03'S, 166°25'E, 830 m alt., on unidentified tree trunk in forest near the road, 2005-12-06, A. Elvebakk 05:633 (O L-186393, holotype; CANB, isotype [not seen]) [TLC: sekikaic and homosekikaic acid; GenBank: MH174285 (ITS)].

Description. Thallus effuse, squamulose; squamules up to 0.4 mm wide, rounded and adnate when young, later becoming somewhat elongated with a crenulate and slightly ascending margin, flattened, green, with scattered patches of red (K+ purple) spots, epruinose, glabrous; margin concolorous with upper side, not fibrillose; lower side white; isidia attached marginally to the squamules, simple or sparingly branched, up to 1.8 mm long and 0.1 mm wide. Upper cortex composed of a few layers of thick-walled, irregularly or mainly periclinally orientated hyphae with angular to shortly cylindrical lumina, 15–30 µm thick, lacking an epinecral layer, not containing crystals (polarised

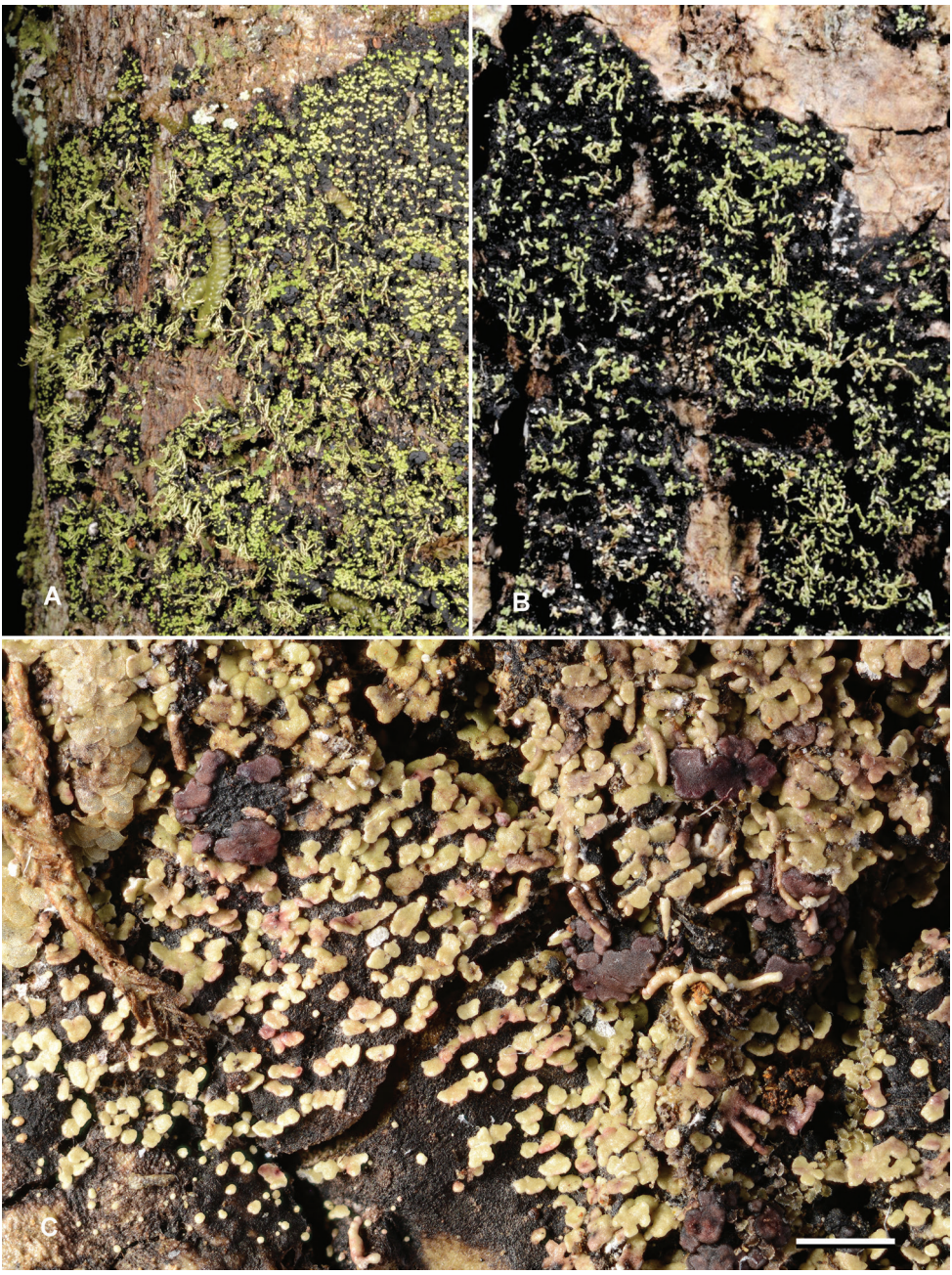

Figure 3. *Krogia isidiata.* **A** field photograph of JR35688 **B** field photograph of JR35034 **C** herbarium photograph of holotype. Scale bar: 1 mm. Photo: J. Rikkinen (**A, B**), E. Timdal (**C**).

light!); algal layer 30–40 µm thick, filled with crystals dissolving in K; medulla composed of loosely interwoven hyphae, containing crystals in the upper part; lower cortex lacking; prothallus brownish-black, well developed. Apothecia up to 0.8 mm diam. when simple, often forming aggregates up to 1.6 mm diam., dark reddish-brown to

brownish-black, more or less plane, with a rather distinct, concolorous or slightly darker, flexuose margin; excipulum dark reddish-brown throughout, composed of radiating, closely conglutinated, thick-walled hyphae with narrowly cylindrical lumina, inner part containing crystals dissolving in K; hypothecium dark reddish-brown, composed of closely conglutinated, thick-walled hyphae with narrowly cylindrical lumina, containing crystals dissolving in K; epithecium colourless, not containing crystals (but crystals present in hymenium below). Ascospores filiform, curved, simple, spirally arranged in ascus, ca. 20–30 × ca. 1.0 µm (estimate of curved spores). Conidiomata not seen.

Chemistry. Sekikaic acid (major), homosekikaic acid (major). Spot tests: all negative, except for red patches being K+ purple.

Distribution. The species is known from four collections at three localities in New Caledonia.

Ecology. The species grows on tree trunks in moist or mesic tropical forests and woodlands (Fig. 5B). All collections are from low-elevation sites and from ultramafic soils typical of the southern part of Grande Terre (main island of New Caledonia). It prefers shaded basal trunks that are otherwise mainly dominated by epiphytic bryophytes and/or leprarioid lichens.

Etymology. The specific epithet refers to its vegetative dispersal units, isidia.

Remarks. This species and *K. macrophylla* are the only isidiate species of *Krogia*. They differ morphologically mainly in the size and shape of the squamules. In *K. isidiata,* they are small (up to 0.4 mm wide), rounded and adnate to somewhat elongated and with a slightly ascending margin and, in *K. macrophylla,* large (up to 3 mm wide), elongated and ascending even when young. In *K. isidiata*, the squamules are attached to a prothallus, whereas in the latter species, a prothallus has not been observed. The former species contains sekikaic and homosekikaic acid, the latter an unknown compound resembling boninic acid.

Krogia isidiata shares the secondary chemistry with *K. borneensis*; see that species for discussion.

Additional specimens examined. New Caledonia. *Province Sud*: Yaté, dense forests along road RP 3 about 5 km west of Yaté, on tree trunk, 22°10'03.63"S, 166°54'10.15"E, 410 m alt., 2016-09-20, J. Rikkinen 34385 (H); Blue River Provincial Park, dense riparian forest near camp site on river bank, on tree trunk, 22°05'54.79"S, 166°38'20.24"E, 200 m alt. 2016-09-22, J. Rikkinen 35034 (H); Blue River Provincial Park, dense forest between camp site and road GR NC1, on tree trunk, 22°05'47.63"S, 166°38'22.54"E, 220 m alt., 2016-09-24, J. Rikkinen 35688 (H, PC).

Krogia macrophylla **Kistenich & Timdal, sp. nov.**
Mycobank: MB825080
Fig. 4

Diagnosis. The species differs from all other species of the genus in forming larger (up to 3 mm wide, vs. up to 0.3–1.5 mm wide in the other species) squamules and, except for *K. coralloides*, in producing an unknown compound resembling boninic acid.

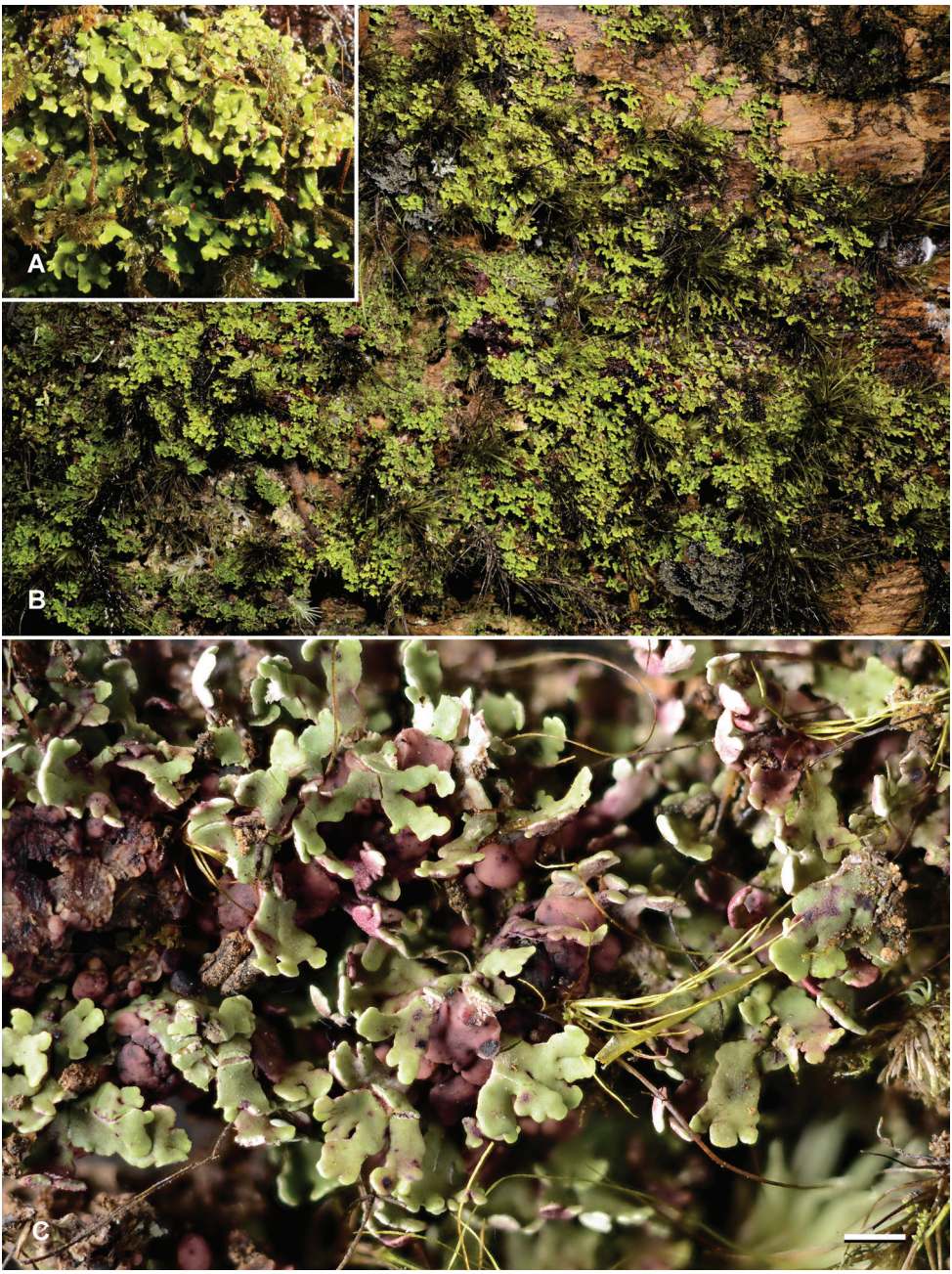

Figure 4. *Krogia macrophylla* **A** field photograph of JR36047 **B** field photograph of holotype **C** herbarium photograph of holotype. Scale bar: 1 mm. Photo: J. Rikkinen (**A, B**), E. Timdal (**C**).

Type. New Caledonia, Province Sud, Mont Mou Nature Reserve, in low dense mist forest along foot path to the mountain summit, on tree trunk, 22°03'39.66"S, 166°20'53.54"E, 1162 m alt., 2016-09-26, J. Rikkinen 36077 (H, holotype [TLC:

unknown compound resembling boninic acid; GenBank: MH174288 (ITS)]; PC, isotype).

Description. Thallus effuse, squamulose; squamules up to 3 mm wide, at first rounded, later becoming incised and deeply divided into up to 1 mm wide lobes, ascending even when young, often imbricate, flattened or with an up-turned tip, greyish-green, with patches of purple (K+ bluish-black) spots, epruinose, glabrous; margin concolorous with upper side, not fibrillose; lower side white; isidia (present in one specimen) attached marginally to the squamules, simple or sparingly branched, up to 1.6 mm long and 0.2 mm wide. Upper cortex composed of thick-walled, irregularly orientated hyphae with angular to cylindrical lumina, 50–80 µm thick, lacking an epinecral layer, not containing crystals (polarised light!); algal layer 25–35 µm thick, filled with crystals dissolving in K; medulla composed of loosely interwoven hyphae, upper part containing crystals dissolving in K; lower cortex lacking; prothallus lacking. Apothecia up to 1 mm diam. when simple, often forming aggregates up to 6 mm diam., pale to medium brown, with purple patches, plane to weakly convex, with an indistinct, slightly paler, often flexuose margin; excipulum pale brown to colourless, composed of radiating, closely conglutinated, thick-walled hyphae with narrowly cylindrical lumina, not containing crystals; hypothecium pale brown to colourless, composed of closely conglutinated, thick-walled hyphae with narrowly cylindrical lumina, not containing crystals; epithecium colourless, not containing crystals; purple pigment occurring patchily in exciple, hypothecium and hymenium. Ascospores filiform, curved, simple, spirally arranged in ascus, ca. 20–30 × ca. 1.0 µm (estimate of curved spores). Conidiomata not seen.

Chemistry. An unknown compound resembling boninic acid (major) and traces of additional compounds. Spot tests: all negative, except for purple patches being K+ deeper purple to bluish-black.

Distribution. The species is known from three localities in New Caledonia.

Ecology. The species grows on tree trunks in moist or wet tropical forests (Figs. 5A–C). Two collections are from montane mist forests and one from a low-elevation rainforest, all on ultramafic soils typical of the southern part of Grande Terre (main island of New Caledonia). It prefers shaded basal trunks that are otherwise mainly dominated by epiphytic bryophytes and/or leprarioid lichens.

Etymology. The specific epithet refers to the large squamules.

Remarks. In the examined material, one specimen (Rikkinen 38565) is isidiate, whereas the others are not. Our first assumption, that two species were involved, was not confirmed by the phylogeny (Fig. 1) and it appears that vegetative dispersal units, isidia, are produced occasionally in *K. macrophylla*. The only other isidiate species of *Krogia* is *K. isidiata*; see that species discussion.

Krogia macrophylla has a similar secondary chemistry to *K. coralloides* (an unknown substance resembling boninic acid as the major constituent) but differs in lacking the boninic acid that co-occurs as the major constituent in *K. coralloides* (Timdal 2002). *Krogia coralloides* forms smaller (up to 1 mm wide), more linear lobes with often down-turned tips.

Figure 5. Habitat images from New Caledonia **A** Mont Humboldt Nature Reserve, site of *K. macrophylla*, with *Araucaria humboldtensis* **B** Blue River Provincial Park, site of *K. isidiata* and *K. macrophylla* **C** Mont Mou Nature Reserve, holotype locality of *K. macrophylla*. Photo: J. Rikkinen.

Additional specimens examined. New Caledonia. *Province Sud*: Blue River Provincial Park, dense riparian forest near camp site on river bank, on tree trunk, 22°05'54.79"S, 166°38'20.24"E, 200 m alt., 2016-09- 22, J. Rikkinen 35037 (H);

locality data as for holotype, J. Rikkinen 36047 (H); Mont Humboldt Nature Reserve, close to Mont Humboldt refuge, in low dense mist forest along foot path from shelter towards the mountain summit, on tree trunk, 21°52'46.79"S, 166°24'49.17"E, 1320 m alt., 2011-11-09, J. Rikkinen 38565 (H).

Key to the species of *Krogia*

1 Squamules large, up to 3 mm wide and with up to 1 mm wide lobes; containing an unknown compound resembling boninic acid..... ***K. macrophylla***
– Squamules smaller, up to 1.5 mm wide and with up to 0.4 mm wide lobes; chemistry various..... **2**
2 Thallus with isidia; containing sekikaic and homosekikaic acid..... ***K. isidiata***
– Thallus without isidia; chemistry various..... **3**
3 Squamules minute, up to 0.3 wide and with up to 0.1 mm, simple lobes, forming a microphyllinous crust; not containing lichen substances..... ***K. microphylla***
– Squamules medium sized, up to 1.5 mm wide and with up to 0.4 mm wide, coralloid elongated lobes; containing lichen substances..... **4**
4 Thallus with brownish black hypothallus; containing sekikaic and homosekikaic acid..... ***K. borneensis***
– Thallus without distinct hypothallus; chemistry different..... **5**
5 Squamules mainly flattened; lobes up to 0.4 mm wide; containing 4-O-methylcryptochlorophaeic acid ..... ***K. antillarum***
– Squamules mainly convex; lobes up to 0.1 mm wide; containing boninic acid and an unknown, similar compound ..... ***K. coralloides***

Acknowledgements

We would like to thank Arve Elvebakk and Alexander Paukov for providing us with their field collections; the specimen of the latter (A. Paukov 2234 (B)) was collected during a sampling trip to Sabah. We are grateful to Mika Bendiksby for assistance in the DNA lab and for valuable discussions. We acknowledge the Sabah Biodiversity Council, the administration units at Danum Valley and Maliau Conservation Areas for granting permits to access and work in the studied sites in the framework of the NHM "Danum – Maliau Quantitative Inventory" (JKM/MBS.1000-2/2 (77), MBMC 2012/15) and for the provision of logistic support. J.R. would like to thank Jérôme Munzinger (Montpellier) for help in the preparation of the fieldwork in New Caledonia and Alexander R. Schmidt and Leyla Seyfullah (University of Göttingen) for planning and organising the field trips. Fieldwork and collection in southern New Caledonia were kindly permitted by the Direction de l'Environnement (Province Sud), permit 17778/DENV/SCB delivered in November 2011 and permit 20112388-2016/ARR/DENV delivered in October 2016.

References

Altekar G, Dwarkadas S, Huelsenbeck JP, Ronquist F (2004) Parallel metropolis coupled Markov chain Monte Carlo for Bayesian phylogenetic inference. Bioinformatics 20: 407–415.

Aptroot A, Sipman HJM, Mercado Diaz JA, Mendonça CO, Feuerstein SC, Cunha-Dias IPR, Pereira TA, Cáceres MES (2018) Eight new species of Pyrenulaceae from the Neotropics, with a key to 3-septate *Pyrgillus* species. The Lichenologist 50: 77–87. https://doi.org/10.1017/S0024282917000573

Ayres DL, Darling A, Zwickl DJ, Beerli P, Holder MT, Lewis PO, Huelsenbeck JP, Ronquist F, Swofford DL, Cummings MP, Rambaut A, Suchard MA (2012) BEAGLE: An Application Programming Interface and High-Performance Computing Library for Statistical Phylogenetics. Systematic Biology 61: 170–173. https://doi.org/10.1093/sysbio/syr100

Bendiksby M, Timdal E (2013) Molecular phylogenetics and taxonomy of *Hypocenomyce* sensu lato (Ascomycota: Lecanoromycetes): Extreme polyphyly and morphological/ecological convergence. Taxon 62: 940–956. https://doi.org/10.12705/625.18

Culberson CF (1972) Improved conditions and new data for the identification of lichen products by a standardized thin-layer chromatographic method. Journal of Chromatography 72: 113–125. https://doi.org/10.1016/0021-9673(72)80013-X

Culberson CF, Johnson A (1982) Substitution of methyl tert.-butyl ether for diethyl ether in standarzided thin-layer chromatographic method for lichen products. Journal of Chromatography 238: 483–487. https://doi.org/10.1016/S0021-9673(00)81336-9

Gardes M, Bruns TD (1993) ITS primers with enhanced specificity for basidiomycetes – application to the identification of mycorrhizae and rusts. Molecular Ecology 2: 113–118.

Katoh K, Standley DM (2013) MAFFT Multiple Sequence Alignment Software Version 7: Improvements in Performance and Usability. Molecular Biology and Evolution 30: 772–780. https://doi.org/10.1093/molbev/mst010

Kearse M, Moir R, Wilson A, Stones-Havas S, Cheung M, Sturrock S, Buxton S, Cooper A, Markowitz S, Duran C (2012) Geneious Basic: an integrated and extendable desktop software platform for the organization and analysis of sequence data. Bioinformatics 28: 1647–1649.

Kistenich S, Timdal E, Bendiksby M, Ekman S (in press) Molecular systematics and character evolution in the lichen family Ramalinaceae (Lecanorales, Ascomycota). Taxon 67. https://doi.org/10.12705/675.1

Lanfear R, Frandsen PB, Wright AM, Senfeld T, Calcott B (2016) PartitionFinder 2: new methods for selecting partitioned models of evolution for molecular and morphological phylogenetic analyses. Molecular Biology and Evolution 34: 772–773.

Lücking R, Johnston MK, Aptroot A, Kraichak E, Lendemer JC, Boonpragob K, Cáceres ME, Ertz D, Ferraro LI, Jia Z-f (2014) One hundred and seventy-five new species of Graphidaceae: closing the gap or a drop in the bucket? Phytotaxa 189: 7–38.

Lumbsch HT, Chaves-Chaves JL, Umaña-Tenorio L, Lücking R (2011) One hundred new species of lichenized fungi: A signature of undiscovered global diversity. Phytotaxa: 1–127.

Masson D, Divakar PK, Sérusiaux E (2015) *Hypotrachyna penduliloba* and *Remototrachyna pandani*, two new species in the hyperdiverse lichen family Parmeliaceae from Réunion in the Mascarene Archipelago. Mycological Progress 14: 1–15.

Menlove JE (1974) Thin-layer chromatography for the identification of lichen products. Bulletin of the British Lichen Society 34: 3–5.

Miller MA, Pfeiffer W, Schwartz T (2010) Creating the CIPRES Science Gateway for inference of large phylogenetic trees. Proceedings of the Gateway Computing Environments Workshop (GCE), 2010, New Orleans, LA, 1–8.

Mirarab S, Nguyen N, Guo S, Wang L-S, Kim J, Warnow T (2015) PASTA: ultra-large multiple sequence alignment for nucleotide and amino-acid sequences. Journal of Computational Biology 22: 377–386.

Naksuwankul K, Kraichak E, Parnmen S, Lücking R, Lumbsch H (2016) Five new species of Graphidaceae (Ascomycota, Ostropales) from Thailand. MycoKeys 17: 47–63.

Rannala B, Zhu T, Yang Z (2011) Tail paradox, partial identifiability, and influential priors in Bayesian branch length inference. Molecular Biology and Evolution 29: 325–335.

Ronquist F, Huelsenbeck JP (2003) MrBayes 3: Bayesian phylogenetic inference under mixed models. Bioinformatics 19: 1572–1574.

Sodamuk M, Boonpragob K, Mongkolsuk P, Tehler A, Leavitt SD, Lumbsch HT (2017) *Kalbionora palaeotropica*, a new genus and species from coastal forests in Southeast Asia and Australia (Malmideaceae, Ascomycota). MycoKeys 22: 15–25.

Stamatakis A (2014) RAxML version 8: a tool for phylogenetic analysis and post-analysis of large phylogenies. Bioinformatics 30: 1312–1313.

Stöver BC, Müller KF (2010) TreeGraph 2: Combining and visualizing evidence from different phylogenetic analyses. BMC Bioinformatics 11: 7. https://doi.org/10.1186/1471-2105-11-7

Timdal E (2002) *Krogia coralloides*, a new lichen genus and species from Mauritius. The Lichenologist 34: 293–296.

Timdal E (2008) Studies on *Eschatogonia* (Ramalinaceae) in Peru. Lichenologist 40: 31–38.

Timdal E (2009) *Krogia antillarum* (Ramalinaceae), a new lichen species from the West Indies. Bryologist 112: 387–389.

White TJ, Bruns T, Lee S, Taylor J (1990) Amplification and direct sequencing of fungal ribosomal RNA genes for phylogenetics. PCR protocols: a guide to methods and applications, 18: 315–322.

Zhang C, Rannala B, Yang Z (2012) Robustness of Compound Dirichlet Priors for Bayesian Inference of Branch Lengths. Systematic Biology 61: 779–784. https://doi.org/10.1093/sysbio/sys030

Zoller S, Scheidegger C, Sperisen C (1999) PCR primers for the amplification of mitochondrial small subunit ribosomal DNA of lichen-forming ascomycetes. The Lichenologist 31: 511–516. https://doi.org/10.1006/lich.1999.0220

Zwickl DJ (2006) Genetic algorithm approaches for the phylogenetic analysis of large biological sequence datasets under the maximum likelihood criterion. PhD Dissertation, University of Texas at Austin, Austin, Texas.

Appendix

Krogia antillarum is reported here as new to Brazil, Guatemala and Mexico from the following examined specimens: Brazil. *Rio de Janeiro*: Parque Nacional do Itatiaia, along trail to Três Picos, 22.4358°S, 44.6118°W, 1090 m alt., on tree trunk in Atlantic rainforest, 2015-11-27, M.S. Dahl, S. Kistenich, E. Timdal & A.K. Toreskaas AM-39 (O L-202829). Guatemala. *Depto. Alta Verapaz*: NE of Cobán-Aragon, at the borders of Rio Cahabon (tierra fría), 1700 m alt., cloud forest, on *Liquidambar tyraciflua*, 2002-09-13, C. Andersohn s.n. (B 60-127330. Mexico. *Chiapas*: Municipio La Trinitaria, Parque Nacional Lagunas de Montebello, Paso del Soldado, 16°07'07"N, 91°43'09"W, 1500 m alt., bosque de *Pinus maximinoi* y *Quercus sapotifolia,* exposición N, epífita, 1994-11-29, J. Wolf & H. Sipman 2052 (B 60-110597).

MycoKeys 40: 89–110 (2018)
doi: 10.3897/mycokeys.40.28337
http://mycokeys.pensoft.net

RESEARCH ARTICLE

A peer-reviewed open-access journal
MycoKeys
Launched to accelerate biodiversity research

Liebetanzomyces polymorphus gen. et sp. nov., a new anaerobic fungus (Neocallimastigomycota) isolated from the rumen of a goat

Akshay Joshi[1], Vikram B. Lanjekar[1], Prashant K. Dhakephalkar[1], Tony M. Callaghan[2,3], Gareth W. Griffith[2], Sumit Singh Dagar[1]

1 *Bioenergy Group, Agharkar Research Institute, Pune, India* **2** *Institute of Biological, Environmental and Rural Sciences, Cledwyn Building, Aberystwyth University, Aberystwyth, SY23 3DD, Wales, UK* **3** *Commercial Mushroom producers Co-Operative Society Ltd., Units 7 & 8, Newgrove Industrial Estate, Ballinode Road, Monaghan, Ireland*

Corresponding author: *Sumit Singh Dagar* (ssdagar@aripune.org)

Academic editor: *K. Voigt* | Received 12 July 2018 | Accepted 5 September 2018 | Published 10 October 2018

Citation: Joshi A, Lanjekar VB, Dhakephalkar PK, Callaghan TM, Griffith GW, Dagar SS (2018) *Liebetanzomyces polymorphus* gen. et sp. nov., a new anaerobic fungus (Neocallimastigomycota) isolated from the rumen of a goat. MycoKeys 40: 89–110. https://doi.org/10.3897/mycokeys.40.28337

Abstract

An extended incubation strategy to culture slow growing members of anaerobic fungi resulted in the isolation of a novel anaerobic fungus from the rumen of a goat after 15 days. The novel genus, represented by type strain G1SC, showed filamentous monocentric thallus development and produced uniflagellate zoospores, hence, showing morphological similarity to the genera *Piromyces*, *Buwchfawromyces*, *Oontomyces* and *Pecoramyces*. However, strain G1SC showed genetic similarity to the genus *Anaeromyces*, which, though produces uniflagellate zoospore, also exhibits polycentric thallus development. Moreover, unlike *Anaeromyces*, strain G1SC did not show hyphal constrictions, instead produced a branched, determinate and anucleate rhizoidal system. This fungus also displayed extensive sporangial variations, both exogenous and endogenous type of development, short and long sporangiophores and produced septate sporangia. G1SC utilised various complex and simple substrates, including rice straw and wheat straw and produced H_2, CO_2, formate, acetate, lactate, succinate and ethanol. Phylogenetic analysis, using internal transcribed spacer 1 (ITS1) and D1/D2 domain of large-subunit (LSU) rRNA locus, clearly showed a separate lineage for this strain, near *Anaeromyces*. The ITS1 based geographical distribution studies indicated detection of environmental sequences similar (93–96%) to this strain from cattle faeces. Based on morphological and molecular characterisation results of strain G1SC, we propose a novel anaerobic fungus *Liebetanzomyces polymorphus* **gen. et sp. nov.**, in the phylum *Neocallimastigomycota*.

Keywords

Anaerobe, fungal diversity, novel genus, phylogeny, rumen fungi, taxonomy

Introduction

Anaerobic fungi inhabit the gut of various herbivorous animals where they play a pivotal role in the degradation of lignocellulosic feed (Gruninger et al. 2014). Some recent reports even suggest the presence of anaerobic fungi outside the gut of terrestrial animals and within the gut of sea animals and sediments (Ivarsson et al. 2016; Edwards et al. 2017; Picard 2017). Taxonomically, anaerobic fungi are the only member of phylum *Neocallimastigomycota*, class *Neocallimastigomycetes*, order *Neocallimastigales* and family *Neocallimastigaceae* (Hibbett et al. 2007). So far, ten genera of these fungi have been reported, namely *Anaeromyces*, *Caecomyces*, *Cyllamyces*, *Neocallimastix*, *Orpinomyces*, *Piromyces*, *Buwchfawromyces*, *Feramyces*, *Oontomyces* and *Pecoramyces*, the last four of which have been described very recently (Callaghan et al. 2015; Dagar et al. 2015; Hanafy et al. 2017; Hanafy et al. 2018).

The total number of anaerobic fungal species is reported to be 29, but this number is not validated due to several taxonomy related issues, including incorrect or repetitive naming (Paul et al. 2018). Several culture-independent studies, moreover, suggest the presence of at least 25 genus- and 119 species-equivalent taxa of anaerobic fungi, highlighting the need for continuous attempts for the cultivation of these additional taxa into axenic cultures (Kittelmann et al. 2012; Koetschan et al. 2014; Paul et al. 2018). This suggested number of total genera and species may even be higher as some of the primers used during routine ITS-based studies are also known to neglect certain cultures (Callaghan et al. 2015). These observations, therefore, reaffirm the need to look into vastly unexplored and unreported diversity of anaerobic fungi.

Many of the anaerobic fungal genera like *Orpinomyces*, *Caecomyces*, *Neocallimastix*, *Piromyces* etc. have a ubiquitous occurrence and can be found in diverse animal species, while some are reportedly host-specific (Paul et al. 2018). The genus *Oontomyces* has been reported to be a camel-specific genus (Dagar et al. 2015) and some uncultured genus designates have been reported to be specific to hosts like Somali ass, wallaby or American bison (Paul et al. 2018). Similarly, the presence of recently described genera *Pecoramyces* and *Feramyces* has been found limited to foregut fermenters and wild undomesticated animals, respectively (Hanafy et al. 2018). However, it is interesting to note that many genera remain uncultured even from the routinely sampled domesticated herbivores, a fact which needs further attention. In this paper, we report the isolation of a novel anaerobic fungus *Liebetanzomyces polymorphus,* isolated from goat rumen after prolonged incubation of 15 days.

Materials and methods

Sampling, cultivation and preservation

The rumen digesta samples were collected from goats (n=3) slaughtered at Kondhwa slaughterhouse, Pune (India). The samples were immediately brought to the labora-

tory (within 1 h), pooled and homogenised for 10 minutes under the gas phase of CO_2 before making dilutions (up to 10^{-4}) in the anaerobic diluent (McSweeney et al. 2005). The serum roll bottle method (Miller and Wolin 1974) was used to isolate pure cultures of anaerobic fungi from different dilutions. Briefly, the inoculum (0.5 ml) was added to 125 ml glass serum bottles containing 10 ml fungal culture medium (pH 6.8 ± 0.1), which comprised (per litre) of 3 g yeast extract, 5 g tryptone, 150 ml each of solution 1 (0.3% K_2HPO_4), solution 2 [0.3% KH_2PO_4, 0.6% $(NH_4)_2SO_4$, 0.6% NaCl, 0.06% $MgSO_4.7H_2O$ and 0.06% $CaCl_2.2H_2O$] and clarified rumen fluid, 1 ml resazurin (0.1%), 1 ml hemin (0.05%), 6 g $NaHCO_3$, 1 g L-cysteine-HCl, 5 g cellobiose and 20 g agar. The antibiotics, benzylpenicillin and streptomycin sulphate (final concentration 200 µg/ml), were also added to inhibit bacterial growth.

All the roll bottles were incubated at 39±1 °C for 3 weeks and inspected regularly for the development of fungal colonies. The morphologically distinct colonies were picked under anaerobic conditions and inoculated into the fresh liquid culture medium. The serum roll bottle method was repeated two more times to get the axenic fungal cultures. All the cultures were cryopreserved at -80 °C and -196 °C for short-term and long-term storage, respectively using ethylene glycol (final concentration 0.64 M) as the cryoprotectant (Callaghan et al. 2015).

Morphological characterisation

The colony morphology of the cultures was measured after 3 d growth on cellobiose roll bottles, using a stereomicroscope (Leica M205 FA) equipped with a digital camera (Leica DFC450 C). For documenting the microscopic features, the cultures were grown on different carbon sources like rice straw, wheat straw, cellulose, xylan, starch, cellobiose, lactose, maltose, sucrose, glucose, xylose and fructose for 3 d. The microscopic features like thallus morphology, shape and size of sporangia, zoospore shape and flagellation etc. were documented using a differential interference contrast (DIC) microscope (Olympus BX53) equipped with a digital camera (Olympus DP 73) and scanning electron microscope (Carl Zeiss EVO MA15), respectively. The samples for scanning electron microscopy were prepared as described by Ho et al. (1988). To determine the monocentric/polycentric growth patterns, nuclei positions were visualised following straining with bisbenzimide (Fliegerova et al. 2002) or DAPI (Callaghan et al. 2015) using a fluorescence microscope (Nikon Eclipse 80i) equipped with a monochrome digital camera (Media Cybernetics) or confocal microscope (Leica TCS SP8), respectively. All images were processed in GIMP (version 2.8.14) and then compiled using Inkscape (version 0.91) software.

Molecular characterisation and phylogenetic analysis

For molecular characterisation, the genomic DNA was extracted using the CTAB DNA extraction protocol (Sirohi et al. 2013). The complete internal transcribed

spacer (ITS1-5.8S-ITS2; ITS) and D1/D2 domain of large-subunit (LSU) ribosomal DNA were amplified using ITS1/ITS4 and NL1/NL4 primer pairs (Edwards et al. 2017). The sequencing was outsourced to 1st BASE (Singapore) and the obtained sequences were compiled and edited manually using BioEdit software (Hall 1999). Since most of the culture-independent studies have generated only ITS1 sequences, the ITS sequence was trimmed to obtain only the partial ITS1 region. Sequence similarity searches were performed using GenBank BLASTn. For phylogenetic analyses, the ITS1 and LSU sequences representing different anaerobic fungal genera and uncultured representatives, were downloaded from the NCBI GenBank database. All the sequences were aligned using the ClustalW programme (Thompson et al. 1994) with default settings in MEGA7 (Kumar et al. 2016). The aligned sequences were used to construct a phylogenetic tree in MEGA7 using the maximum-likelihood method based on the Tamura-Nei model (Tamura and Nei 1993) and tested by 500 bootstrap replications. The genus *Gromochytrium mamkaevae* was used as the outgroup for both ITS1 (accession number: KF586842) as well as LSU (accession number: NR_132054) based trees. The ITS1 and LSU alignments have been submitted to TreeBASE under submission ID 22988.

Substrate utilisation, enzyme activities and fermentation product analyses

The obtained strains were grown in a fungal culture medium without yeast extract or tryptone and cellobiose was replaced by different substrates (Table 1) as a carbon source (Hanafy et al. 2017; Hanafy et al. 2018). Following initial growth for 2 d on monosaccharides and disaccharides and 5 d on polysaccharides, the cultures were subcultured three times at 10% inoculum size to evaluate their substrate utilisation abilities. The growth was measured in terms of visible biomass accumulation and total gas production. The cultures were scored based on their ability to grow luxuriantly (++) or slowly (+) within the stipulated incubation periods or following extended incubation up to 10 days. The avicelase, CMCase, xylanase and β-glucosidase activities of type strain were also determined following its growth on cellulose, xylan, wheat straw and rice straw for 5 d as per the method described previously (Dagar et al. 2018). The fermentation gases (H_2, CO_2), volatile fatty acids (VFAs; acetate, propionate, butyrate etc.) and alcohols (ethanol and butanol) of growth positive substrates were determined using gas chromatographs equipped with flame ionisation or thermal conductivity detectors, similar to previous reports (Dighe et al. 1998; Kamalaskar et al. 2010; Singh et al. 2016). The organic acids (formate, lactate, succinate, malate etc.) were analysed using HPLC LC20A (Shimadzu, Japan) equipped with a refractive index detector (Thakker et al. 2006). An ordination of the obtained fermentation products was also generated to see if there is any pattern of substrate utilisation using Non-metric Multidimensional Scaling (NMDS) analysis based on the distance matrix in PAST 3.20 software (Hammer et al. 2001).

Table 1. Substrate utilisation pattern of *Liebetanzomyces polymorphus* strains G1SC and G6SC compared with other genera of monocentric and uniflagellate filamentous anaerobic fungi.

Substrate		Lp	Am	Pc	Pr
Polysaccharide	Rice straw	++	ND	ND	ND
	Wheat straw	++	ND	ND	ND
	Cellulose	++	++	++	++
	Xylan	++	++	++	++
	Starch	++	++	++	++
	Inulin	–	–	–	++
	Raffinose	–	–	++	++
	Chitin	–	ND	ND	–
	Alginate	–	ND	ND	–
	Pectin	++	–	–	–
Disaccharide	Cellobiose	++	++	++	++
	Sucrose	+	++	++	++
	Maltose	++	++	++	++
	Trehalose	–	ND	ND	+
	Lactose	+	+	++	–
Monosaccharide	Glucose	++	++	++	++
	Xylose	++	++	++	++
	Mannose	–	–	–	++
	Fructose	++	++	++	++
	Arabinose	–	–	–	–
	Ribose	–	ND	–	–
	Glucuronic acid	–	ND	ND	–
	Galactose	–	–	–	–
Peptide	Peptone	–	ND	ND	–
	Tryptone	–	ND	ND	–

Strains: **Lp** *Liebetanzomyces polymorphus* strain G1SC and G6SC **Am** *Anaeromyces mucronatus* strain BF2 (Breton et al. 1990) **Pc** *Piromyces communis* strain SM5 (Trinci et al. 1994) **Pr** *Pecoramyces ruminantium* strain C1A and S4B (Hanafy et al. 2017). – (negative), ++ (positive), + (weak growth/ slow growth/ growth visible after 4–10 d of incubation), ND (not documented)

Results and discussion

Growth and morphological characterisation

For the routine anaerobic fungal isolation, the inoculated roll tubes are usually incubated for 2–4 d after which the developed colonies are picked anaerobically and pure cultures are obtained. However, we chose to incubate the roll tubes for an extended period of time i.e. up to 3 weeks. The decision for extended incubation was taken in the wake of the fact that several genera of anaerobic fungi remain to be uncultured and incubation time may be one of the limiting factors. As shorter incubation times favours fast-growing cultures, some slow growing cultures might be omitted and which may grow after prolonged incubation. The prolonged incubation might

also help some cultures to cope better in stressed conditions of different growth environment, the presence of antibiotics or some oxygen exposure during sample collection or processing. In a previous study, prolonged incubation was recommended for the isolation of anaerobic bacteria from clinical specimens and correct bacteriological diagnosis (Wren 1980). Janssen et al. (2002) also speculated that the extended incubation period may help isolation of previously uncultured groups of soil bacteria. In this case, the extended incubation of 15 d resulted in the development of two fungal colonies, but no further growth even after 21 d of incubation. Following isolation and establishment of pure cultures, the morphological, molecular and substrate utilisation characteristics of both strains, namely G1SC and G6SC were found to be identical. Therefore, one of them, i.e. strain G1SC, was denoted as the type strain and used for detailed characterisation. The type strain has been deposited to the MACS collection of microorganisms (MCM), Agharkar Research Institute, Pune, India under the accession number MCMB-1469.

The colony morphology of strain G1SC is shown in Fig. 1A–C, showing 1–2 mm sized colony, attached to rice straw (Fig. 1A) and at different stages of growth. A large number of newly formed sporangia at the periphery of the colony were observed, as shown by numerous dot-like structures of varying sizes (Fig. 1B–C). A similar observation was also made in broth culture, where numerous fungal thalli, attached to the bottom of glass bottles, were seen on the initial period of growth (Suppl. material 1: Figure S1), which later developed into a thin mat or biofilm-like structure (Fig. 1D) similar to *Pecoramyces* (Hanafy et al. 2017). Zoospores were abundantly produced, mostly uniflagellate (Fig. 1E–F) and rarely biflagellate (Fig. 1G), spherical to ovoid in size (5–6 μm in diameter) and the flagellum 15–20 μm in length. The zoospores were found to germinate either endogenously or exogenously (Fig. 1H–I) into different shapes of sporangia (Fig. 1J) like globose or ellipsoidal at the very early stages of development. Different forms of rhizoidal development, like long single rhizoid (Fig. 1K), two rhizoids (Fig. 1L) and even multiple rhizoids originating from sporangia (Fig. 1M), were also seen.

We also noticed pleomorphism in sporangial and rhizoidal structures of strain G1SC on different substrates like rice straw (Fig. 2A), wheat straw (Fig. 2B), cellulose (Fig. 2C), xylan (Fig. 2D), starch (Fig. 2E), cellobiose (Fig. 2F), lactose (Fig. 2G), maltose (Fig. 2H), sucrose (Fig. 2I), glucose (Fig. 2J), xylose (Fig. 2K) and fructose (Fig. 2L). In the case of complex substrates like rice straw, wheat straw, cellulose and xylan, the rhizoidal growth was observed to be more extensively branched. Conversely, thicker and less branched rhizoidal growth was noticed on dimeric and monomeric substrates, probably due to the ready availability of fermentable sugars. It was also observed that, on rice and wheat straw, an exogenous type of sporangia development with short or long sporangiophores was more prominent in comparison to endogenous sporangia on all other substrates. The presence of sporangiophores on complex straw particles might be helpful for sporangia to come out of straw and release zoospores to further areas for faster colonisation. The pleomorphism, in morphological features with a change in culture conditions, particularly with carbon source, is also well de-

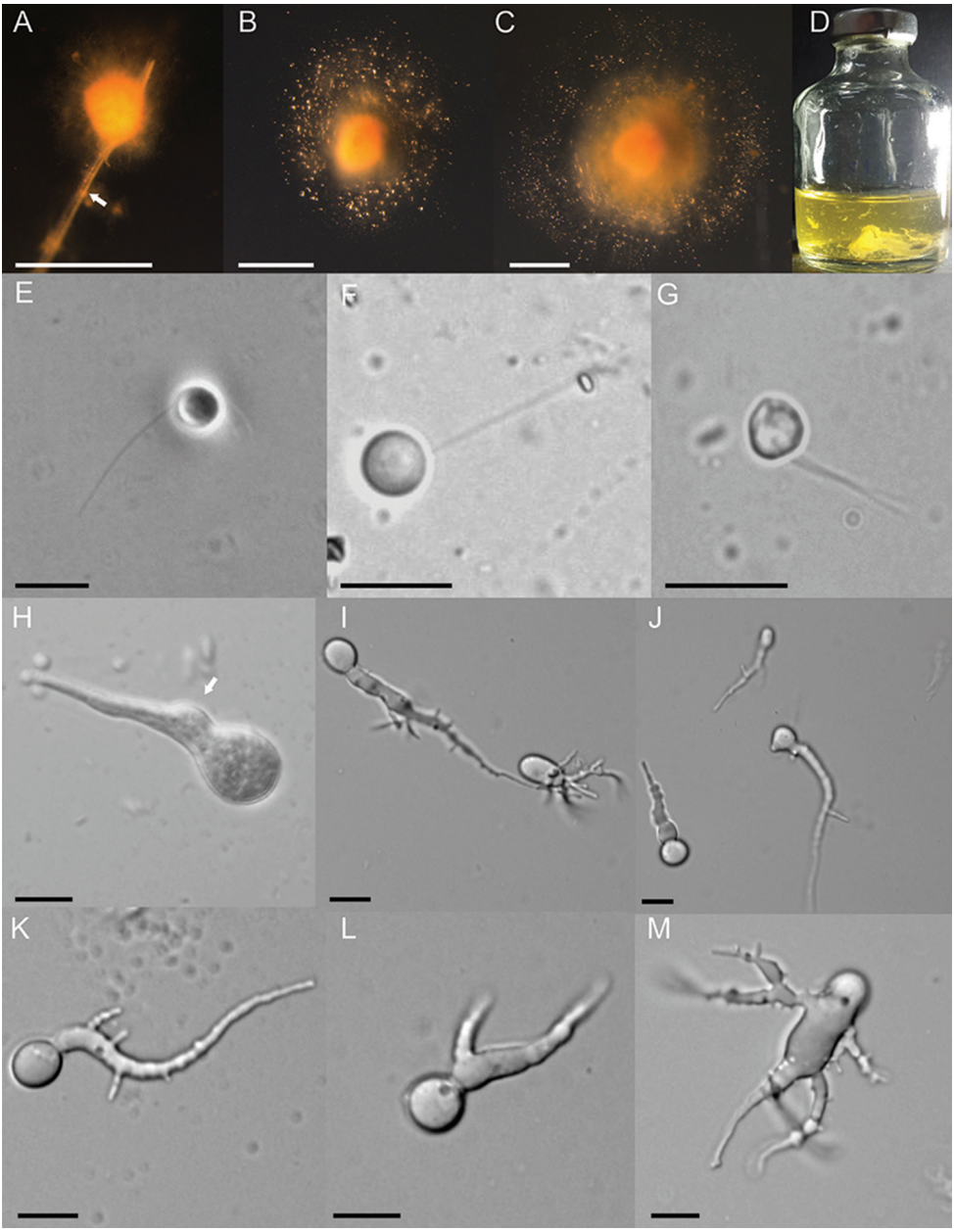

Figure 1. Macroscopic and microscopic features of *Liebetanzomyces polymorphus*. Colony morphology on agar roll tubes (**A–C**), showing the development of a colony attached (**A**) to a straw particle (arrowed), dense growth in the centre surrounded by numerous sporangia and zoospores (**B–C**) causing expansion of colony size. Growth in liquid medium showing a biofilm-like growth (**D**). Zoospores are spherical and Uniflagellate (**E–F**) or biflagellate (**G**). Germinating zoospore (**H**) showing a zoospore cyst (arrowed), presence and absence of sporangiophore indicating the endogenous and exogenous type of sporangial development (**I**) and different shapes of sporangia (**I, J**). Early stages of thallus development showing a single (**K**), bifurcated (**L**) and multifurcated (**M**) rhizoidal system. Scale bar: 1 mm (**A–C**); 10 μM (**E–M**).

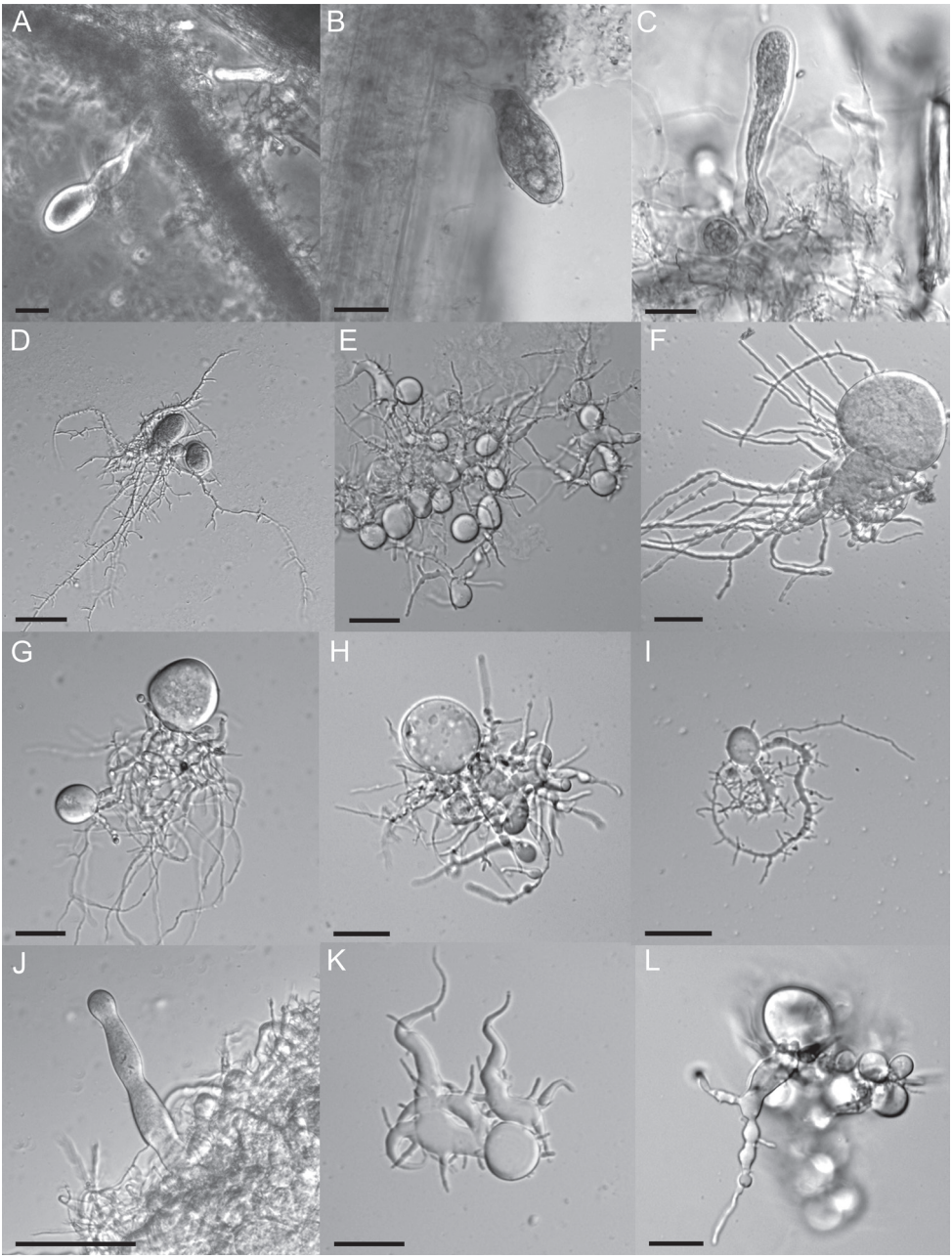

Figure 2. Microscopic features of *Liebetanzomyces polymorphus* showing pleomorphism in sporangial and rhizoidal structures, when grown on different carbon sources like rice straw (**A**), wheat straw (**B**), cellulose (**C**), xylan (**D**), starch (**E**), cellobiose (**F**), lactose (**G**), maltose (**H**), sucrose (**I**), glucose (**J**), xylose (**K**) and fructose (**L**). The exogenous sporangia appearing on a sporangiophore (**A–B**) and endogenous sporangia of different shapes (**C–L**) are shown. Scale bar: 20 μM.

scribed earlier (Brookman et al. 2000; Gruninger et al. 2014). However, the sporangial shapes varied, not only on different carbon sources, but also on the same carbon source (Fig. 3). Different sporangial shapes like globose, ellipsoid, clavate, ovoid, with or without a papilla were noticed on the same substrate i.e. rice straw as shown in Fig. 3A–F. Similar polymorphism was also observed on several other substrates, e.g. xylose (Fig. 3G–I) and cellobiose (Fig. 3J–L), where conspicuous irregular sporangial structures were seen. These findings, therefore, highlight the pleomorphic nature of strain G1SC, irrespective of the carbon sources used in the growth medium.

The sporangial size also varied in diameter (10–90 µm wide, 10–75 µm long), always borne at the terminal end of a variable length sporangiophore (15–80 µm), in the case of exogenous development. Several cyst-like structures were also visible on the sporangiophore (Fig. 3A–C) highlighting bipolar germination of zoospores. In some cases, an eggcup shaped sporangiophore at the bottom of sporangium (Fig. 3C) and a constricted sporangiophore were also noted (Fig. 3E). In the case of soluble substrates, few pseudo-intercalary sporangia, similar to *Oontomyces* and *Feramyces* (Dagar et al. 2015; Hanafy et al. 2018), were also noted (Fig. 3J–L). The thallus development was clearly monocentric as evident by the mature sporangia full of zoospores (Fig. 4A–D, I), anucleated rhizoids (Fig. 4E–I) and a single thallus having a single sporangium (Fig. 4J–K). All these morphological features were similar to various *Piromyces* spp., *Buwchfawromyces, Oontomyces* and *Pecoramyces*, which also have the monocentric thallus and extensive variations in sporangial shape and size and produce uniflagellate zoospores (Ho and Barr 1995). Similar to *P. rhizinflatus*, the sporangia of strain G1SC showed a constricted, isthmus-like neck (Fig. 2C, J), sporangiophore appearing like an eggcup (Fig. 3C) like in *P. communis* and sporangium with a papilla (Fig. 3D) similar to *P. mae* (Ho and Barr 1995; Li et al. 1990).

The similarities in morphological features of monocentric and uniflagellate genera make it very difficult to identify and differentiate this group of anaerobic fungi. It is also interesting to note that, so far, the maximum number of species has been described in the *Piromyces* genus and most of the newly described genera of anaerobic fungi share morphological similarities with these different species, including strain G1SC. These observations point towards the possibility that some of these newly described genera might have been isolated previously as well but were identified as different species of *Piromyces*. It is also worth noting that all newly described genera have primarily been described using molecular tools, thus emphasising the need to use these modern tools.

Molecular characterisation and phylogenetic analysis

The successful amplification of ITS and LSU regions yielded product sizes of ca. 700 bp and 750 bp, respectively. The obtained sequences were submitted to NCBI GenBank to obtain the accession numbers for strain G1SC (MH468765 and MH468763; ITS

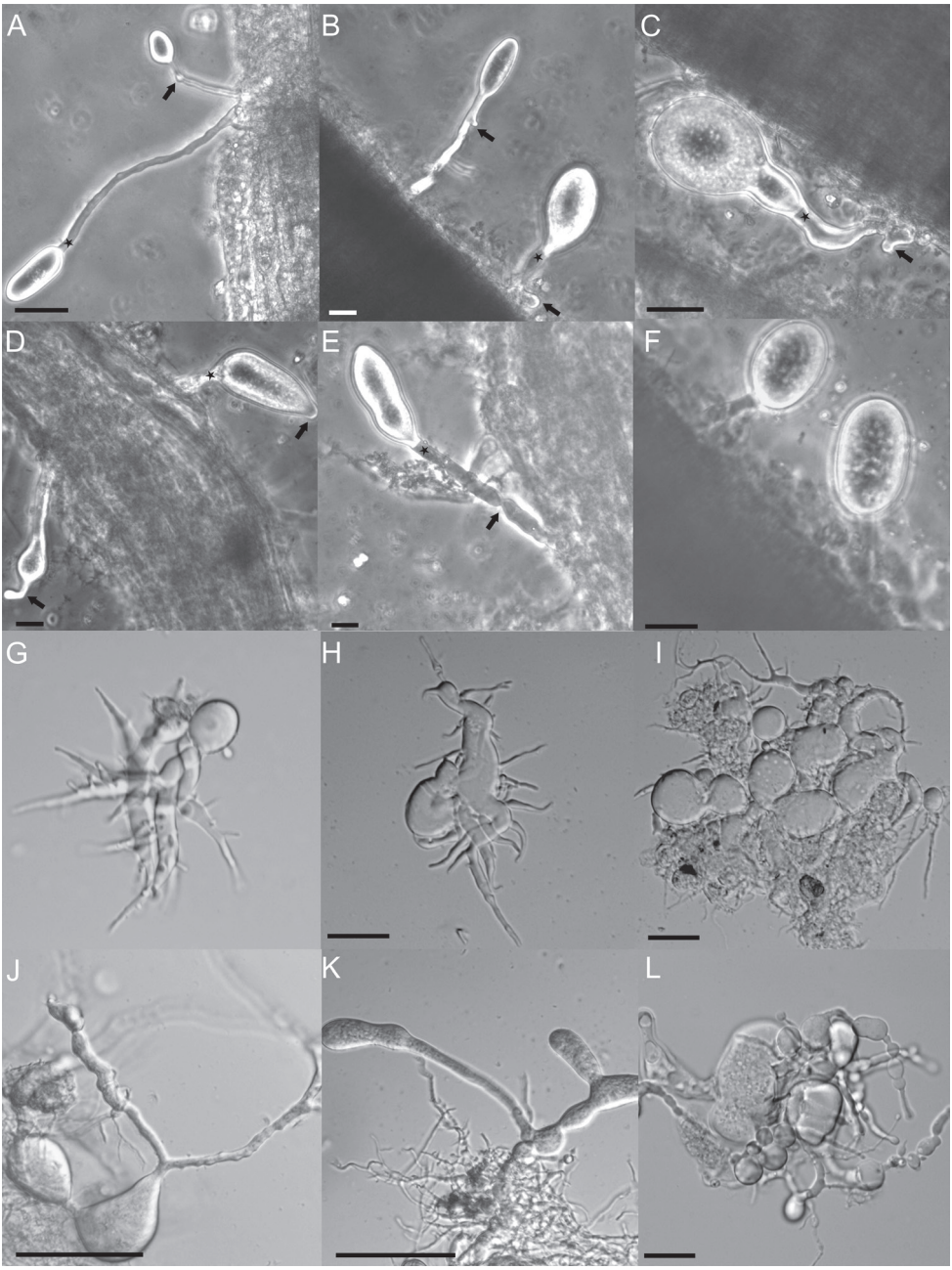

Figure 3. Microscopic images of *Liebetanzomyces polymorphus*. On rice straw (**A–F**) sporangia of varying sizes and shapes, like elongate (**A**), ellipsoid (**B**), ovoid (**C**), clavate (**E**) and globose (**F**). The zoospore cyst (**A–C** arrowed) is also visible, highlighting bipolar germination. Sporangiophore of varying length and shape, from short to long (**A**), sometimes eggcup shaped (**C**) and constricted (**E** arrowed) is shown. The sporangia with a papilla (**D** arrowed) and septum (**B, C, D, E** starred) are also indicated. Sporangia and thalli of irregular morphology on xylose (**G–I**) and cellobiose (**J–L**), including some pseudo-intercalary sporangia (**J–L**) can be observed. Scale bar: 20 μM.

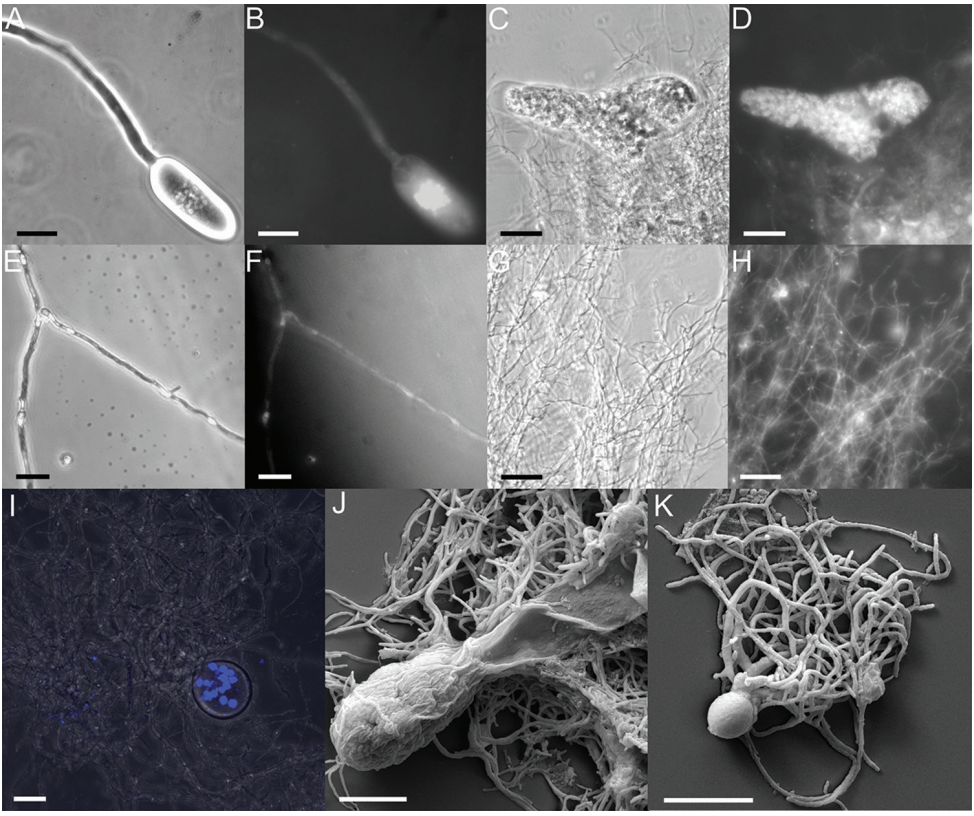

Figure 4. Phase contrast (**A, C, E, G**), fluorescence (**B, D, F, H**) and confocal (**I**) microscopic images of *Liebetanzomyces polymorphus* showing elongate (**A–B**) and triangular (**C–D**) sporangium filled with zoospores. Nuclei were seen in sporangium but not in sporangiophore (**B**) or rhizoidal system (**F, H, I**). No constrictions were observed in rhizoids. Scanning electron microscopy images of elongate (**J**) and globose (**K**) sporangium showing monocentric thallus. Scale bar: 20 μM (**A–I**); 10 μM (**J–K**).

and LSU) and G6SC (MH468766 and MH468764; ITS and LSU). The ITS region based sequence similarity search results showed that strain G1SC was 88.14% and 87.03% similar to *A. robustus* (accession number: NR 148182) and *A. contortus* (accession number: MG605706), respectively. Likewise, the LSU region of strain G1SC was most closely similar (97.71%) to *A. contortus* (accession number: MG605690). Although the sequence similarity of ca. 97% usually relates to a novel culture at the species level with its nearest match, the stark morphological dissimilarities of strain G1SC with *A. contortus* led to its classification as a novel genus.

To better understand the ecological distribution of strain G1SC, only ITS1 based searches were performed, which indicated <96% sequence similarities with several uncultured representatives of phylum Neocallimastigomycota (Suppl. material 2: Figure S2) reported from the USA (Liggenstoffer et al. 2010). The nearest matches were with different clones obtained from cattle (93–96%) and other clones of cattle, sheep and llama (88%-92%), indicating the presence of members of the G1SC clade in cat-

tle and close relatives in sheep and llama. The nearest matches of G1SC clade were also found in the SP4 clade designated by Paul et al. (2018), represented by accession number GQ767184, which consisted of 120 sequences of uncultured fungi, all from cattle faeces. The results, hence, indicate the presence of related fungi in both large as well as small ruminants. Surprisingly, no similar sequences were obtained from goat, which might be due to a lesser number of culture-independent studies conducted on these animals. The phylogenetic analysis of LSU and ITS1 regions showed distinct lineage for the G1SC clade, supported by high bootstrap values (Fig. 5 and Fig. 6), nearest to the Anaeromyces cluster. The results, therefore, underscore the importance of morphology-based identifications along with molecular tools, as none on its own can be relied on for accurate identification of anaerobic fungi.

Substrate utilisation, enzyme activities and fermentation product analyses

The substrate utilisation profiles of strains G1SC and G6SC exhibited exactly identical patterns (Table 1). Both these strains could utilise various polymeric and monomeric substrates. Our results were also compared to substrate utilisation profiles of other genera of monocentric and uniflagellate filamentous anaerobic fungi. All these genera were found to utilise cellulose, xylan, starch, cellobiose, sucrose, maltose, glucose and fructose, while none utilised chitin, ribose, peptone and tryptone as the sole carbon and energy source. For inulin, raffinose, alginate, pectin, trehalose, mannose, arabinose, glucuronic acid and galactose, varying results were obtained. Interestingly, only strains G1SC and G6SC were found positive for pectin utilisation amongst compared genera.

The enzyme activities (μmol/ml/h) of type strain G1SC showed maximum enzyme activities on crude substrates like rice straw and wheat straw, instead of pure cellulose and xylan (Table 2). The highest avicelase (1.05 ± 0.19) and xylanase (88.33 ± 1.00) activities were obtained on rice straw, while highest CMCase (7.73 ± 0.31) and β-glucosidase (1.64 ± 0.08) activities were measured in wheat straw. When compared to the enzyme activities of *Neocallimastix*, *Piromyces*, *Orpinomyces* and *Anaeromyces,* grown on wheat straw (Dagar et al. 2018), the strain G1SC displayed poor β-glucosidase activities. The avicelase activities of strain G1SC were comparable to *Orpinomyces* and *Anaeromyces*, but lower than most strains of *Neocallimastix* and *Piromyces*. The CMCase and xylanase activities of strain G1SC were comparable to *Orpinomyces*, *Neocallimastix* and most strains of *Piromyces*, but higher than *Anaeromyces*. These results suggest that strain G1SC is a moderate lignocellulose degrader and can be of use in applications involving lignocellulose degradation.

Figure 5. The LSU based maximum-likelihood tree is showing the phylogenetic position of *Liebetanzomyces polymorphus* with other members of phylum *Neocallimastigomycota*. Bootstrap values (>50%) based on 500 replicates are indicated at branching points. The GenBank accession number of each strain is listed in parentheses. Scale bar: 0.1 substitutions per site.

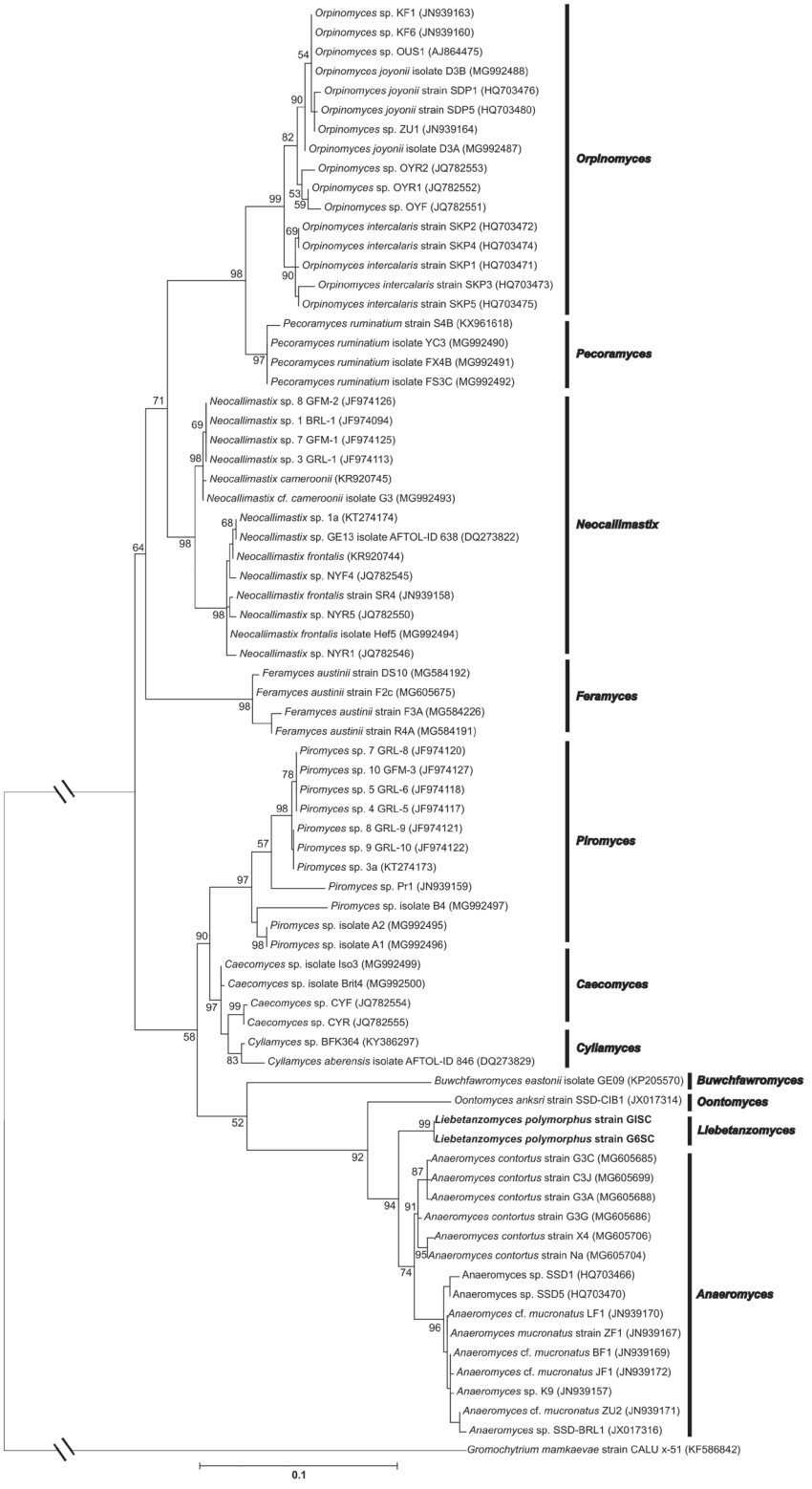
Orpinomyces sp. KF1 (JN939163)
Orpinomyces sp. KF6 (JN939160)
Orpinomyces sp. OUS1 (AJ864475)
Orpinomyces joyonii isolate D3B (MG992488)
Orpinomyces joyonii strain SDP1 (HQ703476)
Orpinomyces joyonii strain SDP5 (HQ703480)
Orpinomyces sp. ZU1 (JN939164)
Orpinomyces joyonii isolate D3A (MG992487)
Orpinomyces sp. OYR2 (JQ782553)
Orpinomyces sp. OYR1 (JQ782552)
Orpinomyces sp. OYF (JQ782551)
Orpinomyces intercalaris strain SKP2 (HQ703472)
Orpinomyces intercalaris strain SKP4 (HQ703474)
Orpinomyces intercalaris strain SKP1 (HQ703471)
Orpinomyces intercalaris strain SKP3 (HQ703473)
Orpinomyces intercalaris strain SKP5 (HQ703475)
Orpinomyces
Pecoramyces ruminatium strain S4B (KX961618)
Pecoramyces ruminatium isolate YC3 (MG992490)
Pecoramyces ruminatium isolate FX4B (MG992491)
Pecoramyces ruminatium isolate FS3C (MG992492)
Pecoramyces
Neocallimastix sp. 8 GFM-2 (JF974126)
Neocallimastix sp. 1 BRL-1 (JF974094)
Neocallimastix sp. 7 GFM-1 (JF974125)
Neocallimastix sp. 3 GRL-1 (JF974113)
Neocallimastix cameroonii (KR920745)
Neocallimastix cf. cameroonii isolate G3 (MG992493)
Neocallimastix sp. 1a (KT274174)
Neocallimastix sp. GE13 isolate AFTOL-ID 638 (DQ273822)
Neocallimastix frontalis (KR920744)
Neocallimastix sp. NYF4 (JQ782545)
Neocallimastix frontalis strain SR4 (JN939158)
Neocallimastix sp. NYR5 (JQ782550)
Neocallimastix frontalis isolate Hef5 (MG992494)
Neocallimastix sp. NYR1 (JQ782546)
Neocallimastix
Feramyces austinii strain DS10 (MG584192)
Feramyces austinii strain F2c (MG605675)
Feramyces austinii strain F3A (MG584226)
Feramyces austinii strain R4A (MG584191)
Feramyces
Piromyces sp. 7 GRL-8 (JF974120)
Piromyces sp. 10 GFM-3 (JF974127)
Piromyces sp. 5 GRL-6 (JF974118)
Piromyces sp. 4 GRL-5 (JF974117)
Piromyces sp. 8 GRL-9 (JF974121)
Piromyces sp. 9 GRL-10 (JF974122)
Piromyces sp. 3a (KT274173)
Piromyces sp. Pr1 (JN939159)
Piromyces sp. isolate B4 (MG992497)
Piromyces sp. isolate A2 (MG992495)
Piromyces sp. isolate A1 (MG992496)
Piromyces
Caecomyces sp. isolate Iso3 (MG992499)
Caecomyces sp. isolate Brit4 (MG992500)
Caecomyces sp. CYF (JQ782554)
Caecomyces sp. CYR (JQ782555)
Caecomyces
Cyllamyces sp. BFK364 (KY386297)
Cyllamyces aberensis isolate AFTOL-ID 846 (DQ273829)
Cyllamyces
Buwchfawromyces eastonii isolate GE09 (KP205570)
Buwchfawromyces
Oontomyces anksri strain SSD-CIB1 (JX017314)
Oontomyces
Liebetanzomyces polymorphus strain GISC
Liebetanzomyces polymorphus strain G6SC
Liebetanzomyces
Anaeromyces contortus strain G3C (MG605685)
Anaeromyces contortus strain C3J (MG605699)
Anaeromyces contortus strain G3A (MG605688)
Anaeromyces contortus strain G3G (MG605686)
Anaeromyces contortus strain X4 (MG605706)
Anaeromyces contortus strain Na (MG605704)
Anaeromyces sp. SSD1 (HQ703466)
Anaeromyces sp. SSD5 (HQ703470)
Anaeromyces cf. mucronatus LF1 (JN939170)
Anaeromyces mucronatus strain ZF1 (JN939167)
Anaeromyces cf. mucronatus BF1 (JN939169)
Anaeromyces cf. mucronatus JF1 (JN939172)
Anaeromyces sp. K9 (JN939157)
Anaeromyces cf. mucronatus ZU2 (JN939171)
Anaeromyces sp. SSD-BRL1 (JX017316)
Anaeromyces
Gromochytrium mamkaevae strain CALU x-51 (KF586842)
0.1

Table 2. Enzyme activities (μmol/mL/h) of *Liebetanzomyces polymorphus* strain G1SC on different substrates at 5 d of incubation.

Enzyme activity	Substrate used			
	Rice straw	Wheat straw	Cellulose	Xylan
Avicelase	1.05 ± 0.19	0.68 ± 0.10	0.73 ± 0.06	–
CMCase	4.55 ± 0.14	7.73 ± 0.31	5.56 ± 0.98	–
Xylanase	88.33 ± 1.00	79.44 ± 0.11	–	54.69 ± 2.31
B-glucosidase	1.53 ± 0.07	1.64 ± 0.08	0.69 ± 0.02	

– ±: standard deviation of three replicates.

Table 3. Fermentation products of *Liebetanzomyces polymorphus* strain G1SC on different substrates after 2 d of incubation.

Substrate	Fermentation product (in mM)						
	Hydrogen	Carbon dioxide	Formate	Acetate	Lactate	Succinate	Ethanol
Rice straw	58.10 ± 3.57	4.82 ± 0.16	16.43 ± 0.04	26.07 ± 0.24	1.79 ± 0.04	0.29 ± 0.00	10.35 ± 0.05
Wheat straw	45.42 ± 2.98	5.46 ± 0.13	11.44 ± 0.07	19.77 ± 0.44	1.72 ± 0.04	0.24 ± 0.00	8.27 ± 0.13
Cellulose	26.86 ± 3.11	6.38 ± 0.05	4.61 ± 0.05	13.26 ± 0.52	0.73 ± 0.02	ND	7.27 ± 0.01
Xylan	27.71 ± 2.48	7.12 ± 0.11	5.01 ± 0.06	8.30 ± 0.12	4.01 ± 0.06	0.12 ± 0.00	6.96 ± 0.03
Starch	44.09 ± 0.54	5.99 ± 0.03	9.45 ± 0.10	14.58 ± 0.28	15.11 ± 0.38	0.34 ± 0.00	7.69 ± 0.13
Pectin	42.59 ± 1.18	6.38 ± 0.09	7.64 ± 0.08	11.32 ± 0.22	3.56 ± 0.04	0.15 ± 0.01	8.01 ± 0.12
Cellobiose	58.05 ± 0.63	5.64 ± 0.03	9.75 ± 0.02	15.69 ± 0.29	9.35 ± 0.04	0.30 ± 0.01	8.46 ± 0.04
Sucrose	29.21 ± 1.02	6.99 ± 0.05	3.77 ± 0.10	7.61 ± 0.44	0.66 ± 0.00	ND	9.11 ± 0.06
Maltose	53.26 ± 3.01	5.59 ± 0.12	8.26 ± 0.13	17.45 ± 0.40	10.16 ± 0.06	0.22 ± 0.00	7.85 ± 0.05
Lactose	39.08 ± 1.83	6.51 ± 0.08	4.26 ± 0.01	8.98 ± 0.13	0.47 ± 0.01	ND	8.52 ± 0.04
Glucose	49.79 ± 0.86	5.84 ± 0.04	10.11 ± 0.18	16.75 ± 0.19	7.18 ± 0.02	0.31 ± 0.00	8.65 ± 0.09
Xylose	53.80 ± 1.41	5.62 ± 0.09	8.38 ± 0.19	12.58 ± 0.47	7.90 ± 0.06	0.16 ± 0.00	8.39 ± 0.03
Fructose	61.05 ± 1.59	5.28 ± 0.06	11.79 ± 0.05	17.05 ± 0.71	15.97 ± 0.03	0.30 ± 0.00	9.10 ± 0.05

– ±: standard deviation of three replicates.

The substrate utilisation results were also confirmed by measuring the fermentation products on each substrate (Table 3). The strain G1SC produced hydrogen, carbon dioxide, formate, acetate, lactate, succinate and ethanol on all substrates, but did not produce propionate, butyrate, butanol or malate which is in line with the previous reports (Trinci et al. 1994; Edwards et al. 2017). The absence of propionate and butyrate also implies that there was no bacterial contamination and all products are solely of fungal origin. The fermentation product quantities also indicated the efficiency of substrate utilisation. The substrates like sucrose and lactose, which recorded poor growth after 2 d of incubation, also showed lesser production of formate, acetate

Figure 6. The ITS1 based maximum-likelihood tree is showing the phylogenetic position of *Liebetanzomyces polymorphus* with nearest uncultured clones and other members of phylum *Neocallimastigomycota*. Bootstrap values (>50%) based on 500 replicates are indicated at branching points. The GenBank accession number of each strain is listed in parentheses. Scale bar: 0.5 substitutions per site.

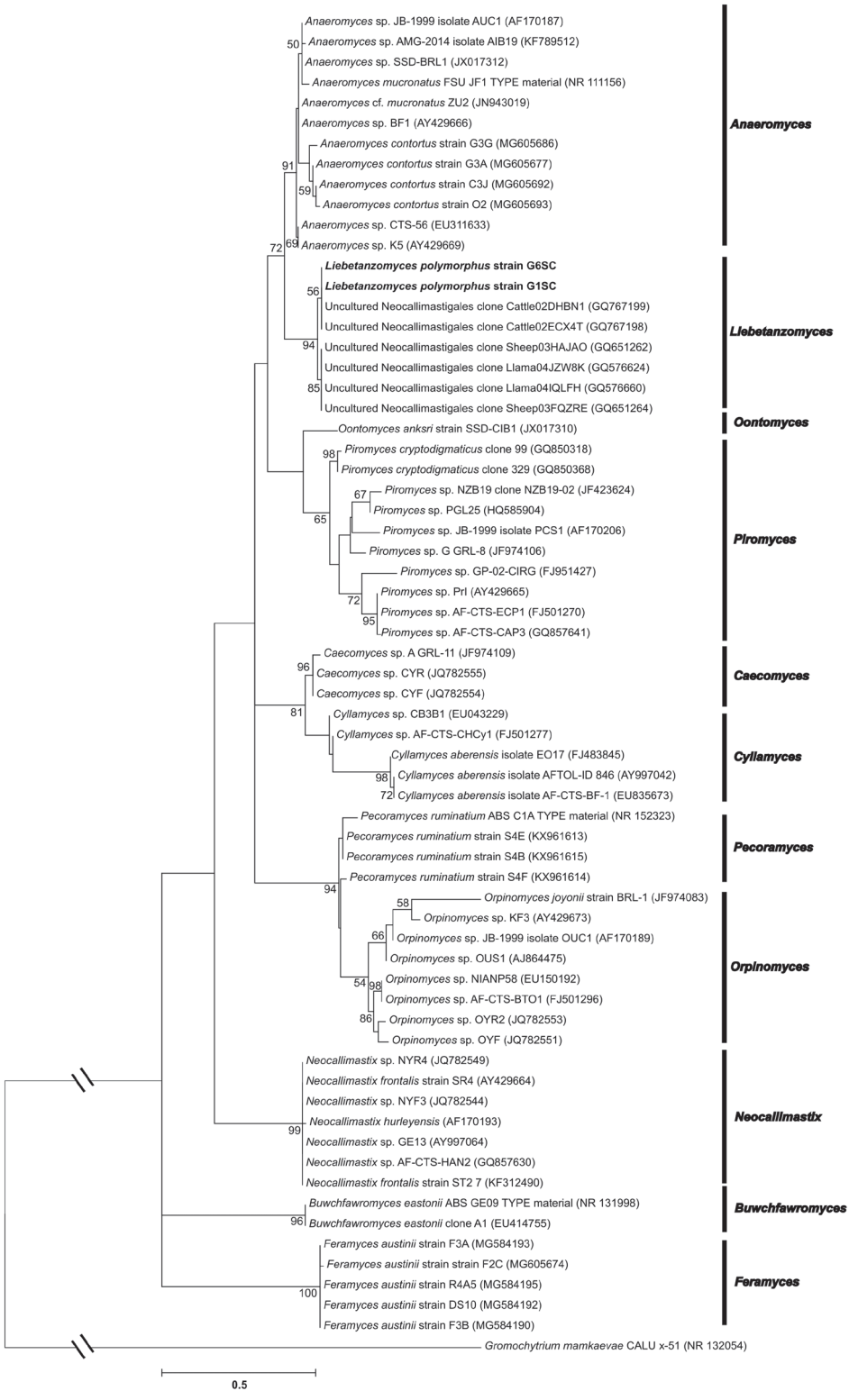
Anaeromyces sp. JB-1999 isolate AUC1 (AF170187)
Anaeromyces sp. AMG-2014 isolate AIB19 (KF789512)
Anaeromyces sp. SSD-BRL1 (JX017312)
Anaeromyces mucronatus FSU JF1 TYPE material (NR 111156)
Anaeromyces cf. mucronatus ZU2 (JN943019)
Anaeromyces sp. BF1 (AY429666)
Anaeromyces contortus strain G3G (MG605686)
Anaeromyces contortus strain G3A (MG605677)
Anaeromyces contortus strain C3J (MG605692)
Anaeromyces contortus strain O2 (MG605693)
Anaeromyces sp. CTS-56 (EU311633)
Anaeromyces sp. K5 (AY429669)
Anaeromyces
Liebetanzomyces polymorphus strain G6SC
Liebetanzomyces polymorphus strain G1SC
Uncultured Neocallimastigales clone Cattle02DHBN1 (GQ767199)
Uncultured Neocallimastigales clone Cattle02ECX4T (GQ767198)
Uncultured Neocallimastigales clone Sheep03HAJAO (GQ651262)
Uncultured Neocallimastigales clone Llama04JZW8K (GQ576624)
Uncultured Neocallimastigales clone Llama04IQLFH (GQ576660)
Uncultured Neocallimastigales clone Sheep03FQZRE (GQ651264)
Liebetanzomyces
Oontomyces anksri strain SSD-CIB1 (JX017310)
Oontomyces
Piromyces cryptodigmaticus clone 99 (GQ850318)
Piromyces cryptodigmaticus clone 329 (GQ850368)
Piromyces sp. NZB19 clone NZB19-02 (JF423624)
Piromyces sp. PGL25 (HQ585904)
Piromyces sp. JB-1999 isolate PCS1 (AF170206)
Piromyces sp. G GRL-8 (JF974106)
Piromyces sp. GP-02-CIRG (FJ951427)
Piromyces sp. PrI (AY429665)
Piromyces sp. AF-CTS-ECP1 (FJ501270)
Piromyces sp. AF-CTS-CAP3 (GQ857641)
Piromyces
Caecomyces sp. A GRL-11 (JF974109)
Caecomyces sp. CYR (JQ782555)
Caecomyces sp. CYF (JQ782554)
Caecomyces
Cyllamyces sp. CB3B1 (EU043229)
Cyllamyces sp. AF-CTS-CHCy1 (FJ501277)
Cyllamyces aberensis isolate EO17 (FJ483845)
Cyllamyces aberensis isolate AFTOL-ID 846 (AY997042)
Cyllamyces aberensis isolate AF-CTS-BF-1 (EU835673)
Cyllamyces
Pecoramyces ruminatium ABS C1A TYPE material (NR 152323)
Pecoramyces ruminatium strain S4E (KX961613)
Pecoramyces ruminatium strain S4B (KX961615)
Pecoramyces ruminatium strain S4F (KX961614)
Pecoramyces
Orpinomyces joyonii strain BRL-1 (JF974083)
Orpinomyces sp. KF3 (AY429673)
Orpinomyces sp. JB-1999 isolate OUC1 (AF170189)
Orpinomyces sp. OUS1 (AJ864475)
Orpinomyces sp. NIANP58 (EU150192)
Orpinomyces sp. AF-CTS-BTO1 (FJ501296)
Orpinomyces sp. OYR2 (JQ782553)
Orpinomyces sp. OYF (JQ782551)
Orpinomyces
Neocallimastix sp. NYR4 (JQ782549)
Neocallimastix frontalis strain SR4 (AY429664)
Neocallimastix sp. NYF3 (JQ782544)
Neocallimastix hurleyensis (AF170193)
Neocallimastix sp. GE13 (AY997064)
Neocallimastix sp. AF-CTS-HAN2 (GQ857630)
Neocallimastix frontalis strain ST2 7 (KF312490)
Neocallimastix
Buwchfawromyces eastonii ABS GE09 TYPE material (NR 131998)
Buwchfawromyces eastonii clone A1 (EU414755)
Buwchfawromyces
Feramyces austinii strain F3A (MG584193)
Feramyces austinii strain strain F2C (MG605674)
Feramyces austinii strain R4A5 (MG584195)
Feramyces austinii strain DS10 (MG584192)
Feramyces austinii strain F3B (MG584190)
Feramyces
Gromochytrium mamkaevae CALU x-51 (NR 132054)
0.5

and lactate and the absence of succinate. Likewise, the polymeric substrate like rice straw, wheat straw, cellulose and xylan showed lesser production of hydrogen, formate, acetate, lactate, succinate and ethanol at 2 d of incubation (Table 3), which increased substantially after 5 d (Suppl. material 4: Table S1). The NMDS plot showed clear clustering of various carbon sources based on fermentation products, an observation duly supported by a low stress value (Suppl. material 3: Figure S3). These results, therefore, signify the usefulness of metabolite profiling for measuring the substrate utilisation abilities of anaerobic fungi.

Liebetanzomyces polymorphus **Joshi, G.W. Griff. & Dagar, gen. et sp. nov.**
Registration identifier (genus): IF554794
Registration identifier (species): IF554795

Diagnosis. Strictly anaerobic fungus with determinate, monocentric thallus with single terminal sporangium of varying shape and size and uniflagellate zoospores. The clade is defined by the sequences accession numbers MH468765 (ITS1, 5.8S, ITS2 complete) and MH468763 (LSU, partial sequence). The most genetically similar genus is *Anaeromyces*, which is defined as forming a polycentric thallus (Breton et al. 1990. FEMS Microbiol. Lett. 58, p.177), in contrast to the monocentric *Liebetanzomyces*.

A strict anaerobic fungus, isolated from the rumen of a goat. In roll tubes of cellobiose agar medium, the fungus forms medium to large circular colonies (0.5–2 mm diam.). In liquid cellobiose medium, the fungal thalli attach to the sides and bottom of glass bottles. Monocentric thallus development, producing a single terminal sporangium per thallus. Also, the fungus produces few pseudo-intercalary sporangia but only on soluble substrates. An extensive anucleate rhizoidal system without constrictions is formed. The sporangia vary in size (10–90 µm wide, 10–75 µm long), shape (globose, ellipsoid, clavate, ovoid, elongate or irregular) and sometimes bear papillae. The sporangium is borne on variable length sporangiophore (15–80 µm), sometimes forming an eggcup-like structure below the sporangium or showing cyst-like structure. Zoospores are produced abundantly, mostly uniflagellate, rarely biflagellate, spherical (5–6 µm in diameter) in size and flagellum of 15–20 µm in length. The zoospores may germinate either endogenously or exogenously. The clade is defined by the sequences accession numbers MH468765 (ITS1, 5.8S, ITS2 complete) and MH468763 (LSU, partial sequence). The ex-type culture (strain G1SC) is stored cryogenically in liquid nitrogen at bioenergy group, Agharkar Research Institute, Pune, India. The holotype is a 3 d old culture of G1SC preserved in 5% glutaraldehyde and deposited at the MACS-collection of microorganisms (MCM) of Agharkar Research Institute, Pune, India and isotype material at the Aberystwyth University biorepository (code ABS).

Etymology. '*Liebetanz*' is assigned to honour Erwin Liebetanz (Liebetanz 1910) by taking all nine letters of his surname (i.e. LIEBETANZ) and who was the first to observe anaerobic gut fungus *Piromyces* as a flagellated organism in 1910; myces = the Greek name for fungus.

The specific epithet *polymorphus* is for different polymorphic sporangial shapes displayed by this fungus.

Conclusions

The morphological and molecular characterisation results clearly indicate that the strain G1SC represents a novel genus *Liebetanzomyces polymorphus* in the phylum *Neocallimastigomycota*. *Liebetanzomyces polymorphus* displays a monocentric thallus and produces uniflagellate zoospores, thus, it is morphologically similar to *Piromyces, Buwchfawromyces*, *Oontomyces* and *Pecoramyces*. *Liebetanzomyces polymorphus* exhibits extensive sporangial variations and is genetically near but dissimilar to *Anaeromyces*. The ITS1 and LSU based phylogenetic analysis also confirmed the distinct lineage of *Liebetanzomyces polymorphus*. The results suggest that both morphological and molecular tools should be used in tandem to determine the uniqueness of any anaerobic fungal culture, as the use of either one independently can result in a wrong identification.

Acknowledgements

The authors acknowledge the support of Department of Biotechnology (DBT) for the financial support (project no. BT/PR15694/PBD/26/506/2015). We are grateful to Dr Karthick Balasubramanian for his valuable help in the suitable presentation of results and Dr Rajesh Kumar K.C. for helpful discussions. We also thank the Director, Agharkar Research Institute for providing the required infrastructure support.

Reference

Breton A, Bernalier A, Dusser M, Fonty G, Gaillard-Martinie B, Guillot J (1990) *Anaeromyces mucronatus* nov. gen., nov. sp. A new strictly anaerobic rumen fungus with polycentric thallus. FEMS microbiology letters 70: 177–182. https://doi.org/10.1111/j.1574-6968.1990.tb13974.x

Brookman J, Mennim G, Trinci A, Theodorou M, Tuckwell D (2000) Identification and characterization of anaerobic gut fungi using molecular methodologies based on ribosomal ITS1 and 18S rRNA. Microbiology 146: 393–403. https://doi.org/10.1099/00221287-146-2-393

Callaghan TM, Podmirseg SM, Hohlweck D, Edwards JE, Puniya AK, Dagar SS, Griffith GW (2015) *Buwchfawromyces eastonii* gen. nov., sp. nov.: a new anaerobic fungus (*Neocallimastigomycota*) isolated from buffalo faeces. MycoKeys 9. https://doi.org/10.3897/mycokeys.9.9032

Dagar SS, Kumar S, Griffith GW, Edwards JE, Callaghan TM, Singh R, Nagpal AK, Puniya AK (2015) A new anaerobic fungus (*Oontomyces anksri* gen. nov., sp. nov.) from the di-

gestive tract of the Indian camel (*Camelus dromedarius*). Fungal Biology 119: 731–737. https://doi.org/10.1016/j.funbio.2015.04.005

Dagar SS, Kumar S, Mudgil P, Puniya AK (2018) Comparative evaluation of lignocellulolytic activities of filamentous cultures of monocentric and polycentric anaerobic fungi. Anaerobe 50: 76–79. https://doi.org/10.1016/j.anaerobe.2018.02.004

Dighe AS, Shouche YS, Ranade DR (1998) *Selenomonas lipolytica* sp. nov., an obligately anaerobic bacterium possessing lipolytic activity. International Journal of Systematic and Evolutionary Microbiology 48: 783–791. https://doi.org/10.1099/00207713-48-3-783

Edwards JE, Forster RJ, Callaghan TM, Dollhofer V, Dagar SS, Cheng Y, Chang J, Kittelmann S, Fliegerova K, Puniya AK, Henske JK, Gilmore SP, O'Malley MA, Griffith GW, Smidt H (2017) PCR and omics based techniques to study the diversity, ecology and biology of anaerobic fungi: insights, challenges and opportunities. Frontiers in Microbiology 8: 1657. https://doi.org/10.3389/fmicb.2017.01657

Fliegerova K, Pažoutová S, Mrazek J, Kopečný J (2002) Special properties of polycentric anaerobic fungus *Anaeromyces mucronatus*. Acta Veterinaria Brunensis 71: 441–444. https://doi.org/10.2754/avb200271040441

Gruninger RJ, Puniya AK, Callaghan TM, Edwards JE, Youssef N, Dagar SS, Fliegerova K, Griffith GW, Forster R, Tsang A, McAllister T, Elshahed MS (2014) Anaerobic fungi (phylum *Neocallimastigomycota*): advances in understanding their taxonomy, life cycle, ecology, role and biotechnological potential. FEMS Microbiology Ecology 90: 1–17. https://doi.org/10.1111/1574-6941.12383

Hall TA (1999) BioEdit: a user-friendly biological sequence alignment editor and analysis program for Windows 95/98/NT. Nucleic acids symposium series. [London]: Information Retrieval Ltd., c1979–c2000., 95–98.

Hammer Ø, Harper DAT, Ryan PD (2001) PAST: Paleontological statistics software package for education and data analysis. Palaeontologia Electronica 4: 1–9.

Hanafy RA, Elshahed MS, Liggenstoffer AS, Griffith GW, Youssef NH (2017) *Pecoramyces ruminantium*, gen. nov., sp. nov., an anaerobic gut fungus from the feces of cattle and sheep. Mycologia 109: 231–243. https://doi.org/10.1080/00275514.2017.1317190

Hanafy RA, Elshahed MS, Youssef NH (2018) *Feramyces austinii*, gen. nov, sp. nov., an anaerobic gut fungus from rumen and fecal samples of wild Barbary sheep and fallow deer. Mycologia. https://doi.org/10.1080/00275514.2018.1466610

Hibbett DS, Binder M, Bischoff JF, Blackwell M, Cannon PF, Eriksson OE, Huhndorf S, James T, Kirk PM, Lucking R, Thorsten Lumbsch H, Lutzoni F, Matheny PB, McLaughlin DJ, Powell MJ, Redhead S, Schoch CL, Spatafora JW, Stalpers JA, Vilgalys R, Aime MC, Aptroot A, Bauer R, Begerow D, Benny GL, Castlebury LA, Crous PW, Dai YC, Gams W, Geiser DM, Griffith GW, Gueidan C, Hawksworth DL, Hestmark G, Hosaka K, Humber RA, Hyde KD, Ironside JE, Koljalg U, Kurtzman CP, Larsson KH, Lichtwardt R, Longcore J, Miadlikowska J, Miller A, Moncalvo JM, Mozley-Standridge S, Oberwinkler F, Parmasto E, Reeb V, Rogers JD, Roux C, Ryvarden L, Sampaio JP, Schussler A, Sugiyama J, Thorn RG, Tibell L, Untereiner WA, Walker C, Wang Z, Weir A, Weiss M, White MM, Winka K, Yao YJ, Zhang N (2007) A higher-level phylogenetic classification of the Fungi. Mycological Research 111: 509–547. https://doi.org/10.1016/j.mycres.2007.03.004

Ho Y, Abdullah N, Jalaludin S (1988) Penetrating structures of anaerobic rumen fungi in cattle and swamp buffalo. Microbiology 134: 177–181. https://doi.org/10.1099/00221287-134-1-177

Ho Y, Barr D (1995) Classification of anaerobic gut fungi from herbivores with emphasis on rumen fungi from Malaysia. Mycologia: 655–677. https://doi.org/10.1080/00275514.1995.12026582

Ivarsson M, Schnürer A, Bengtson S, Neubeck A (2016) Anaerobic Fungi: A Potential Source of Biological H(2) in the Oceanic Crust. Frontiers in Microbiology 7: 674. https://doi.org/10.3389/fmicb.2016.00674

Janssen PH, Yates PS, Grinton BE, Taylor PM, Sait M (2002) Improved culturability of soil bacteria and isolation in pure culture of novel members of the divisions *Acidobacteria*, *Actinobacteria*, *Proteobacteria*, and *Verrucomicrobia*. Applied and Environmental Microbiology 68: 2391–2396. https://doi.org/10.1128/aem.68.5.2391-2396.2002

Kamalaskar LB, Dhakephalkar P, Meher K, Ranade D (2010) High biohydrogen yielding *Clostridium* sp. DMHC-10 isolated from sludge of distillery waste treatment plant. International Journal of Hydrogen Energy 35: 10639–10644. https://doi.org/10.1016/j.ijhydene.2010.05.020

Kittelmann S, Naylor GE, Koolaard JP, Janssen PH (2012) A proposed taxonomy of anaerobic fungi (Class *Neocallimastigomycetes*) suitable for large-scale sequence-based community structure analysis. PLoS One 7: e36866. https://doi.org/10.1371/journal.pone.0036866

Koetschan C, Kittelmann S, Lu J, Al-Halbouni D, Jarvis GN, Müller T, Wolf M, Janssen PH (2014) Internal transcribed spacer 1 secondary structure analysis reveals a common core throughout the anaerobic fungi (*Neocallimastigomycota*). PLoS One 9: e91928. https://doi.org/10.1371/journal.pone.0091928

Kumar S, Stecher G, Tamura K (2016) MEGA7: molecular evolutionary genetics analysis version 7.0 for bigger datasets. Molecular Biology and Evolution 33: 1870–1874. https://doi.org/10.1093/molbev/msw054

Li J, Heath IB, Bauchop T (1990) *Piromyces mae* and *Piromyces dumbonica*, two new species of uniflagellate anaerobic chytridiomycete fungi from the hindgut of the horse and elephant. Canadian Journal of Botany 68: 1021–1033. https://doi.org/10.1139/b90-129

Liebetanz E (1910) Die parasitischen Protozoen des Wiederkauermagens. Archiv für Protistenkunde 19: 19–80.

Liggenstoffer AS, Youssef NH, Couger M, Elshahed MS (2010) Phylogenetic diversity and community structure of anaerobic gut fungi (phylum Neocallimastigomycota) in ruminant and non-ruminant herbivores. The ISME Journal 4: 1225. https://doi.org/10.1038/ismej.2010.49

McSweeney CS, Denman SE, Mackie RI (2005) Rumen bacteria. In: Makkar HPS, McSweeney CS (Eds) Methods in Gut Microbial Ecology for Ruminants. Springer Netherlands, Dordrecht, 23–37. https://doi.org/10.1007/1-4020-3791-0_2

Miller TL, Wolin MJ (1974) A Serum bottle modification of the hungate technique for cultivating obligate anaerobes. Applied Microbiology 27: 985–987.

Paul SS, Bu D, Xu J, Hyde KD, Yu Z (2018) A phylogenetic census of global diversity of gut anaerobic fungi and a new taxonomic framework. Fungal Diversity 89: 253–266. https://doi.org/10.1007/s13225-018-0396-6

Picard KT (2017) Coastal marine habitats harbor novel early-diverging fungal diversity. Fungal Ecology 25: 1–13. https://doi.org/10.1016/j.funeco.2016.10.006

Singh KG, Lapsiya KL, Gophane RR, Ranade DR (2016) Optimization for butanol production using Plackett-Burman Design coupled with Central Composite Design by *Clostridium beijerenckii* strain CHTa isolated from distillery waste manure. International Research Journal of Biochemical Technology 7: 1063–1068.

Sirohi SK, Choudhury PK, Dagar SS, Puniya AK, Singh D (2013) Isolation, characterization and fibre degradation potential of anaerobic rumen fungi from cattle. Annals of Microbiology 63: 1187–1194. https://doi.org/10.1007/s13213-012-0577-6

Tamura K (1992) Estimation of the number of nucleotide substitutions when there are strong transition-transversion and G+ C-content biases. Molecular Biology and Evolution 9: 678–687. https://doi.org/10.1093/oxfordjournals.molbev.a040752

Tamura K, Nei M (1993) Estimation of the number of nucleotide substitutions in the control region of mitochondrial DNA in humans and chimpanzees. Molecular Biology and Evolution 10: 512–526. https://doi.org/10.1093/oxfordjournals.molbev.a040023

Thakker C, Bhosale S, Ranade D (2006) Formation of succinic acid by *Klebsiella pneumoniae* MCM B-325 under aerobic and anaerobic conditions. Journal of Microbiology and Biotechnology 16: 870–879.

Thompson JD, Higgins DG, Gibson TJ (1994) CLUSTAL W: improving the sensitivity of progressive multiple sequence alignment through sequence weighting, position-specific gap penalties and weight matrix choice. Nucleic Acids Research 22: 4673–4680. https://doi.org/10.1093/nar/22.22.4673

Trinci APJ, Davies DR, Gull K, Lawrence MI, Bonde Nielsen B, Rickers A, Theodorou MK (1994) Anaerobic fungi in herbivorous animals. Mycological Research 98: 129–152. https://doi.org/10.1016/S0953-7562(09)80178-0

Wren M (1980) Prolonged primary incubation in the isolation of anaerobic bacteria from clinical specimens. Journal of Medical Microbiology 13: 257–264. https://doi.org/10.1099/00222615-13-2-257

Supplementary material 1

Figure S1

Authors: Akshay Joshi, Vikram B. Lanjekar, Prashant K. Dhakephalkar, Tony M. Callaghan, Gareth W. Griffith, Sumit Singh Dagar

Data type: multimedia

Explanation note: Photographs showing fungal thalli (marked by arrows) of *Liebetanzomyces polymorphus* attached to the sides (A) and bottom (B) of glass bottles when grown in liquid medium.

Link: https://doi.org/10.3897/mycokeys.40.28337.suppl1

Supplementary material 2

Figure S2

Authors: Akshay Joshi, Vikram B. Lanjekar, Prashant K. Dhakephalkar, Tony M. Callaghan, Gareth W. Griffith, Sumit Singh Dagar

Data type: multimedia

Explanation note: The ITS1 based maximum-likelihood tree based on the Tamura 3-parameter model (Tamura 1992) is showing the phylogenetic position of *Liebetanzomyces polymorphus* with nearest uncultured clones. The genus *Anaeromyces mucronatus* (accession number: NR_111156) was used as the outgroup. Bootstrap values (>50%) based on 500 replicates are indicated at branching points. The GenBank accession number of each strain is listed before the name. Bar, 0.02 substitutions per site.

Link: https://doi.org/10.3897/mycokeys.40.28337.suppl2

Supplementary material 3

Figure S3

Authors: Akshay Joshi, Vikram B. Lanjekar, Prashant K. Dhakephalkar, Tony M. Callaghan, Gareth W. Griffith, Sumit Singh Dagar

Data type: multimedia

Explanation note: The Non-metric multidimensional scaling (NMDS) plot showing clustering of various carbon sources based on fermentation products. Stress value, 0.012.

Link: https://doi.org/10.3897/mycokeys.40.28337.suppl3

Supplementary material 4

Table S1

Authors: Akshay Joshi, Vikram B. Lanjekar, Prashant K. Dhakephalkar, Tony M. Callaghan, Gareth W. Griffith, Sumit Singh Dagar

Data type: species data

Explanation note: Fermentation products of *Liebetanzomyces polymorphus* strain G1SC on different substrates after 5 d of incubation.

Link: https://doi.org/10.3897/mycokeys.40.28337.suppl4

MycoKeys 40: 111–126 (2018)
doi: 10.3897/mycokeys.40.28700
http://mycokeys.pensoft.net

RESEARCH ARTICLE

A peer-reviewed open-access journal
MycoKeys
Launched to accelerate biodiversity research

Taxonomy and phylogeny of *Dichostereum* (Russulales), with descriptions of three new species from southern China

Shi-Liang Liu[1], Shuang-Hui He[1]

1 *Institute of Microbiology, Beijing Forestry University, Beijing 100083, China*

Corresponding author: *Shuang-Hui He* (shuanghuihe@yahoo.com)

Academic editor: *R. Henrik Nilsson* | Received 28 July 2018 | Accepted 24 September 2018 | Published 10 October 2018

Citation: Liu S-L, He S-H (2018) Taxonomy and phylogeny of *Dichostereum* (Russulales), with descriptions of three new species from southern China. MycoKeys 40: 111–126. https://doi.org/10.3897/mycokeys.40.28700

Abstract

Nine species of *Dichostereum* were subjected to phylogenetic analyses, based on a combined dataset of ITS1-5.8S-ITS2-nrLSU-*tef1* sequences. The morphology of specimens collected from China and Australia were studied. Three species, *D. austrosinense*, *D. boidinii* and *D. eburneum*, collected from southern China, are described and illustrated as new to science, based on the morphological and molecular evidence. *Dichostereum austrosinense* is characterised by the relatively large gloeocystidia (80–130 × 8–15 μm) and basidiospores (7.3–8 μm in diam.) with large warts and crests. *Dichostereum boidinii* is distinguished by its thick basidiomata and relatively small basidiospores (5.5–6.5 μm in diam.) with large warts and crests. *Dichostereum eburneum* is unique in having pale basidiomata growing on bark of living *Castanopsis*, abundant crystals in the context and basidiospores with dense and large ornamentations. A key to the 5 species of *Dichostereum* in China is given.

Keywords

Amyloid basidiospores; corticioid fungi; dichohyphae; Peniophoraceae; *Vararia*

Introduction

Dichostereum Pilát, typified with *D. durum* (Bourdot & Galzin) Pilát, is a small and well-delimited corticioid genus in Russulales. It is characterised by resupinate basidiomata with smooth or grandinioid hymenophore, dimitic hyphal system with dextrinoid dichohyphae and clamped generative hyphae, gloeocystidia and ellipsoid or

subglobose, ornamented basidiospores with a strong amyloid reaction in Melzer's reagent (Hallenberg 1985; Bernicchia and Gorjón 2010). Previously, *Dichostereum* was placed in Lachnocladiaceae, which includes genera with dextrinoid skeletal hyphae (Reid 1965; Parmasto 1968, 1970; Hallenberg 1985). However, recent phylogenetic analyses, based on DNA sequences, showed that *Dichostereum* formed a monophyletic lineage in the Peniophoraceae clade, which includes genera with or without dextrinoid hyphae (Larsson and Larsson 2003; Miller et al. 2006; Larsson 2007).

Dichostereum was once treated as a subgenus of *Vararia* P. Karst. (Peniophoraceae, Russulales) by some mycologists since the two genera are very similar in morphology except that the latter has smooth basidiospores (Boidin 1967; Parmasto 1970; Lanquetin 1973). Boidin and Lanquetin (1977) emended the description of *Dichostereum* and retained it as a separate genus. Later, Boidin and Lanquetin (1980) monographed the genus and provided a key to its 11 species based on evidence of morphology, distribution and intercompatibility tests of cultures. Based on limited sampling, their results showed that *D. effuscatum* (Cooke & Ellis) Boidin & Lanq. and *D. granulosum* (Pers.) Boidin & Lanq. were widely distributed, while the other species seemed to be rather endemic (Boidin and Lanquetin 1980). Few studies on the genus have been carried out since then and many regions including East Asia need further collecting and study (Boidin et al. 1987, Boidin and Michel 1998).

Previously, two species, *Dichostereum boreale* (Pouzar) Ginns & M.N.L. Lefebvre (= *D. granulosum*) and *D. pallescens* (Schwein.) Boidin & Lanq., were reported in temperate China (Dai 2011). The species diversity of the genus in China is still unclear. In the present paper, we provide a morphological and phylogenetic study of the genus based on specimens mostly collected from southern China. This is part of an ongoing study of the corticioid fungi of the Russulales in China.

Materials and methods

Morphological studies

Voucher specimens were deposited in the herbaria of Beijing Forestry University, Beijing, China (**BJFC**) and in the Centre for Forest Mycology Research, U.S. Forest Service, Madison, USA (**CFMR**). Freehand sections were made from dried basidiomata and mounted in 2% (w/v) potassium hydroxide (KOH), 1% phloxine (w/v) or Melzer's reagent. Microscopic examinations were carried out with a Nikon Eclipse 80i microscope (Nikon Corporation, Japan) at magnifications up to 1000×. Drawings were made with the aid of a drawing tube. All measurements were carried out with sections mounted in Melzer's reagent. Ornamentations were excluded from the measurements of basidiospores. Scanning electron micrographs (SEM) were taken with a JEOL JSM-6700F microscope (JEOL, Japan). Dried specimens were mounted directly in gold and platinum and examined and photographed at 10.0 kV. Colour names and codes follow Kornerup and Wanscher (1978). Herbarium code designations are from Index Herbariorum (Thiers, continuously updated).

DNA extraction and sequencing

The CTAB plant genome rapid extraction kit DN14 (Aidlab Biotechnologies Co. Ltd, Beijing) was used for DNA extraction and PCR amplification from dried specimens or cultures. The ITS, partial nrLSU and *tef1* markers were amplified with the primer pairs ITS5/ITS4 (White et al. 1990), LR0R/LR7 (Vilgalys and Hester 1990) and 983F/1567R (Rehner and Buckley 2005), respectively. The PCR procedures followed Dai and He (2016). DNA sequencing was performed at Beijing Genomics Institute and the sequences were deposited in GenBank (Benson et al. 2018). The sequence quality control followed Nilsson et al. (2012). BioEdit v.7.0.5.3 (Hall 1999) and Geneious v.11.1.15 (Kearse et al. 2012) were used for chromatogram check and contig assembly.

Phylogenetic analyses

The molecular phylogeny was inferred from a combined dataset of ITS1-5.8S-ITS2-nrLSU-*tef1* sequences of representative members of Peniophoraceae *sensu* Larsson (2007) (Table 1). *Echinodontium tinctorium* (Ellis & Everh.) Ellis & Everh. was selected as the outgroup (Liu et al. 2017a). The sequences of the three markers (ITS, nrLSU and *tef1*) were aligned separately using MAFFT v.7 (Katoh et al. 2017, http://mafft.cbrc.jp/alignment/server/) with the G-INS-i iterative refinement algorithm and optimised manually in BioEdit v.7.0.5.3. The programme Gblocks v.0.91b (Castresana 2000) was then used to exclude poorly aligned positions of the ITS alignment. The separate alignments were concatenated using Mesquite v.3.5.1 (Maddison and Maddison 2018). The combined alignments were deposited in TreeBase (http://treebase.org/treebase-web/home.html, submission ID: 23332).

For both Maximum Likelihood (ML) and Bayesian Inference (BI), a partitioned analysis was performed with the following five partitions: ITS1, 5.8S, ITS2, nrLSU and *tef1*. The ML analysis was performed using RAxML v.8.2.10 (Stamatakis 2014) with the bootstrap values (ML-BS) obtained from 1,000 replicates and the GTRGAMMA model of nucleotide evolution. The maximum parsimony (MP) analysis was performed using PAUP* 4.0a162 (Swofford 2003). Trees were generated using 100 replicates of random stepwise addition of sequence and tree-bisection reconnection (TBR) branch-swapping algorithm with all characters given equal weight. Branch supports (MP-BS) for all parsimony analyses were estimated by performing 1,000 bootstrap replicates with a heuristic search of 10 random-addition replicates for each bootstrap replicate. The BI was performed using MrBayes 3.2.6 (Ronquist et al. 2012). The best-fit substitution model for each partitioned locus was estimated separately with jModeltest v.2.17 (Darriba et al. 2012). Four Markov chains were run for 6,000,000 generations until the split deviation frequency value was lower than 0.01. The convergence of the runs was checked using Tracer v.1.7 (Rambaut et al. 2018). Trees were sampled every 100th generation. The first quarter of the trees, which represented the burn-in phase of the analyses, was discarded and the remaining trees were used to calculate Bayesian posterior probabilities (BPP) in the majority rule consensus tree. All trees were visualised in FigTree 1.4.2 (Rambaut 2014).

Table 1. Species and sequences used in the phylogenetic analyses. Newly generated sequences are set in bold. Holotypes are marked with *.

Taxa	Voucher	Locality	ITS	nrLSU	*tef1*
Asterostroma bambusicola	He 4132	Thailand	KY263865	KY263871	**MH669240**
A. cervicolor	He 4020	China	KY263859	KY263869	–
Baltazaria eurasiaticogalactina	CBS 666.84	France	–	AY293211	–
B. octopodites	FLOR 56449	Brazil	MH260025	MH260047	–
Dichostereum austrosinense	He 4871*	China	**MH538317**	**MH538334**	–
	He 4316	China	**MH538316**	**MH538335**	–
	He 3551	China	**MH538314**	–	**MH550363**
D. boidinii	He 5026*	China	**MH538324**	**MH538330**	–
	He 1662	China	**MH538309**	–	**MH550360**
	He 4410	China	**MH538315**	**MH538331**	**MH550361**
	He 462	China	**MH538311**	–	–
	Dai 16117	China	**MH538312**	**MH538327**	**MH550362**
D. durum	Fungi Gallici 1985	France	AF506429	AF506429	–
D. eburneum	He 5374*	China	**MH538318**	**MH538337**	**MH550366**
D. effuscatum	GG 930915	France	AF506390	AF506390	–
	FP 101758 Sp	USA	**MH538323**	**MH538336**	**MH550367**
	CBS 516.80	USA	–	AF323739	–
D. granulosum	NH 7137	Canada	AF506391	AF506391	–
	FP 133479 Sp	USA	**MH538321**	**MH538333**	**MH550368**
	He 1887	China	**MH538313**	**MH538332**	**–**
D. pallescens	Kropp 2	USA	**MH538320**	**MH538326**	**MH550365**
	CBS 717.81	USA	–	AF518614	–
	He 3266	China	**MH538310**	**MH538325**	**MH550364**
D. aff. *pallescens*	KHL 10258	Puerto Rico	AF506428	AF506428	–
D. rhodosporum	Dai 18625A	Australia	**MH538319**	**MH538329**	**MH550370**
D. sordulentum	FP 11735 Sp	USA	**MH538322**	**MH538328**	**MH550369**
Duportella tristicula	He 4775	China	**MH669235**	**MH669239**	**MH669245**
Echinodontium tinctorium	HHB 12866 Sp	USA	KY172888	KY172903	**MH550371**
Gloiothele lactescens	EL 8-98	Sweden	AF506453	AF506453	–
G. lamellosa	KHL11031	Venezuela	AF506454	AF506454	–
Lachnocladium cf. *brasiliense*	CALD 161213-1	Brazil	MH260037	MH260055	–
L. schweinfurthianum	KM 49740	Cameroon	MH260033	MH260051	–
L. sp.	KHL10556	Jamaica	AF506461	AF506461	–
Parapterulicium subarbusculum	FLOR 56456	Brazil	MH260026	MH260026	–
	FLOR 56459	Brazil	MH260027	MH260049	–
Peniophora polygonia	He 3668	China	**MH669233**	**MH669237**	**MH669243**
P. rufa	He 2788	China	**MH669234**	**MH669238**	**MH669244**
Scytinostroma portentosum	EL11-99	Sweden	AF506470	AF506470	–
Vararia investiens	He 2104	USA	–	**MH669236**	**MH669242**
	FP 151122	USA	**MH971976**	**MH971977**	**–**
Vesiculomyces citrinus	He 3716	China	KY860369	KY860429	**MH669241**

Results

Phylogenetic inference

The ITS-nrLSU-*tef1* sequence dataset contained 37 ITS, 38 nrLSU and 18 *tef1* sequences from 40 samples representing 26 ingroup taxa and the outgroup (Table 1). Twenty ITS, 18 nrLSU and 18 *tef1* sequences were generated for this study. The dataset had an aligned length of 2239 characters, of which 1596 were constant, 163 variable characters were parsimony-uninformative and 480 were parsimony-informative. MP analysis yielded six most parsimonious trees. jModelTest suggested TIM2ef+G, K80+G, TPM1uf+G, TIM2+I+G and TrN+I+G to be the best-fit models of nucleotide evolution for ITS1, 5.8S, ITS2, nrLSU and *tef1* markers, respectively, for the Bayesian analysis. The average standard deviation of split frequencies of BI was 0.004704 at the end of the run. MP and BI analyses resulted in an almost identical tree topology compared to the ML analysis. Only the ML tree is shown in Fig. 1 with ML and MP bootstrap values ≥50% and Bayesian posterior probabilities ≥0.95 labelled along the branches.

In the tree (Fig. 1), the nine sampled species of *Dichostereum* formed a strongly supported clade in Peniophoraceae (ML-BS = 91, MP-BS = 97, BPP = 1.00). *Vararia investiens* (Schwein.) P. Karst., the generic type of *Vararia*, formed a sister lineage to *Dichostereum*, but this close relationship did not receive significant support. Of the three new species, samples of *D. austrosinense* and *D. boidinii* formed two strongly supported lineages, whilst the single specimen of *D. eburneum* formed the sister taxon to *D. boidinii* and *D.* aff. *pallescens*. *Dichostereum effuscatum* from France and USA and both *D. granulosum* and *D. pallescens* from north America and China, formed three strongly supported lineages. Single samples of *D. durum* from France, *D. rhodosporum* from Australia and *D. sordulentum* from USA formed their own distinct lineages.

Taxonomy

Dichostereum austrosinense **S.H. He & S.L. Liu, sp. nov.**
MycoBank: MB826931
Figs 2a, 3, 6a

Typification. CHINA. Guangxi Autonomous Region, Jinxiu County, Dayaoshan Nature Reserve, Shengtangshan, on fallen angiosperm trunk, 15 Jul 2017, He 4871 (holotype, BJFC 024390, ITS GenBank accession number: MH538317; isotype in CFMR).

Etymology. "*austrosinense*" referring to the distribution in southern China.

Basidiomata. Perennial, resupinate, effused, closely adnate, inseparable from substrates, coriaceous to soft corky, at first as irregular small patches, later confluent up to 15 cm long, 4.5 cm wide, up to 1 mm thick. Hymenophore surface smooth, greyish-orange

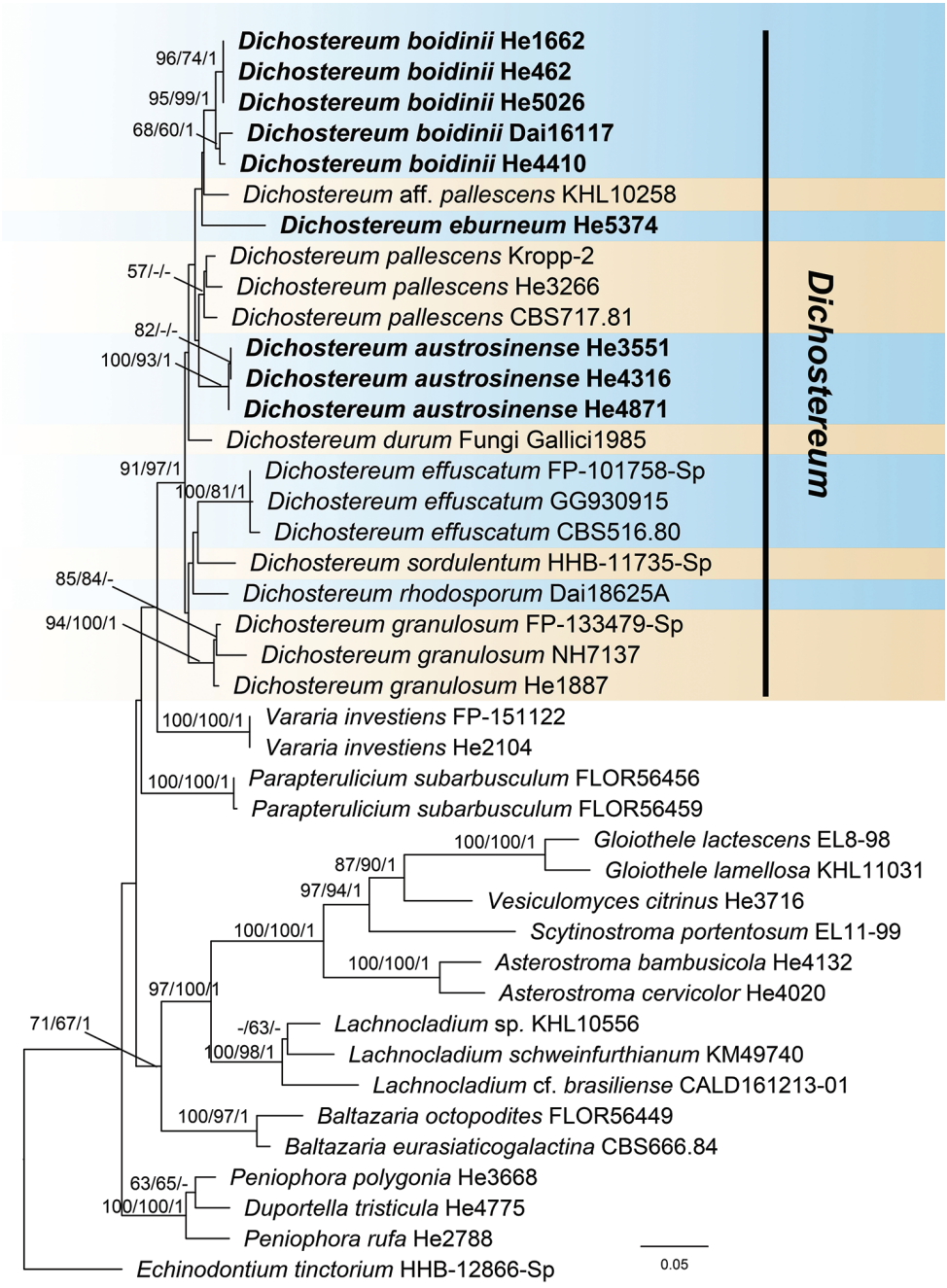

Figure 1. Phylogeny of *Dichostereum* and representatives of Peniophoraceae inferred from ITS-nrLSU-*tef1* sequences. Topology is from ML analysis with maximum likelihood bootstrap support values (≥50, former), parsimony bootstrap support values (≥50, middle) and Bayesian posterior probability values (≥0.95, latter) shown along the branches. Different species of *Dichostereum* are indicated as coloured blocks. The new species are set in bold. Scale bar: 0.05 nucleotide substitutions per site.

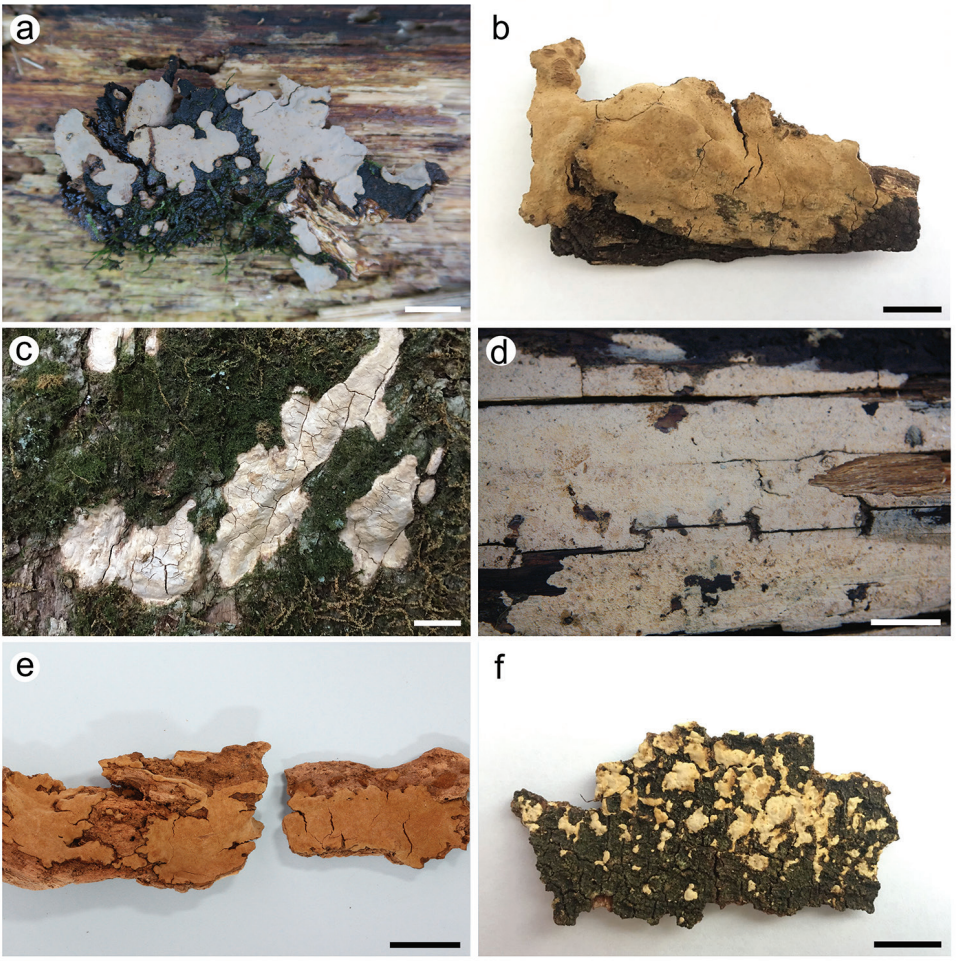

Figure 2. Basidiomata of *Dichostereum* species. **a** *D. austrosinense* (holotype, He 4871) **b** *D. boidinii* (holotype, He 5026) **c** *D. eburneum* (holotype, He 5374) **d** *D. granulosum* (He 1887) **e** *D. pallescens* (He 3266) **f** *D. rhodosporum* (Dai 18625A). Scale bar: 1 cm.

[5B(4–5)], brownish-yellow [5C(7–8)] to light brown [6D(4–8)], not cracking; margin abrupt, concolorous or darker than hymenophore surface.

Microscopic structures. Hyphal system dimitic. Context thickening, compact, composed of generative hyphae, dichohyphae, embedded basidiospores and scattered crystals. Generative hyphae rare, with clamp connections, hyaline, thin- to slightly thick-walled, 2–3 µm in diam. Dichohyphae dominant, hyaline to yellow, distinctly thick-walled, dichotomously branched with acute tips, weakly dextriniod. Catahymenium composed of dichohyphae, gloeocystidia, basidia and basidioles. Dichohyphae in this layer abundant, similar to those in the context, but strongly dextrinoid, more slender and more frequently branched, 20–50 µm across, 2–4 µm wide at lowest part. Gloeocystidia abundant, subcylindrical to subfusiform, hyaline, slightly thick-walled,

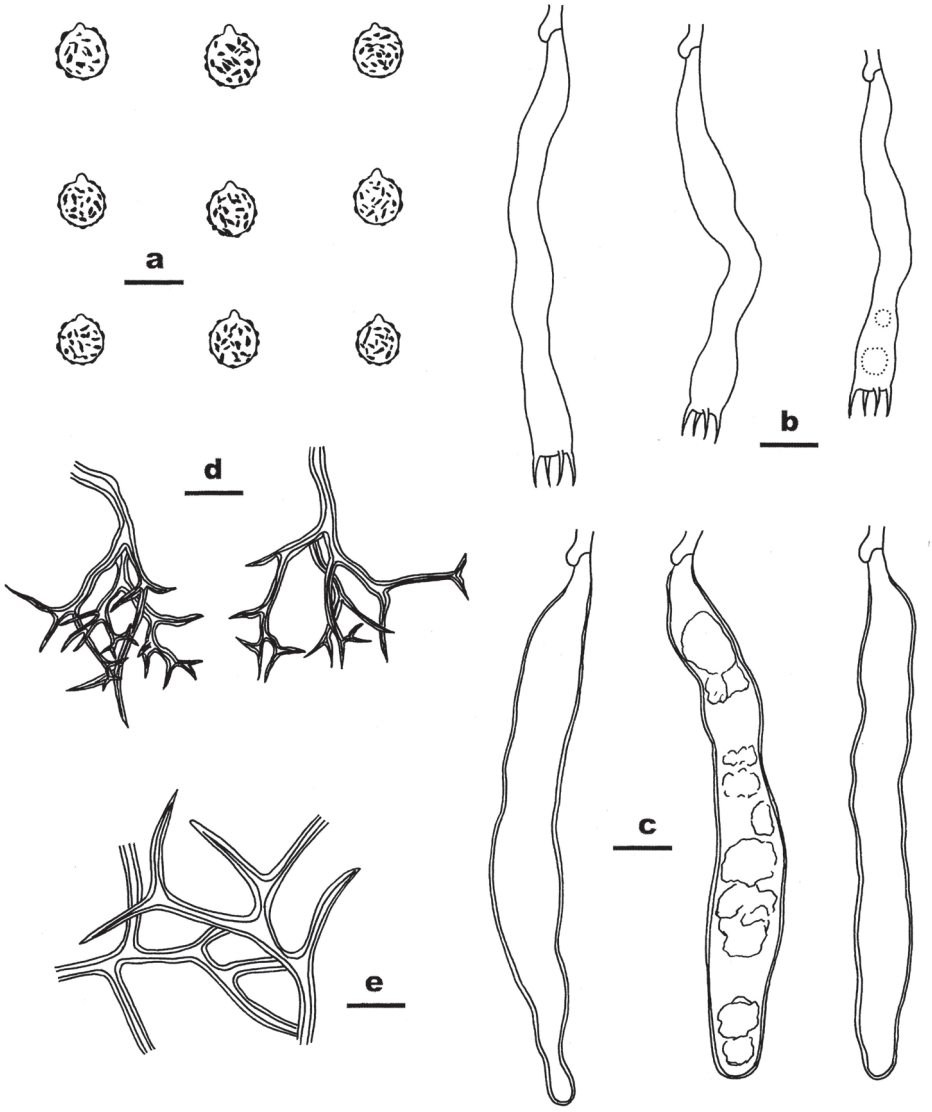

Figure 3. Microscopic structures of *Dichostereum austrosinense* (drawn from the holotype). **a** Basidiospores **b** Basidia **c** Gloeocystidia **d** Dichohyphae from hymenium **e** Dichohyphae from subiculum. Scale bar: 10 μm.

with or without solidified contents, 80–130 × 8–15 μm. Basidia narrowly cylindrical, usually slightly sinuous, hyaline, thin-walled, with 4 sterigmata and a basal clamp connection, 50–80 × 5–8 μm; basidioles in shape similar to basidia, but slightly smaller. Basidiospores abundant, subglobose with a distinct apiculus, hyaline to pale yellowish-brown in KOH, thick-walled, strongly amyloid, (7–) 7.3–8 (–9) μm in diam.; walls ornamented with large warts and crests.

Additional specimens examined. CHINA. Hainan Province, Lingshui County, Diaoluoshan Nature Reserve, on fallen angiosperm trunk, 17 Mar 2016, He 3551 (BJFC 022052); Jiangxi Province, Lianping County, Jiulianshan Nature Reserve, on fallen angiosperm branch, 13 Aug 2016, He 4316 (BJFC 023758).

Remarks. *Dichostereum austrosinense* is overall characterised by the relatively large gloeocystidia and basidiospores with large warts and crests. *Dichostereum peniophoroides* (Burt) Boidin & Lanq. is similar to *D. austrosinense* but differs in having wider gloeocystidia (7–22 μm), slightly larger basidiospores (7–9 μm) with larger ornamentations and a distribution in Caribbean regions (Lanquetin 1973; Boidin and Lanquetin 1980). *Dichostereum austrosinense* is also similar to *D. rhodosporum* (Wakef.) Boidin & Lanq. which differs in having paler basidiomata, smaller ornamentations of basidiospores and a distribution in Australia and New Zealand (Boidin and Lanquetin 1980, Figs. 2 and 6).

Dichostereum boidinii **S.H. He & S.L. Liu, sp. nov.**
MycoBank: MB826932
Figs 2b, 4, 6b

Typification. CHINA. Hubei Province, Wufeng County, Breeding base of *Magnolia*, on angiosperm stump, 14 Aug 2017, He 5026 (holotype, BJFC 024544, ITS GenBank accession number: MH538324; isotype in CFMR).

Etymology. "*boidinii*" (Lat.), named to honour Dr. Jacques Boidin (Lyon, France) for his contribution to the taxonomy of *Dichostereum*.

Basidiomata. Perennial, resupinate to effused-reflexed with slightly elevated margin, closely adnate, inseparable from substrates, coriaceous to soft corky, up to 8 cm long, 4 cm wide, 1.5 mm thick. Hymenophore surface smooth, greyish-orange [6B(3–4)], brownish-orange [6C(4–6)] to light brown [6D(4–6)], not cracking; margin abrupt, concolorous or darker than hymenophore surface.

Microscopic structures. Hyphal system dimitic. Context thickening, compact, composed of generative hyphae, dichohyphae, embedded basidiospores and scattered crystals. Generative hyphae rare, with clamp connections, hyaline, thin-walled, 2–3 μm in diam. Dichohyphae dominant, hyaline to yellow, distinctly thick-walled, dextriniod. Catahymenium composed of dichohyphae, gloeocystidia, basidia and basidioles. Dichohyphae in this layer abundant, similar to those in the context, but strongly dextrinoid, more frequently branched with short terminal branches, 20–40 μm across, 2–4 μm wide at lowest part. Gloeocystidia abundant, fusiform to subulate, hyaline, slightly thick-walled, with solidified contents, 20–60 × 7–12 μm. Basidia subclavate to subcylindrical, hyaline, thin-walled, with 4 sterigmata and a basal clamp connection, 25–40 × 5–7 μm; basidioles in shape similar to basidia, but slightly smaller. Basidiospores subglobose with a distinct apiculus, hyaline to pale yellowish-brown in KOH, thick-walled, strongly amyloid, (5–) 5.5–6.5 (–7) μm in diam.; walls ornamented with warts and crests.

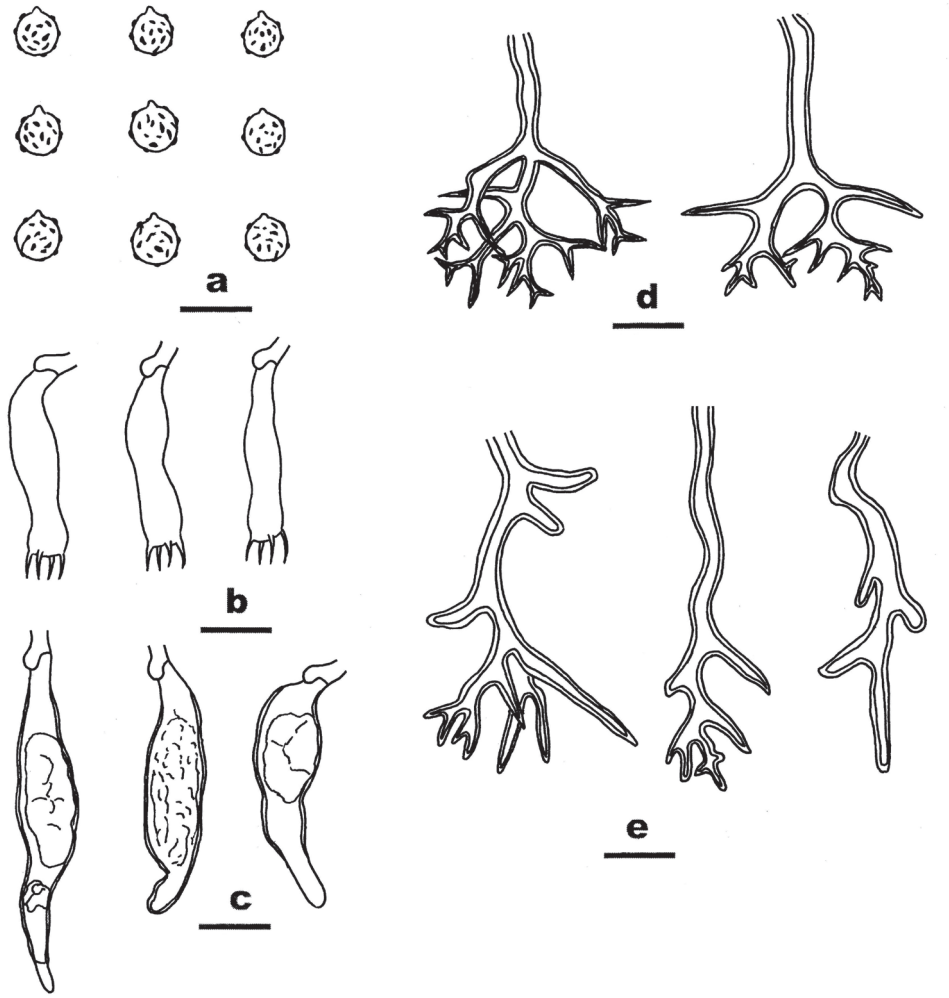

Figure 4. Microscopic structures of *Dichostereum boidinii* (drawn from the holotype). **a** Basidiospores **b** Basidia **c** Gloeocystidia **d** Dichohyphae from hymenium **e** Dichohyphae from subiculum. Scale bar: 10 μm.

Additional specimens examined. CHINA. Anhui Province, Huangshan County, Huangshan Nature Reserve, on fallen angiosperm trunk, 21 Oct 2011, He 462 (BJFC 012101); Hainan Province, Lingshui County, Diaoluoshan Nature Reserve, on rotten wood of *Dacrydium*, 13 Nov 2015, Dai 16117 (BJFC 020210); Jiangxi Province, Anyuan County, Sanbaishan Forest Park, on fallen angiosperm trunk, 15 Aug 2016, He 4410 (BJFC 023851); Yunnan Province, Kunming, Xishan Park, on angiosperm stump, 17 Jul 2013, He 1662 (BJFC 016129).

Remarks. *Dichostereum boidinii* is widely distributed in southern China and mainly characterised by the thick, brownish basidiomata and relatively small basidiospores with large warts and crests. *Dichostereum pallescens* is similar to *D. boidinii* but differs in

having slender dichohyphae and smaller and sparser ornamentations of basidiospores (Boidin and Lanquetin 1980, Fig. 6). *Dichostereum orientale* Boidin & Lanq. resembles *D. boidinii* by sharing short terminal branches of dichohyphae, but differs in having smaller basidiospores (5–5.5 μm in diam.) and a distribution in Africa (Boidin and Lanquetin 1980). The ornamentation of basidiospores of *D. boidinii* is similar to *D. austrosinense*, but the latter species has larger gloeocystidia, basidia and basidiospores.

***Dichostereum eburneum* S.H. He & S.L. Liu, sp. nov.**
MycoBank: MB826933
Figs 2c, 5, 6c

Typification. CHINA. Fujian Province, Wuyishan County, Wuyishan Nature Reserve, on bark of living *Castanopsis*, 6 Apr 2018, He 5374 (holotype, BJFC, ITS GenBank accession number: MH538318; isotype in CFMR).

Etymology. "*eburneum*" referring to the white colour of hymenophore.

Basidiomata. Perennial, resupinate, effused, closely adnate, inseparable from substrate, coriaceous, at first as irregular small patches, later confluent up to 7 cm long, 2 cm wide, 200–500 μm thick. Hymenophore surface smooth, white (5A1), orange white (5A2) to greyish-orange [5B(3–4)], cracking with age; margin thinning out, concolorous with hymenophore.

Microscopic structures. Hyphal system dimitic. Context thickening, compact, composed of generative hyphae, dichohyphae, embedded basidiospores and abundant crystals. Generative hyphae rare, with clamp connections, hyaline, thin- to slightly thick-walled, 2–3 μm in diam. Dichohyphae dominant, hyaline to yellow, distinctly thick-walled, dextriniod, frequently branched, aseptate, 1–2 μm in diam. Catahymenium composed of dichohyphae, gloeocystidia, basidia and basidioles. Dichohyphae in this layer abundant, hyaline to pale yellow, distinctly thick-walled, strongly dextriniod, dichotomously branched with acute terminal tips, 15–30 μm across, 2–4 μm wide at lowest part. Gloeocystidia abundant, fusiform to subclavate, hyaline, thin-walled, with solidified contents, 20–50 × 5–10 μm. Basidia subcylindrical with basal part slightly swollen, hyaline, thin-walled, with 4 sterigmata and a basal clamp connection, 30–45 × 6–9 μm; basidioles in shape similar to basidia, but slightly smaller. Basidiospores subglobose with a distinct apiculus, hyaline to pale yellowish-brown in KOH, thick-walled, strongly amyloid, 6–7 (–8) μm in diam.; walls ornamented with dense, large warts and crests.

Remarks. *Dichostereum eburneum* is characterised by the pale basidiomata on bark of living tree, the presence of abundant crystals in context and basidiospores with dense and large ornamentations. Ecologically and macroscopically, *D. eburneum* resembles *Dendrothele* Höhn. & Litsch., but the microscopic features are largely different (Nakasone and Burdsall 2011). *Dichostereum kenyense* Boidin & Lanq. is similar to *D. eburneum* by sharing the large ornamentations of basidiospores, but differs in having wider span of dichohyphae, slightly larger basidiospores (7–8 μm) and a distribution in Africa (Boidin and Lanquetin 1980).

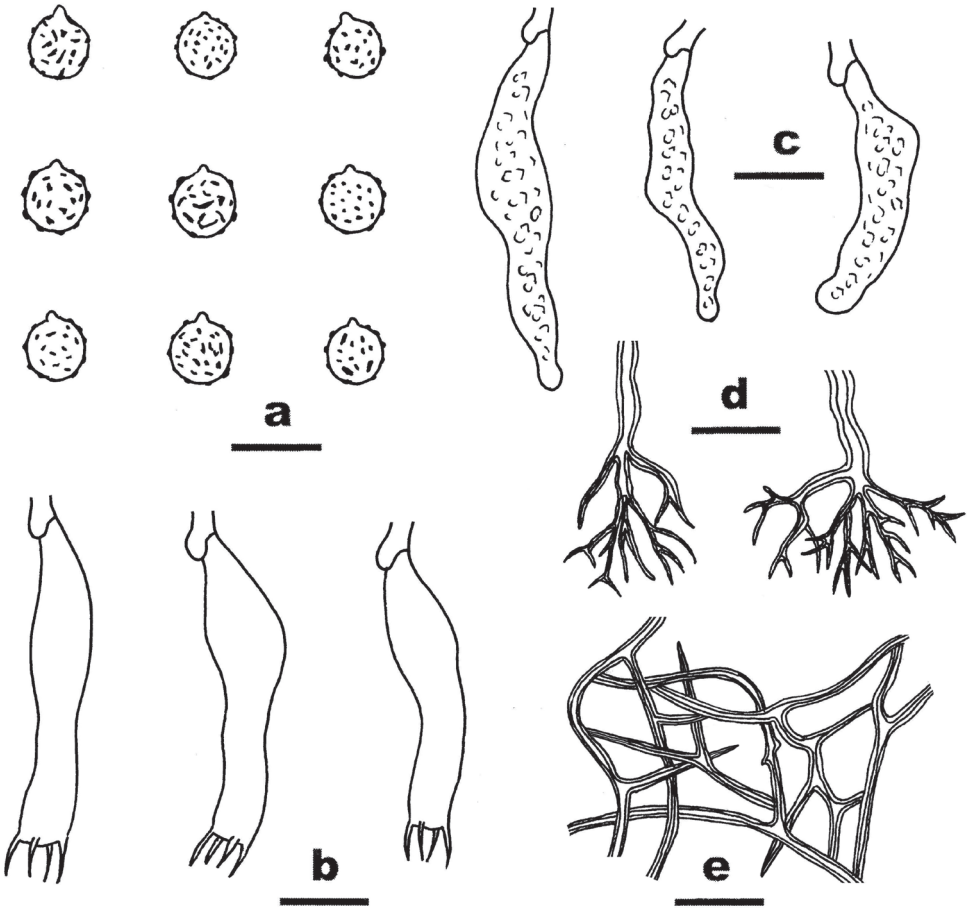

Figure 5. Microscopic structures of *Dichostereum eburneum* (drawn from the holotype). **a** Basidiospores; **b** Basidia **c** Gloeocystidia **d** Dichohyphae from hymenium **e** Dichohyphae from subiculum. Scale bar: 10 μm.

Key to 5 species of Dichostereum in China

1	Hymenophore grandinioid; basidiospores ellipsoid	***D. granulosum***
–	Hymenophore smooth; basidiospores subglobose	**2**
2	Basidiomata white; on bark of living *Castanopsis*	***D. eburneum***
–	Basidiomata brownish; on dead wood	**3**
3	Gloeocystidia ≥80 μm long	***D. austrosinense***
–	Gloeocystidia <80 μm long	**4**
4	Basidiospores 6.5–7.5 μm in diam, ornamentation sparse	***D. pallescens***
–	Basidiospores 5.5–6.5 μm in diam, ornamentation dense	***D. boidinii***

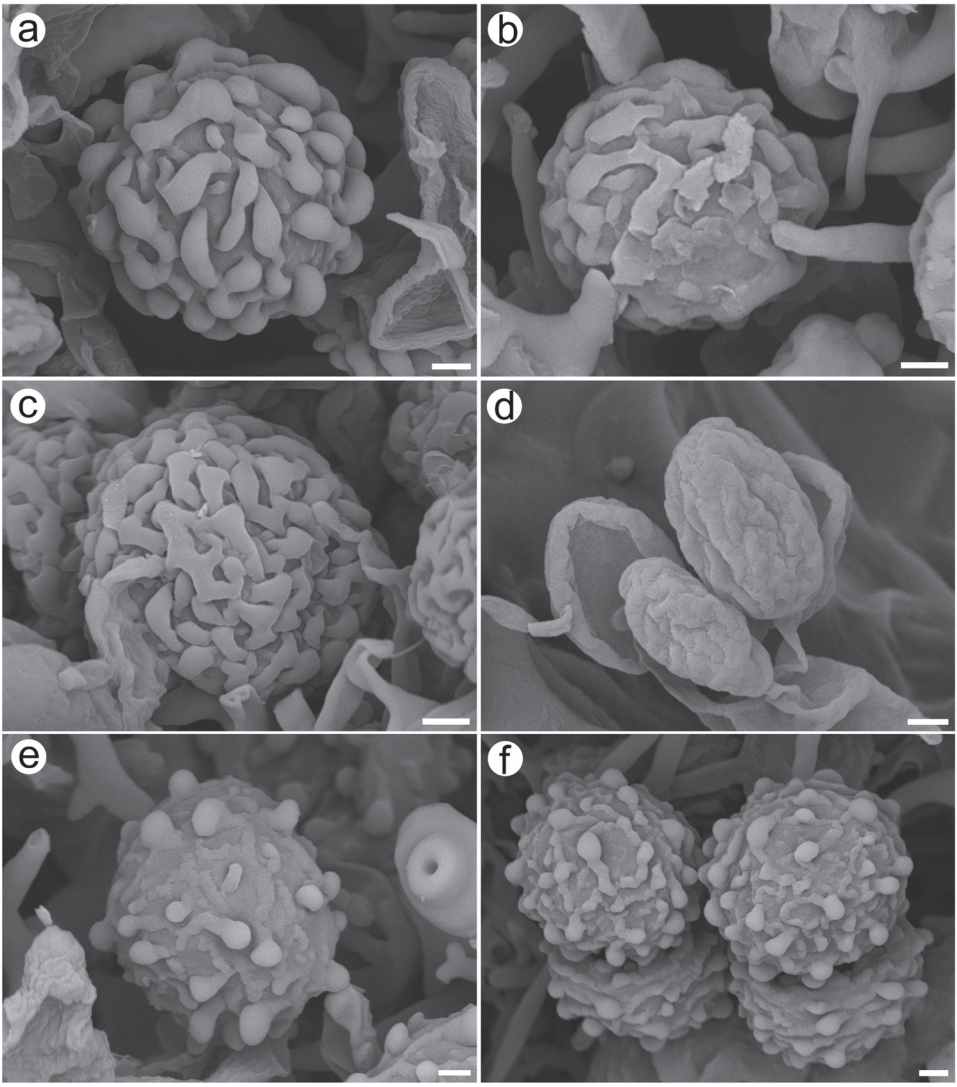

Figure 6. Scanning electron micrographs (SEM) of basidiospores of *Dichostereum*. **a** *D. austrosinense* (holotype, He 4871) **b** *D. boidinii* (holotype, He 5026) **c** *D. eburneum* (holotype, He 5374) **d** *D. granulosum* (He 1887) **e** *D. pallescens* (He 3266) **f** *D. rhodosporum* (Dai 18625A). Scale bar: 1 μm.

Discussion

To date, 14 species of *Dichostereum* have been described worldwide including the three new species in the present paper (Boidin and Lanquetin 1980). Amongst them, 5 species, *D. brevisporum* (S.S. Rattan) Boidin & Lanq. from India, *D. kenyense*, *D. orientale* and *D. ramulosum* (Boidin & Lanq.) Boidin & Lanq. from Africa and *D. peniophoroides* from Caribbean regions, were not included in the present analyses. In order to

resolve the infra-generic phylogenetic relationships of *Dichostereum*, samples of these species and any additional undescribed taxa should be included.

The family Peniophoraceae *sensu* Larsson (2007) formed a strongly supported clade in Russulales and included about 15 genera (Larsson and Larsson 2003; Miller et al. 2006; Larsson 2007; Leal-Dutra et al. 2018). Except for the coralloid *Lachnocladium* Lév. and the insect symbiont *Entomocorticium* H.S. Whitney, Bandoni & Oberw., all the other genera in the family are corticioid fungi, such as *Asterostroma* Massee, *Peniophora* Cooke, *Scytinostroma* Donk and *Vararia*. However, recent molecular and morphological studies showed that two species of *Parapterulicium* Corner with coralloid basidiomata belong to Peniophoraceae in the Russulales rather than Pterulaceae of the Agaricales (Leal-Dutra et al. 2018). In the phylogenetic tree, the type species, *Parapterulicium subarbusculum* Corner formed a distinct lineage, while *P. octopodites* Corner is closely related to *Scytinostroma galactinum* (Fr.) Donk and its relatives. More studies on the taxonomy and phylogeny of Peniophoraceae are needed, since some large genera such as *Scytinostroma* and *Vararia* are still polyphyletic and many species are undescribed.

Acknowledgements

The authors thank Drs. Rita Rentmeester and Karen Nakasone (Center for Forest Mycology Research, Northern Research Station, U.S. Forest Service, Madison, USA) for culture and literature loan. The authors acknowledge Dr. Yu-Cheng Dai (Beijing Forestry University, China) for providing specimens. This study was supported by the National Natural Science Foundation of China (Nos. 31670013 & 31470144) and the Fundamental Research Funds for the Central Universities (No. 2017PT09).

References

Benson DA, Cavanaugh M, Clark K, Karsch-Mizrachi I, Ostell J, Pruitt KD, Sayers EW (2018) GenBank. Nucleic Acids Research 46: 41–47. https://doi.org/10.1093/nar/gkx1094

Bernicchia A, Gorjón SP (2010) Fungi Europaei 12. Corticiaceae s.l. Edizioni Candusso, Italia. 1008 pp.

Boidin J (1967) Basidiomycètes Lachnocladiaceae résupinés de la Republique Centrafricaine. Cahiers de La Maboké 5: 23–35.

Boidin J, Lanquetin P (1977) Les genres *Dichostereum* et *Vararia* en Guadeoloupe (Basidiomycetes, Lachnocladiaceae). Mycotaxon 6: 277–336.

Boidin J, Lanquetin P (1980) Contribution a l'étude du genre *Dichostereum* Pilàt (Basidiomycètes, Lachnocladiaceae). Bulletin de la Société Mycologique de France 96: 381–406.

Boidin J, Michel H (1998) Les genres *Vararia* et *Dichostereum* en Europe (Basidiomycotina, Lachnocladiaceae). Bulletin de la Société Mycologique de France 114: 1–4.

Boidin J, Gilles G, Lanquetin P (1987) Basidiomycètes Aphyllophorales de l'île de la Réunion. IX – Les genres *Dichostereum* Pilát et *Vararia* Karsten. Bulletin de la Société Mycologique de France 103: 119–135.

Castresana J (2000) Selection of conserved blocks from multiple alignments for their use in phylogenetic analysis. Molecular Biology and Evolution 17: 540–552. https://doi.org/10.1093/oxfordjournals.molbev.a026334

Dai LD, He SH (2016) New species and new records of *Aleurodiscus* s.l. (Basidiomycota) in China. Mycological Progress 15: 717–730. https://doi.org/10.1007/s11557-016-1202-z

Dai YC (2011) A revised checklist of corticioid and hydnoid fungi in China for 2010. Mycoscience 52(1): 69–79. https://doi.org/10.1007/S10267-010-0068-1

Darriba D, Taboada GL, Doallo R, Posada D (2012) jModelTest 2: more models, new heuristics and parallel computing. Nature Methods 9: 772. https://doi.org/10.1038/nmeth.2109

Hall TA (1999) Bioedit: a user-friendly biological sequence alignment editor and analysis program for Windows 95/98/NT. Nucleic Acids Symposium Series 41: 95–98.

Hallenberg N (1985) The Lachnocladiaceae and Coniophoraceae of North Europe. Fungiflora, Oslo, 96 pp.

Kearse M, Moir R, Wilson A, Stones-Havas S, Cheung M, Sturrock S, Buxton S, Cooper A, Markowitz S, Duran C, Tierer T, Ashton B, Meintjes P, Drummond A (2012) Geneious Basic: An integrated and extendable desktop software platform for the organization and analysis of sequence data. Bioinformatics 28(12): 1647–1649. https://doi.org/10.1093/bioinformatics/bts199

Kornerup A, Wanscher JH (1978) Methuen handbook of colour (3rd edn). Eyre Methuen, London, 252 pp.

Katoh K, Rozewicki J, Yamada KD (2017) MAFFT online service: multiple sequence alignment, interactive sequence choice and visualization. Briefings in Bioinformatics: bbx108. https://doi.org/10.1093/bib/bbx108

Lanquetin P (1973) Utilisation des cultures dans la systématique des *Vararia* Karst subg. *Dichostereum* (Pilat) Boid. (Basidiomycètes Lachnocladiaceae). Bulletin Mensuel De La Société Linnéenne De Lyon 42(7) :167–192. https://doi.org/10.3406/linly.1973.10071

Larsson E, Larsson KH (2003) Phylogenetic relationships of russuloid basidiomycetes with emphasis on aphyllophoralean taxa. Mycologia 95: 1037–1065. https://doi.org/10.1080/15572536.2004.11833020

Larsson KH (2007) Re-thinking the classification of corticioid fungi. Mycological Research 111: 1040–1063. https://doi.org/10.1016/j.mycres.2007.08.001

Leal-Dutra CA, Neves MA, Grifth GW, Reck MA, Clasen LA, Dentinger BTM (2018) Reclassifcation of *Parapterulicium* Corner (Pterulaceae, Agaricales), contributions to Lachnocladiaceae and Peniophoraceae (Russulales) and introduction of *Baltazaria* gen. nov. MycoKeys 37: 39–56. https://doi.org/10.3897/mycokeys.37.26303

Liu SL, Zhao Y, Dai YC, Nakasone KK, He SH (2017a) Phylogeny and taxonomy of *Echinodontium* and related genera. Mycologia 109: 568–577. https://doi.org/10.1080/00275514.2017.1369830

Liu SL, Tian Y, Nie T, Thawthong A, Hyde KD, Xu LL, He SH (2017b) Updates on East Asian *Asterostroma* (Russulales, Basidiomycota): new species and new records from Thailand and China. Mycological Progress 16: 667–676. https://doi.org/10.1007/s11557-017-1301-5

Maddison WP, Maddison DR (2018) Mesquite: a modular system for evolutionary analysis. Version 3.51. http://www.mesquiteproject.org

Miller SL, Larsson E, Larsson KH, Verbeken A, Nuytinck J (2006) Perspectives in the new Russulales. Mycologia 98: 960–970. https://doi.org/10.1080/15572536.2006.11832625

Nakasone KK, Burdsall, Jr HH (2011) The genus *Dendrothele* (Agaricales, Basidiomycota) in New Zealand. New Zealand Journal of Botany 49: 107–131. https://doi.org/10.1080/00288825X.2010.512636

Nilsson RH, Tedersoo L, Abarenkov K, Ryberg M, Kristiansson E, Hartmann M, Schoch CL, Nylander JAA, Bergsten J, Porter TM, Jumpponen A, Vaishampayan P, Ovaskainen O, Hallenberg N, Bengtsson-Palme J, Eriksson KM, Larsson K-H, Larsson E, Kõljalg U (2012) Five simple guidelines for establishing basic authenticity and reliability of newly generated fungal ITS sequences. MycoKeys 4: 37–63. https://doi.org/10.3897/mycokeys.4.3606

Parmasto E (1968) Conspectus Systematis Corticiacearum. Institutum Zoologicum et Botanicum Academiae Scientiarum R.P.S.S. Estonicae, Tartu, 261 pp.

Parmasto E (1970) The Lachnocladiaceae of the Soviet Union. Academy of Sciences of the Estonian S.S.R. Institute of Zoology and Botany, Tartu, 180 pp.

Rambaut A (2014) FigTree, a graphical viewer of phylogenetic trees. http://tree.bio.ed.ac.uk/software/fgtree/

Rambaut A, Drummond A, Xie D, Baele G, Suchard M (2018) Tracer v1.7. http://beast.community/tracer

Rehner SA, Buckley E (2005) A *Beauveria* phylogeny inferred from nuclear ITS and EF1-alpha sequences: evidence for cryptic diversification and links to *Cordyceps* teleomorphs. Mycologia 97: 84–98. https://doi.org/10.1080/15572536.2006.11832842

Reid DA (1965) A monograph of the stipitate stereoid fungi. Beihefte zur Nova Hedwigia 18: 1–382.

Ronquist F, Teslenko M, van der Mark P, Ayres DL, Darling A, Hőhna S, Larget B, Liu L, Suchard MA, Huelsenbeck JP (2012) MrBayes 3.2: Efficient Bayesian phylogenetic inference and model choice across a large model space. Systematic Biology 61: 539–542. https://doi.org/10.1093/sysbio/sys029

Stamatakis A (2014) RAxML Version 8: A tool for phylogenetic analysis and post-analysis of large phylogenies. Bioinformatics 30: 1312–1313. https://doi.org/10.1093/bioinformatics/btu033

Swofford DL (2003) PAUP*: Phylogenetic analysis using parsimony (*and other methods). Version 4. Sinauer Associates, Sunderland, Massachusetts.

Thiers B (continuously updated) Index Herbariorum: A global directory of public herbaria and associated staff. New York Botanical Garden's Virtual Herbarium. http://sweetgum.nybg.org/ih/

Vilgalys R, Hester M (1990) Rapid genetic identification and mapping of enzymatically amplified ribosomal DNA from several Cryptococcus species. Journal of Bacteriology 172: 4238-4246. https://doi.org/10.1128/jb.172.8.4238-4246.1990

White TJ, Bruns TD, Lee S, Taylor J (1990) Amplification and direct sequencing of fungal ribosomal RNA genes for phylogenetics. In: Innis MA, Gelfand DH, Sninsky JJ, White TJ (Eds) PCR protocols, a guide to methods and applications. Academic, San Diego, 315–322. https://doi.org/10.1016/B978-0-12-372180-8.50042-1